UNIVERSITÀ DEGLI STUDI DELLA TUSCIA DI VITERBO

DIPARTIMENTO DELL' AGRICOLTURA, FORESTE, NATURA ED ENERGIA

CORSO DI DOTTORATO DI RICERCA

____BIOTECNOLOGIE VEGETALI_____ - XXIV Ciclo.

INTEGRATION OF NATIVE AND ENGINEERED PHOTOSYNTHETIC MICROORGANISMS INTO ARTIFICIAL ASSEMBLIES FOR THE DEVELOPMENT OF PROMISING BIOSENSORS TARGETED TO ENVIRONMENTAL MONITORING

Settore Scientifico-Disciplinare
BIO/13

Coordinatore: Prof. Stefania Masci

Firma .....

Tutor: Dott.ssa Maria Teresa Giardi

Firma .....

Dottorando: Giuseppe Rodio

Firma .....

TABLE OF CONTENTS

1.Introduction

1.1 Biosensor description

Biosensors are devices which use a biological recognition element retained in direct spatial contact with transduction system (IUPAC definition) [1]. Biosensors can be straightforwardly depicted as devices that convert a physical or biological event into a measurable signal [2] they are composed of a biosensing element (i.e. enzyme, tissue, living cell) that provides selectivity and a transducer that converts chemical signal into a processable signal [3]. Specifically, biosensor consists of three parts: the first element is the biomediator (a biomimic or biologically derived material e.g. tissue, microorganisms, organelles, cell receptors, enzymes, antibodies, nucleic acids, and biological sensitive elements created with genetic engineering), the second element is the transducer (physicochemical, optical, piezoelectric, electrochemical, etc.) that transforms the signal resulting from the analyte's interaction with the biological element into a signal that can be measured and quantified; the third element is the associated electronics or signal processor, responsible of the results visualization in a user-friendly way [4]. Biosensors require immobilization of biomediator to the surface of the sensor (metal, polymer or glass and other materials) using physical or chemical techniques (Figure 1)

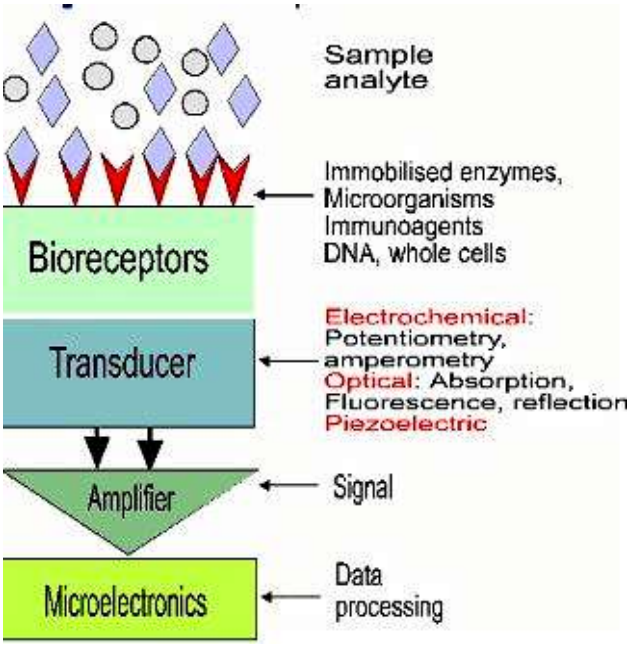

Figure 1.1 Biosensor scheme

Looking at the past it is clear that the concept of biosensor has evolved. The first example of biosensor was illustrated by entrapping the enzyme glucose oxidase in a dialysis membrane over an oxygen probe. Later, the same term "enzyme electrode" was used to describe a similar device where again the enzyme glucose oxidase was immobilized in a polyacrylamide gel onto a surface of an oxygen electrode for the rapid and quantitative determination of glucose. Since the beginning of the '80s, several authors started to prove the concept of biosensor as a system in which an enzyme is coupled to electrochemical-optical sensors. In the electrochemical community at that period the research on Ion Selective Electrodes (ISE) was very active with the idea to extend the range of sensors, and even to non ionic compounds, like glucose. Enzymes, multiple enzymes, organelles, bacteria, specialized biological tissues containing specific enzymes were coupled to potentiometric or amperometric, then optical, thermometric, piezoelectric devices, etc. Recently, the concept evolved again in the attempt to replace or mimic the biological material with synthetic chemical compounds, such as MIPs (Molecular Imprinted Polymers). Enzymes and all biological elements based on the enzymes represent the classes of what is now called "catalytic elements". The other important class is represented by the "affinity elements", namely antibodies, lectins, nucleic acids (DNA and RNA) and recently also synthetic ligands. The exploitation of the selectivity of the biological element is the "driving force" of the biosensor [5].

Catalytic events or affinity events have not the same scheme of transduction. If the biological recognition element present in the sensing layer is an enzyme or generally a biocatalyst, a reaction takes place in the presence of the specific target analyte and an increasing amount of co-reactant or product is consumed or formed, respectively, in a short time depending on the turnover. In this scheme, the amplification step is inherent and a large chemical amount can be obtained from the sensing layer. In contrast, the use of antibodies for the detection of antigens does not involve an amplification stage and the "affinity" reaction should be amplified in order to have a clearly readable transduction. We have two possibilities, one is the use of a bioconjugate involving a bound enzyme, like in the classical ELISA test; the second is the inherent amplification given by the mass of the biological element involved where a piezoelectric device (sensitive to mass) can detect minute amount of large proteins (like antibodies) if they are attracted on the surface of the sensor. With the same scheme, surface plasmon resonance can be sensitive to a small amount of large molecule reacting at the surface of the electrode. The main problem of the biological system, catalytic or affinity, is the associated fragility and the operational activity. Most proteins have an

optimal pH range in which their activity is maximal; this pH range should be compatible with the transducer. Moreover, most of the biological systems have a very narrow range of operating temperature (15÷40°C). The most important problem and main drawback for industrial exploitation is the short lifetime associated with the biological elements. Lifetime of at least months or few years is the prerequisite for a suitable market and the fragility of the assembled systems has always limited the diffusion of biosensors into the market.

In practice the number of biosensors that are likely to be produced and used as "real" commercial devices is very low and the commercial applicability has to be deeply evaluated. Several companies put on the market pre-activated membranes suitable for the immediate preparation of any bioactive membrane and this appeared as a real improvement at least for the easy use of enzyme sensors. The removal of interference has been also another important aspect for the wide use of biosensors in industrial processes. These two main problems have been solved by using multilayer membranes, such as those developed by Yellow Springs Instrument Co. (for glucose or lactate electrodes), where the enzyme is sandwiched between a special cellulose acetate membrane and a polycarbonate nucleopore membrane. The main role of the membrane is to prevent proteins and other macromolecules from passing into the bioactive layer. Cellulose acetate membrane allows only molecules of the size of hydrogen peroxide to cross and contact the platinum anode, thus preventing interference from ascorbic acid or uric acid, for example, at the fixed potential. Such configuration has been used by several researchers in the biosensor assembly. But at the same time several recipes of immobilization of enzymes were published and several laboratories developed their own procedures for immobilizing the biological element, sometimes also patented. One approach was also the development of disposable sensor, based on combination of screen printed electrochemical sensors with enzyme adsorbed on the electrode surface. The use of the sensor just for one measurement limited the use of complicated immobilization procedures to as simple as possible, like the physical adsorption on carbon surface. This electrode surface acted as a sponge, and the large protein was easily immobilized even if the bond was weak. This approach is useful only for a quick and rapid measurement.

Concerning immobilization technology, many other methods have been tested to improve bio-receptor stability and to conserve its bioactivity. The most widely used methods of immobilization are: (i) physical or chemical adsorption on a solid surface; (ii) covalent binding; (iii) entrapment within a membrane, surfactant matrix, polymer or microcapsule; (iv) cross-linking between molecules [6].

The transducer varies depending on the measured parameter; electrochemical, optical, mass and thermal signals are the most common [7]. The measured parameters may be converted into an electrical signal, depending on the type and application of the biosensor. The biosensor advantages are simplicity, small size, robustness, low cost, ability to generate reliable and continuous information, high selectivity and sensitivity, depending on the biomediator type and immobilization methods. This innovative technology represents a valid support to other efficient analytical methods (HPLC, or GC-MS etc.), and finds for instance useful applications in pre-screening analyses.

Biosensors have various application fields: 1) medical applications e.g. glucose monitoring in diabetes patients [8] and other medical health related targets [9] ; 2) environmental applications, e.g. detection of pesticides and river water contaminants [10]; 3) remote sensing of airborne bacteria, e.g. in counter-bioterrorist activities [11]; 4) detection of pathogens [12] 5)determination of toxic levels of substances before and after bioremediation, and of drug residues in food, such as antibiotics and growth promoters, particularly meat and honey [13], 6) analysis of food quality (e.g. phenols in wine, tea and oil) [14].

1.1.1 Transducer System

The current concept of biosensor date back to 1962 thanks to Leland C. Clarke Jr and his collaborators work [15] proposing an enzymes us biomediator immobilized on a sensor using an electrochemical measurement. The electrochemical biosensors could be divided into three main classes conductimetric, potenziometric, amperometric ones.

1.1.1.1 Electrochemical Biosensors

1.1.1.1.1 Conductimetric biosensors

The conductimetric principle of measurement is widely applicable to chemical systems, because many chemical reactions produce or consume ionic species and thereby alter the overall electrical conductivity of the solution, its resistance being determined by migration of all ions that are present. The principle of operation of a conductimetric biosensor involves the application of an electric field across a pair of microelectrodes surrounded by an electrolyte or a buffered solution containing an enzyme immobilized on a sensor and the species to be detected. An electric field is generated by a sinusoidal voltage waveform across the electrode to minimize or to eliminate the undesirable electric process and to overcome the problems related to temperature variation in the single cell device. An example of conductimetric biosensors is the “urea biosensor”, where the urease enzyme

is immobilized on a chip to detect urea, it catalyzes the decomposition of urea which produce bicarbonate ions (as show below in Reaction R1.1) increasing the conductivity of tested solution [16].

R 1.1) $NH_2CONH_2 + 3H_2O \xrightarrow{\text{Urease}} 2NH^+_4 + HCO^-_3 + OH^-$

1.1.1.1.2 Potenziometric biosensors

Potentiometric biosensors use an Ion-selective electrode (ISE) to transduce a biological reaction into an electrical signal, the reactions involving the release or absorption of ions that may be utilised by potentiometric biosensors. An immobilized enzyme layer catalyses the biological reaction which generates or absorbs ions, when the reaction involves H+ ions, a pH meter is the ISE used.

The potential that develops across an ion-selective membrane separating two solutions is measured at virtually zero current, meaning high impedance and no interference to the reaction [17].

A biorecognition element is immobilized on the outer surface or captured inside the membrane. In the past the pH glass electrode was used as a physicochemical transducer [18]. The Nernst potential of the pH glass electrode is described by the Nicolsky-Eisenman equation, of which the generalized form for ISE is as follows [19] (Equation E 1.1) :

E 1.1) $$E = E^0 + \frac{RT}{ZaF} ln\left[a_a + \sum_{i=1}^{n} K_{a,i}(a_i)^{Za/Zi} \right]$$

(E potential, R the universal gas constant, T temperature, F Faraday constant, za followed and zi interfering ion valence, *aa* activity of measured and *ai* activity of interfering ion and *Ka,i* is the selectivity coefficient).

Potentiometric measurements involve, exactly non-faradaic electrode processes, with no net current flow, and operate on the principle of an accumulation of charge density at an electrode surface, resulting in the development of a significant potential at that electrode. This potential is proportional to the logarithm of the analyte activity present in the sample and is measured relative to an inert reference electrode, also in contact with the sample. These sensors are mainly based on field effect transistors (FETs) and were first proposed by Peter Bergveld [20] in 1970 as the ion sensitive field-effect transistor (ISFET). Enzyme-sensitive field-effect transistors (ENFETs) can be fabricated from ISFETs by applying a thin overlayer of enzyme- loaded gel on the ion-selective membrane [21]. Three types of potenziometric biosensors are the morest used: glass electrodes for

cations (which normally is a pH electrode) pH electrode with a gas permeable membrane, solid state electrodes.

Different example of potenziometric biosensors are developed, for examples o detect urea, penicillin, glucose [22]. as show below in Reaction R 1.2, R 1.3, R 1.4

Pennicillin

R 1.2) $\text{penicillin} \rightarrow \text{penicilloate} + H^+$

Glucose

R 1.3) $\text{glucose} + O_2 \xrightarrow{\text{GOD}} \text{gluconic acid} + H_2O_2$

(Gluconic acid change pH, the reaction can be monitored by pH measurement)

Urea

R 1.4) $CO(NH_2)_2 + 2H_2O \xrightarrow{\text{urease}} 2NH_2^+ + CO_3^{2-}$

(Urea the first analyte detected by biosensor (Guillbaut and Kuan, 1987. Urea is hydrolysed by ureas)

1.1.1.1.3 Amperometric biosensor

The signal of these biosensors is generated by the electron exchange between the biological system in the bioreceptor layer and one electrode. Generally speaking, when using amperometric biosensors, the analyte undergoes or is involved in a redox reaction that can be followed by measuring the current in an electrochemical cell.

The analytes, or the species involved with it via a (bio)chemical reaction, change the oxidation state at one electrode then the electron flux is monitored and is proportional to the amount of the species electrochemically transformed at the electrode [23].

The most common biosensors are based on chronoamperometric experiments, where the current is monitored as a function of time. Usually a single potential step is used for a single experiment.

The analysis of chronoamperometry data is based on the Cottrell equation, which defines the current-time dependence for linear diffusion control (Equation E 1.2):

E 1.2) $i = nFACD^{1/2}\pi^{-1/2}t^{-1/2}$

where:

n = number of electrons transferred/molecule

F= Faraday's constant (96,500 C mol^{-1})

A= electrode area (cm^2)

C= concentration (mol cm^3)

D= diffusion coefficient (cm^2s^{-1})

That indicates that, under this conditions there is a linear relationship between the current and the 1/square root of time. A plot of *i vs. t -1/2* is often referred to as the Cottrell plot [24].

Amperometric biosensors can work in two- or three-electrode configurations. The former case consists of reference and working (containing immobilized biorecognition component) electrodes. The main disadvantage of the two-electrode configuration is a limited control of the potential on the working electrode surface with higher currents, and because of this, the linear range could be shortened. To solve this problem, a third auxiliary electrode is employed. Now voltage is applied between the reference and the working electrodes, and current flows between the working and the auxiliary electrodes. An example of three electrode sensors is Figure 1.2 [25]:

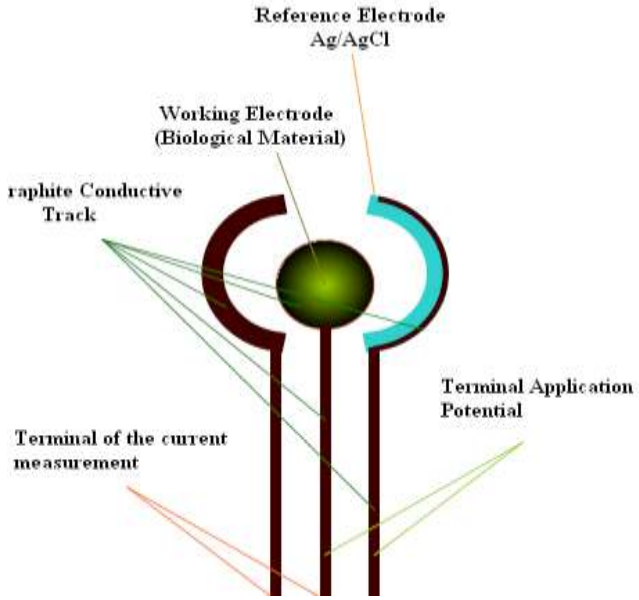

Figure 1.2 Principal Features of Screen Printed Electrode (SPE)

The amperometric biosensors are among the most common biosensors studied both in the past and today, using different types of biological material (enzymes, cells, tissues, proteins, antibodies, nucleic acids) and analytes for clinical use, to detect infection-marker antibodies, acetylcholine, biological oxygen demand, as well as other electrode-attached mediators or to determine simple molecule analytes, such as glutathione, L-alanine and pyruvate, lactate, and cholesterol [26], or for

food analysis such as lactate, citrate, glutamate, ethanol, ecc. [27], and for environmental analysis to detect toxic substance us pesticide (in the water samples), different type of phenols, surfactants, antibiotics, toxins etc. [28][29].

1.1.1.1.3.1 Cyclic Voltammetry

Electrolysis, cyclic voltammetry (CV) , amperometry and several other techniques might be described as "active" electrochemical methods because the experimenter drives an electrochemical reaction by incorporating the chemistry into a circuit and then controlling the reaction by circuit parameters such as voltage.

Cyclic voltammetry is one of the techniques which electrochemists employ to investigate electrolysis mechanisms, series of voltages are applied to the electrode and the corresponding current that flows monitored, to identify the specific potential of electrochemical reaction.

In typical cyclic voltammetry, a solution component is electrolyzed (oxidized or reduced) by placing the solution in contact with an electrode surface, and then making that surface sufficiently positive or negative in voltage to force electron transfer. In simple cases, the surface is started at a particular voltage with respect to a reference half-cell such as calomel or Ag/AgCl, the electrode voltage is changed to a higher or lower voltage at a linear rate, and finally, the voltage is changed back to the original value at the same linear rate. When the surface becomes sufficiently negative or positive, a solution species may gain electrons from the surface or transfer electrons to the surface. This results in a measurable current in the electrode circuitry. However, if the solution is not mixed, the concentration of transferring species near the surface drops, and the electrolysis current then falls off. When the voltage cycle is reversed, it is often the case that electron transfer between electrode and chemical species will also be reversed, leading to an "inverse" current peak.

Principles and concepts illustrated by this technique are: 1) quantitation of concentrations; 2) diffusion effects; 3) irreversibility; 4) study of reaction intermediates; 5) identification of electron transfer steps; and 6) relationships to the Nernst equation.[30] [31] [32] [33]

Voltammetric analysis are an important tool to help develop an amperometric biosensor.

1.1.1.2 Other transducer system

1.1.1.2.1 Piezo-electric biosensor

Piezo-electric biosensors are principally based on the measurement of change in resonant frequency of a piezo-electric crystal as a result of mass changes on its surface . These are caused by the interaction of tested species or analytes with a biospecific agent immobilized on the crystal surface

and its resonant frequency changes as molecules adsorb or desorb from the surface of the crystal, obeying the relationships present in E 1.3:

E 1.3) $\Delta f = \frac{Kf^2 \Delta m}{A}$

Where Δf is the change in resonant frequency (Hz), Δm is the change in mass of adsorbed material (g), K is a constant for the particular crystal dependent on such factors as its density and cut, and A is the adsorbing surface area (cm^2).

The frequency of vibration of the oscillating crystal normally decreases when the analyte binds to the receptor coating the surface. Such sensors generally operate by the propagation of acoustoelectric waves, either along the surface of the crystal or through a combination of bulk and surface, and are commonly referred to as surface acoustic (SAW) wave devices [34].

Most common piezoelectric biosensors are immunological biosensor including microgravimetric immunoassays, microbial assays, DNA hybridization, enzyme based detections and gas phase biosensors [35].

1.1.1.2.2 Optical biosensors

In the most commonly used form of an optical biosensor, the transduction process induces a change in the phase, amplitude, polarization, or frequency of the input light in response to the physical or chemical change produced by the biorecognition process Some of the advantages offered by an optical biosensor are selectivity and specificity, remote sensing, isolation from electromagnetic interference, fast, real-time measurements, multiple channels/multi parameters detection, compact design, minimally invasive for in vivo measurements, choice of optical components for biocompatibility, detailed chemical information on analytes, The main components of an optical biosensor are: light source, optical transmission medium (fiber, waveguide, etc.), immobilized biological recognition element (enzymes, antibodies or microbes, cells, protein, ect), optical detection system. The optical biosensors are classified in based at transduction methods (absorption, fluorescence, luminescence), geometry (bioptrode, Surface Plasmon Resonance, Fiber Grating Based Sensors) and Evanescent Wave Fiber Optic Biosensors.

The simplest optical biosensors use absorptions phenomenon to determine changes in the concentration of analytes. Chemiluminescence is same way similar to fluorescence. The difference is that chemiluminescence occurs by exciting molecules with a chemical reaction whereas fluorescence occurs by exciting molecules via light and then reemission of light at a longer wavelength [36].

1.1.2 Immobilization methods in electrochemical biosensors

Biosensors often need that the biological material (enzymes, proteins, cells, tissues, nucleic acids) to perform its activity must be immobilized on the transducer of signal.

The choice of immobilization method depends on many factors, such as the nature of the biological element, the type of transducer, the physicochemical properties of the analyte and the operating conditions in which the biosensor is to function, and overriding all these considerations is necessary for the biological element to exhibit maximum activity in its immobilized microenvironment [37].

Generally there are 4 main immobilization methods: the adsorption, entrapment, covalent bonding and cross-linking immobilization.

The first one can roughly be divided into two others classes: physical adsorption and chemical adsorption. Physical adsorption is weak and occurs mainly via Van der Waals interaction. Chemical adsorption is stronger and involves the formation of covalent bonds. The physical adsorption is mostly used for enzyme immobilization in ZnO-based glucose biosensors.

The entrapment method refers to mixture of the biomaterial with monomer solution and then polymerised to a gel, trapping the biomaterial. However, this method can give rise to barriers to the diffusion of substrate, leading to reaction delay. Besides, loss of bioactivity may occur through pores in the gel. The gels commonly used include polyacrylamide, starch gels, nylon, silastic gels, conducting polymers, alginates etc.

In the covalent immobilization, the bond occurs between a functional group in the biomaterial to the support matrix. Some functional groups which are not essential for the catalytic activity of an enzyme can be covalently bonded to the support matrix. It requires mild conditions under which reactions are performed, such as low temperature, low ionic strength and pH in the physiological range.

In the cross linking method, usually, biomaterial is chemically bonded to solid supports or to another supporting material by a cross-linking agent. It is an useful method to stabilize adsorbed biomaterials. Glutaraldehyde is the mostly used bifunctional agent however the agents can also interfere with enzyme activity, especially at higher concentrations [19][38][39].

1.1.3 Biosensors to detect pesticides

In environmental pollution monitoring, it is becoming a general opinion that chemical analysis by itself does not provide sufficient information to assess the ecological risk of polluted waters and wastewaters. In the European Union, along with more stringent demands for water treatment (Council Directive 91/271/EEC), industrial and urban wastewater effluents shall reach certain limits

of nontoxicity before the effluent can be discharged into the environment. Thus, much effort has been made during the last years to develop and use varius biosensors for toxicity evaluation of water samples [40].

The extensive use of pesticides for agricultural purposes is the cause of their widespread presence in natural waters. Concern about their toxicity and persistence in the environment has led the European Community to set limits on the concentration of pesticides in different environmental waters: The directive 98/83/EC on the quality of water for human consumption has set a limit of 0.1 μg/l for individual pesticides and of 0.5 μg/l for total pesticides.

To meet the demand for faster, sensitive and economic analytic methods to detect the environmental pollutants different biosensors have been developed, for example for the detection of organophosphorous and carbamate pesticides [41][42][43] by acetyl cholinesterase (AChE) and colin oxidase enzymes. Although sensitive, biosensors based on AchE inhibition are not selective (since the AchE is inhibited by neurotoxins, which include organophosphorous pesticides (OPs), carbamate pesticides, and many other compounds) and cannot, therefore, be used for quantitation of either an individual or a class of pesticides. Many others enzymes have been explored to developed biosensors to detect pesticides: the organophosphorous hydrolase (OPH) to detect organophosphate, [44], the tyrosinase and laccase to find phenols [45], diethyldithiocarbamates [46], and hydrazines [47]; Dithiocarbamate fungicides have been measured by their ability to inhibit the enzyme aldehyde dehydrogenase (AlDH) [48].

Photosynthesis inhibition is an interesting indicator that rapidly reflects the toxic effect of certain pollutants. Taking advantage of this feature, some biosensors based on Photosystem II (PSII) have been reported to be able to detect herbicides in the environment [49]. About 30 % of herbicides, including phenylurea, triazine, and phenolic herbicides, inhibit photosynthetic electron flow by blocking the PSII quinone-binding site and thus modify chlorophyll fluorescence [50]. Different amperometric biosensor are developed to detect different kind of herbicides too [51][10]. Heavy metals were also able to inhibit the activity of the PSII biosensor, but their effect is usually found at much higher concentrations than those typical for herbicides.

1.2 Photosynthesis

1.2.1 Higher plants and green algae photosynthesis

In higher plants (and in the green algae) photosynthetic apparatus is represented by chloroplasts, special cell organellae which contain membrane-made closed structures (thylakoids) tightly leant one on the other to form piles, named grana (Figure 1.3).

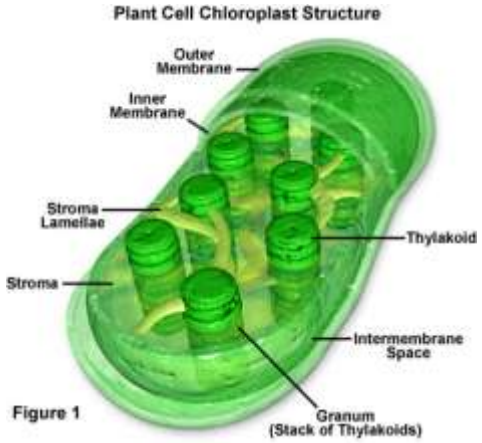

Figure 1.3 A chloroplast. Thylakoids are packed in grana (is a stack of thylakoids folded on top of one another) or not. The stroma is the fluid space within the chloroplast. The lumen is the fluid filled space within a thylakoid.

Within thylakoid membranes the chlorophyll is associated in complexes containing up to 250 molecules, among which only very few are directly involved in the photochemical reactions producing ATP, most of them instead serving only as light-harvesting antennae. The function of these latter is just to collect and funnel light to the already mentioned [52][53] [54] [55] [56] .

Such functional aggregates of a specific photosynthetic protein - as Photosystem II (PSII) for green plants - together with light harvesting complexes containing many chlorophyll and carotenoids with similar organization in both higher plants and photosynthetic bacteria [57].

The Photosynthetic apparatus is arranged in two photosystems, named Photosystem I (PSI) and II, (PSII, Figure 1.4) present in the thylakoids. They are an ensemble of several proteins and pigment-protein complexes working in concert building up functional units of metabolic importance. The final results of these interactions are: (1) the generation of a transmembrane proton gradient necessary to the ATP synthesis; (2) the production of the reducing power necessary to the NADPH biosynthesis [52] [54].

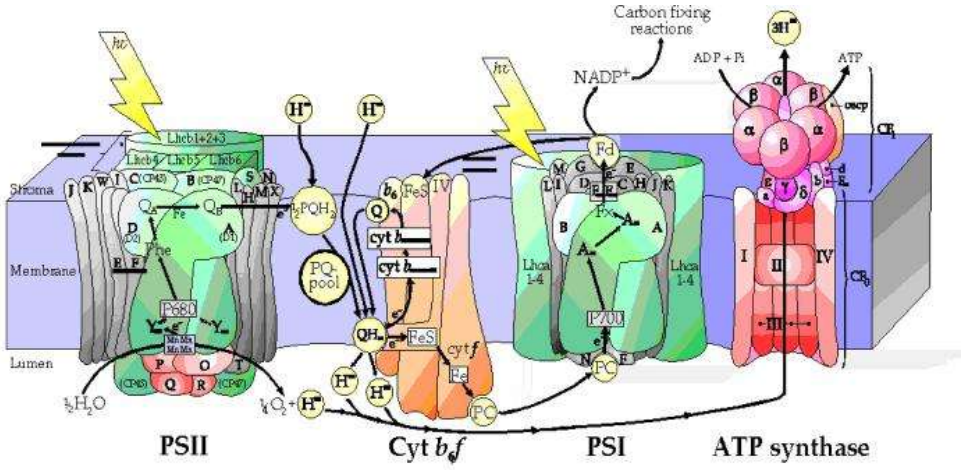

Figure 1.4 The Photosynthetic apparatus is arranged in two photosystems, named Photosystem I (PSI) and II, (PSII) present in the thylokoids

The radiation absorbed by chlorophylls belonging to the light-harvesting complex of PSII is transferred to the pigment P680, made of two chlorophyll molecules arranged in such a way to form an excitonic dimer (the so-called "special pair") and located at the interface between two similar subunits.

Within PSII light is absorbed by chlorophyll-protein harvesting complexes, then it is funnelled to the photochemically active reaction centre, made of D1, D2 and Oxygen Evolving Complex (OEC) subunits (Figure 1.5).

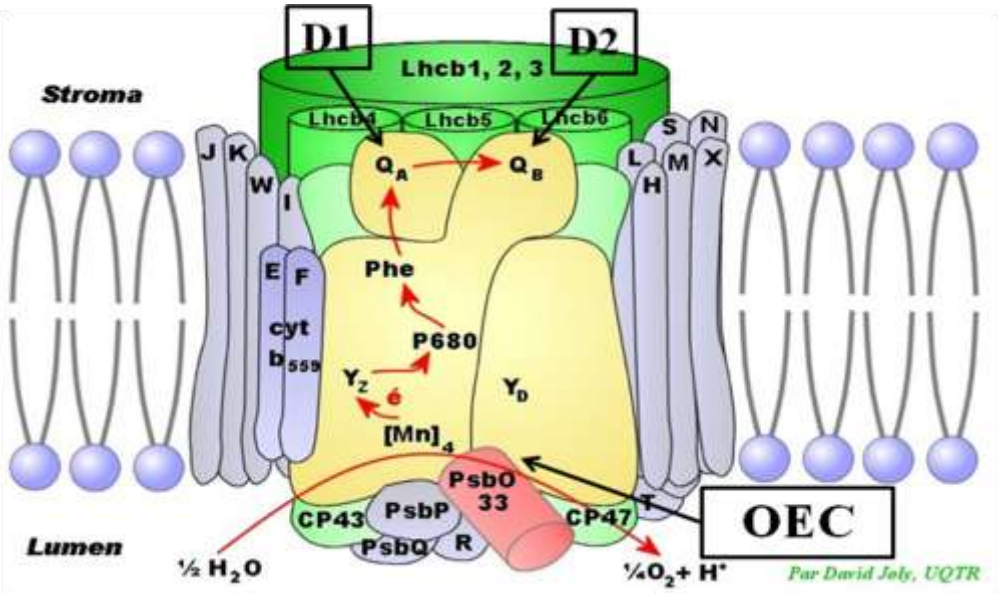

Figure 1.5 Representative PSII scheme, it is possible to see the principal protein D1 and D2, Oxygen Evolving Complex (OEC), Qa and Qb binding site

Here photoexcitation converts a special dimer of Chl *a* molecules (P680, primary electron donor of PSII) , into its oxidized form $P680^{+}$, thus triggering a single electron transfer first to a pheophytin cofactor, then to a plastoquinone molecule, Qa (located in D2) and finally to a second plastoquinone, Qb within D1 (Figure 1.5). Because of the homology in the structure and functions (e.g. for the sensitivity of both Reaction Center and PSII to triazine herbicides), the whole PSII is considered the "eukaryotic analogous" of the bacterial photosynthetic Reaction Center (RC) [52], (Figure 1.6) whose properties will be discussed later.

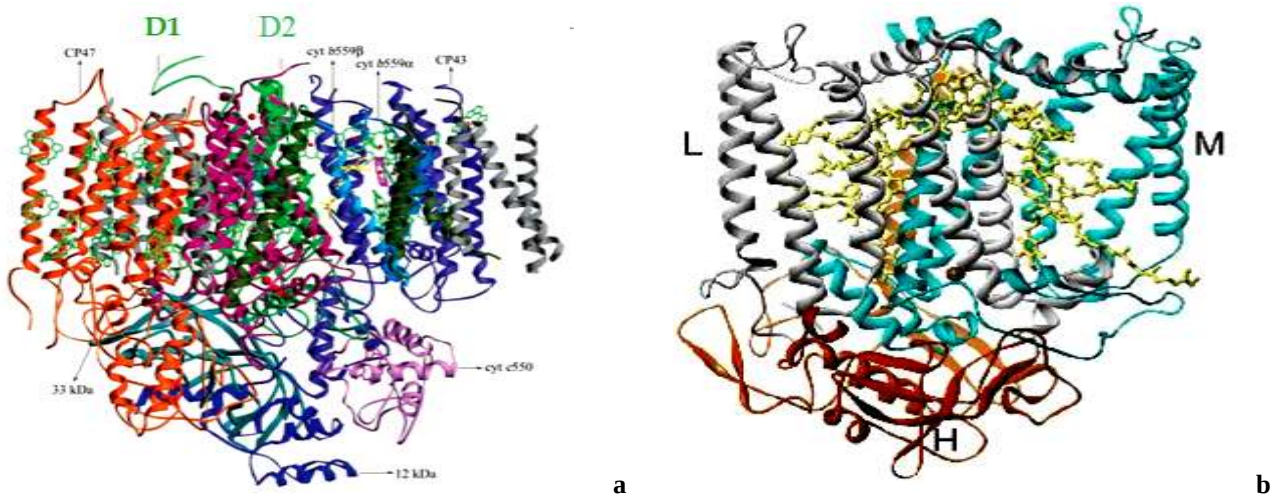

a **b**

Figure 1.6 Homology in the structure between PSII and bacterial photosynthetic Reaction Center (RC)

The photooxided P680 dimer is then reduced by the electrons recovered from the oxidation of water to molecular oxygen operated by a Mn-containing complex bound to the reaction centre (Figure 1.5). Then the global reaction catalyzed by PSII is the light induced electron transfer from water - with the concomitant release of O_2 to the second plastoquinone, together with the production of a transmembrane proton gradient.

The structured model [58] and the analysis of effects on the redox properties of cytochrome (Cyt) b559 induced by PSII herbicides [59] a third plastoquinone Qc was recently found, although its function is not fully clarified it could regular the redox potential in Cyt b559, which is characterized by an unusually high redox potential providing a mechanism of protection of PS II from photoinhibition. A representation of Qc and Qc binding sit is shown in Figure 1.7.

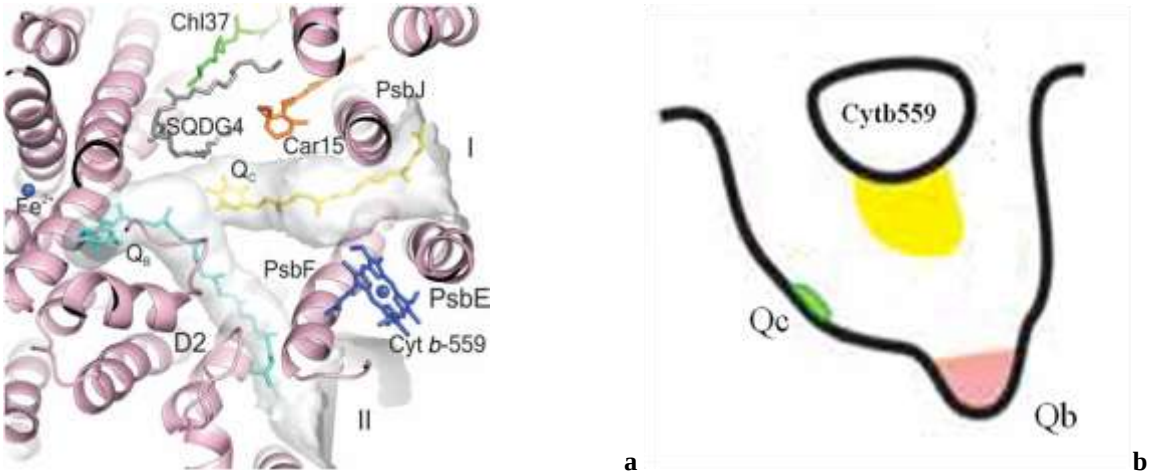

Figure 1.7 Schematic representation of the hypothetical collocation of Qc (a) and Qc binding site (b).

Subsequently electrons coming from PSII arrive to the PSI through the transmembrane cytochrome *bf* complex (cytochrome complex in scheme), that moves protons inside the thylakoid space (the space internal to thylakoid membranes of the grana) when electrons are transferred from PQH_2 to plastocyanine (Pc) (a water soluble protein). At this point the thermodynamic driving force of the electron transfer is definitely exhausted: it is necessary a second photosystem, PSI, to promote a light-induced electron transfer from Pc through the pigment P700 (at the interface between identical subunits of the PSI) and then, through chlorophyll molecules, to ferredoxine (Fd) (a strong reducing agent).

Hence the ferredoxine-$NADP^+$ reductase, a flavoprotein located on the stromal side of the membrane, will catalyze the NADPH synthesis. By this way the connection between PSII and PSI allows the electron transfer from H_2O to NADPH to proceed and, moreover, it leads to the formation of a proton gradient necessary for the ATP synthesis.

The global reaction of the passage through PSII, Cyt bf and PSI follows (R 1.5):

R 1.5) $2NADP + 2H_2O \xrightarrow{\text{LIGHT}} 2NADPH_2 + 2H^+ + O_2$

Alternatively, electrons can be transferred from Fd to PSI through the cytochrome bf complex, instead of going to $NADP^+$: this cyclic photophosphorylation leads to production of the proton gradient without NADPH synthesis (as in bacteria with NADH). This biochemical shunt is active when no $NADP^+$ is available: following this pathway, PSII is not involved in the photosynthetic process and therefore no oxygen production is observed. Subsequently ATP and NADPH so formed

other organic compounds, through the "dark phase", the so-called Calvin-Benson cycle, whose global reaction is [52] (R 1.6):

R 1.6) $CO_2 + 2H_2O + 3ATP + 2NADPH \rightarrow (CHOH) + 3ADp + 3Pi + NADP^+ + H^+$

It is possible summarize the reaction R5 and R6 in with the basic follow equation where CHOH is carbohydrate unit (Reaction R 1.7):

R 1.7) $CO_2 + H_2O \xrightarrow{LIGHT} (CHOH) + O_2$

1.2.2 Purple Bacteria

Purple bacteria are unicellular prokariotes: they are phototrophic since they are able to use solar energy to oxidize reduced substrates, being carbon dioxide the final acceptor of the electrons, they are divided in Thiorhodaceae or Chromatiaceae (purple sulphur bacteria); or Athiorhodaceae or Rhodospirillaceae (purple non-sulphur bacteria) [60] depending on whether they use sulphur compounds as reducing agents for photosynthetic carbon dioxide fixation (water for high plant and green algae). For our purposes, we work with *Rhodobacter sphaeroides* part of Rhodospirillaceae, many of them are facultative anaerobes, but lose most of their photosynthetic pigmented proteins when they are grown aerobically (which may be in the dark or not). In the presence of oxygen, the cells of the Rhodospirillaceae carry out respiration, behaving like eukaryote's mitochondria.

They constitute the largest group of photosynthetic bacteria and account for 8 genera and 30 species identified up to now. To this group belongs, rod-like bacterium provided with flagella.

Purple bacteria carry out a photosynthetic process called anoxygenic, (no produce oxygen). They are able to utilize either the products of the anaerobic metabolism of the sea depths (hydrogen sulfide, hydrogen gas, carbon dioxide) or the product of the anaerobic fermentations and of the partial oxidations taking place in the intermediate layers of the stagnant waters (lakes, pounds, lagoons). For this reason they are able to grow even in the dark, aerobically oxidizing the reduced carbon compounds, even though their optimal oxygen concentration is low. Their native environment is limited to the water layers closer to the surface, at the border between oxygen-containing and oxygen-free waters, where the oxygen concentration is low.

As already specified, the anoxygenic photosynthesis of purple bacteria is different from the oxygenic one of green plants. In prokaryotes there are no chloroplasts and the photosynthetic

pigments are localized just on the plasmic membrane organized in structures deriving from its extensive folding.

R.sphaeroides photosynthetic apparatus is formed by two main integral-membrane enzymes, the Light Harvesting Complex (LH, type I and II), harvesting the electromagnetic radiation, and only one RC, that utilizes the light absorbed (only one compared to the two of the green plants, one for each photosystem) (Figure 1.8).

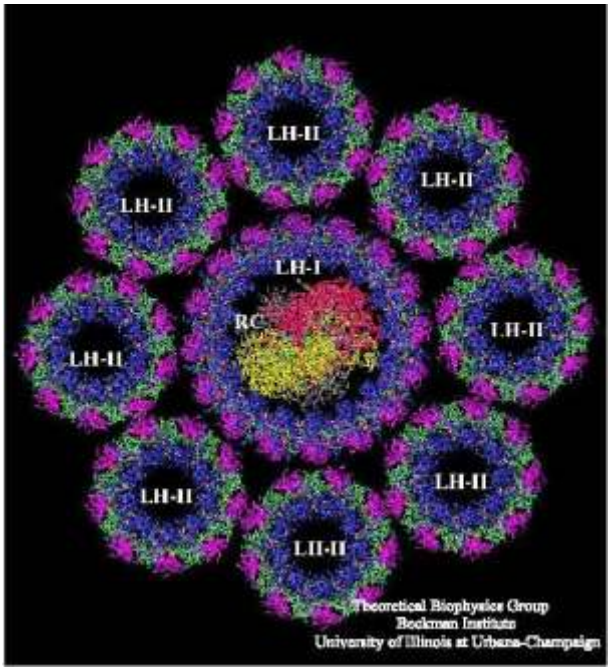

Figure 1.8 LH type I and II harvest the electromagnetic radiation to RC that utilizes the light absorbed to photosynthesis

A single RC molecule is made of up to 25÷30 bacteriochlorophyll molecules, although only very few of them are directly involved in the photochemical reactions leading to the ATP synthesis.

The RC is composed of three subunits termed H (heavy), M (medium) (corresponding to D2 protein of PSII in higher plant and green algae) , and L (light) (corresponding to D1 protein o of PSII in higher plant and green algae) on the basis of their migration properties in sodium dodecyl sulfate (SDS)-polyacrylamide gel electrophoresis (PAGE) (Figure 1.6b and 1.9a).

The three subunits are present in a 1:1:1 stoichiometry and contain a Bchl a dimer, two monomeric molecules of Bchl a, two monomeric molecules of bacteriopheophytin a, two ubiquinones Qa and Qb, and a nonheme iron [61] (Figure 1.9b). The binding sites for each quinones were present in H and L protein respectively, as the high plant homologues protein D2, D1(Figure 1.6).

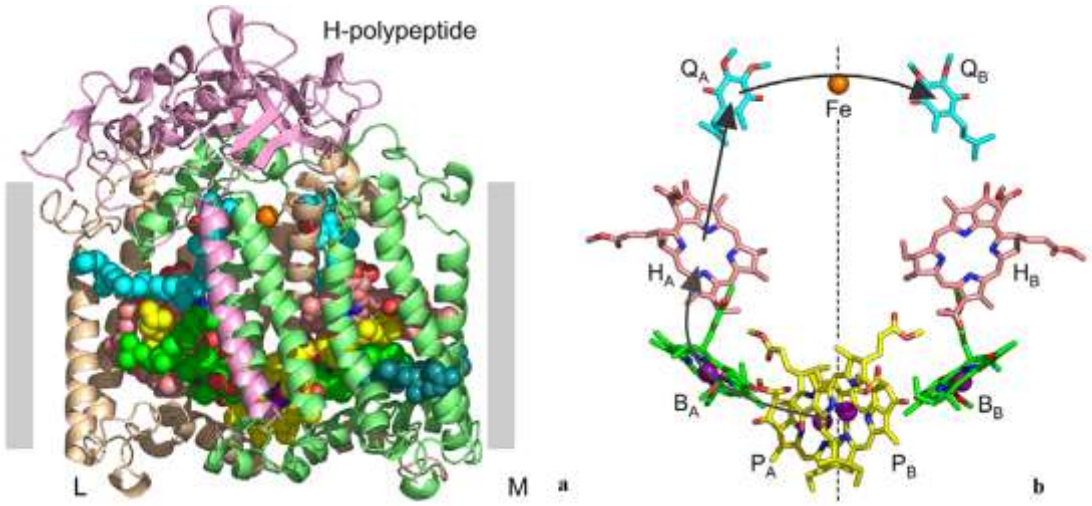

Figure 1.9 Structure, mechanism and environment of the *R. sphaeroides* RC. (a) The ten cofactors (spheres) are held in place by a scaffold consisting of L and M polypeptides (ribbons). The H-polypeptide has a single TM helix and a cytoplasmic domain. (b) The BChl, BPhe and ubiquinone cofactors.

Purple bacteria do not produce oxygen and do not use water us external electron donor as explained in the reaction R 1.8 where H_2A and A are the external not specific electron donor in according to the available environmental sources. and to the bacterial type. They can be H_2S and S, or H_2 and CHOH it is the carbonit unit) [62]:

R 1.8) $CO_2 + 2H_2A \xrightarrow{\text{LIGHT}} (CHOH) + 2A + O_2$

The Calvin-Benson cycle, utilizing as reducing agents the NADPH or the NADH coenzyme, besides ATP for energetic needs. The NAD^+ reduction to NADH is performed by the NADH dehydrogenase, operating in an opposite direction in relation to that of the cell respiration: the electrons are extracted from the reduced substrates (H_2A) and that represents the conclusions of the light-dependent part of the bacterial photosynthesis, whose complete reaction – in analogy with the equation R 1.9:

R 1.9) $2NAD^+ + 2H_2A \xrightarrow{\text{LIGHT}} 2NADH_2 + 2A + 2H^+$

The light, harvested by LHCI and LHCII, is funnelled to the RC primary photoinduced electron donor (a bacteriochlorophyll dimer), the RC being another of the three complexes. An electron is therefore raised to an energy level suitable to initiate the electron transfer that, through a series of intermediate acceptors, reaches the final acceptor, usually an ubiquinone molecule. Once fully reduced - i.e.: after taking up two electrons as well as two protons from the cell cytoplasm - the

ubiquinol can leave the RC exchanging with a pool of ubiquinone molecules present in the core of the bacterial membrane (Figure 1.10). The reduction of a single ubiquinone molecule requires, therefore, the absorption of two photons by the RC. This means that at the end of the first turn of the photocycle (leading to the formation of a semiquinone radical), the photooxidized bacteriochlorophyll dimer needs to be reduced.. To close the cycle the cytochrome (cyt) bc1 (the last of the three complexes of the photosystem) oxidizes the ubiquinol just arrived from the membrane quinone pool, with the concomitant release of two protons in the periplasm. As a consequence, results of the absorption of two photons is the traslocation of two protons from the cytoplasmic to the periplasmic side of the bacterial cell. Within this perspective, RC can be assimilated to a light driven pump producing the proton gradient required for the right function of both the ATP synthase - the third photosynthetic membrane complex – and the NAD^+- reductase.

Purple bacteria are also able to vary their proportions of light-harvesting to RC complexes in response to changes in the level of light [62] - as it happens for the extent of membrane invagination. In the high-light conditions, moreover, higher amounts of quinone (electron acceptor), of cyt bc1 complex (electron transporter), and of ATPase particles have been found, always in relation to RC proteins: in these conditions the arrangement of the antenna complexes in the membranes is modified, smaller units would be more efficient and the RC turns over more often, allowing faster electron transfer within the photosystem. Size and efficiency of the photosystem are regulated by light intensity, the synthesis of the whole photosynthetic apparatus has been found to be controlled by oxygen at a transcriptional level [62].

A schematic representation of Rhodobacter photosynthesis is shown in Figure 1.10.

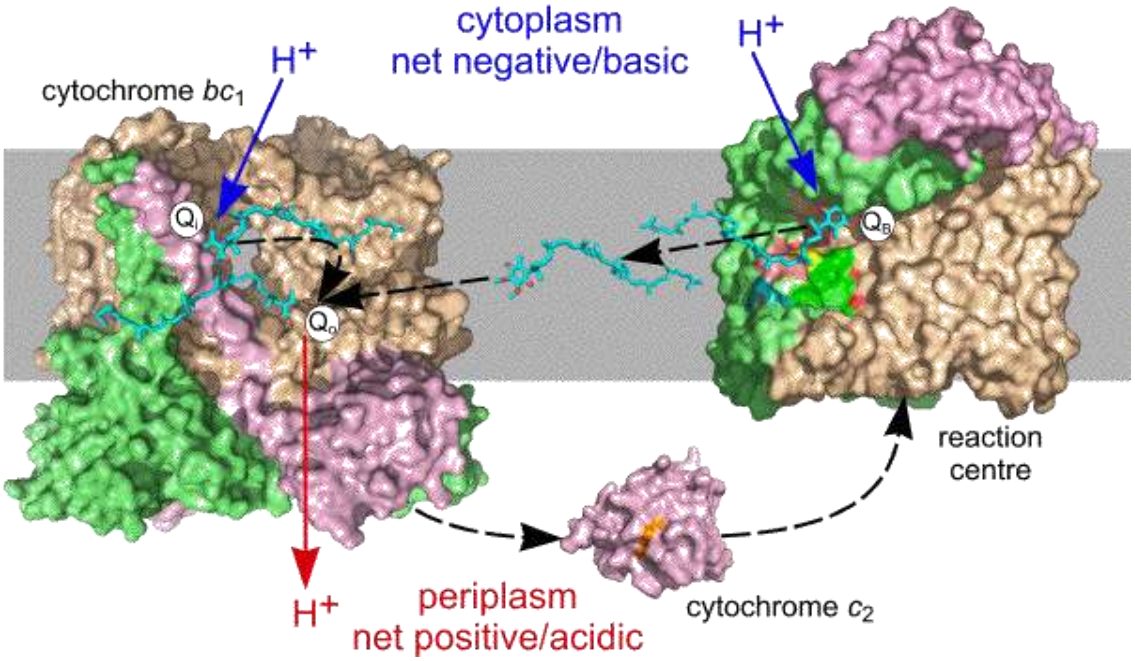

Figure 1.10: A schematic representation of cyclic-anoxogenic photosynthesis in *R.sphaeroides*

1.3 Photosynthesis biosensor

In recent years concern for drinking water contamination from industrial and agricultural activities has been rising. Consequently, the need for efficient environmental monitoring strategies became urgent. Monitoring devices have to be rapid, easy to operate, and offer low-cost screening procedures possibly applicable on field.

Even low levels of chemicals may cause strong adverse effects on humans, animals, plants and ecosystems.

Herbicides represent a specific class of pesticides employed in the chemical weeding of various crops. The most commonly used in agriculture (about 30 % of the total) are urea derivatives, triazines, diazines and phenols, acting as inhibitors of photosynthesis [63]. In particular, triazines (atrazine, simazine, terbuthylazine etc.) and ureas (linuron, diuron, etc.) from agricultural runoff can contaminate soils, surface and ground waters with severe toxic effects on humans. Moreover, their widespread use may lead to the natural selection of resistant weed species, in turn requiring higher amounts of herbicides in agriculture. Although the use of atrazine and simazine was banned by law in European Union (EU) in 2004 (after a 12-year review period) [63][64]. their persistence in soil and water is many years- long due to the combination of a very low water solubility and difficulties in being metabolized by microorganisms [65].

Moreover, up to date the European Commission has published a priority list of substances, which is setting up a framework for an action in the field of water policy, in order to preserve, protect and improve the quality of environment (2455/2001/EC Water Framework Directive, WFD). According to WFD, an efficient monitoring of priority pollutants is required, together with assessment of biological/ecological quality elements and measurement of physic-chemical parameters. Since then developing biosensor devices for rapid and accurate prescreening and determination of pesticides in water samples became a crucial objective.

Biosensors are designed to match many scientific, medical, industrial and environmental applications due to the advantage of being generally sensitive, rapid, economical and easy-to-handle for on-field measurements (see above) [66], from 1980s onwards many biosensors focused on photosynthetic processes. Representing the heart of photosynthesis, the Photosystem II (PSII) multi-subunit pigment protein complex is embedded within thylakoidal membranes of plants, algae and cyanobacteria. PSII. Light triggers an intraprotein electron transfer chain proceeding also beyond PSII, up to other photosynthetic proteins such as cytochrome *bf*, plastocyanine and Photosystem I (PSI), until the final double electron reduction of $NADP^+$ to NADPH.

Among several advantages, the usefulness of using biosensors based on photosynthetic particles containing PSII is due to the fact that the D1 protein specifically recognizes and binds herbicide molecules within its so called Qb binding site, where they act as inhibitors of the photosynthetic activity in competition with a native plastoquinone cofactor. Depending on their concentration, herbicides partially or fully block the electron transfer between Qa and Qb quinones, leading to interruption of water photolysis and oxygen production (Hill reaction) [67] the inhibitor's effect depends on the structural conformation of the Qb site, in turn depending on the arrangement of the D1/D2 subunits. This binding property has paved the way for the use of PSII as an analytical tool for the design and detection of herbicides [68] [69]. Biosensors based on photosynthetic particles containing eukaryotic PSII complexes, as well as their prokaryotic precursors bacterial Reaction Centre (RC) proteins, from whole cells to photosynthetic organelles and isolated proteins of various organisms (algae, cyanobacteria, purple bacteria and green plants such as spinach) have been reported to be able to detect triazine, diazine, urea and phenol pesticides in water samples, both by optical [70][71][72][73], and electrochemical transduction systems [10][74][75][76][77]. Although a variety of whole-cell-based bacterial sensors have been applied in environmental assays for pollutant monitoring, the molecular details of RCs bacterial compared to PSII D1/D2 subunits (analogous in eukaryotes, with very high sequence homology) make RCs biosensors generally less sensitive to herbicides in comparison to algal and cyanobacterial basel devices [72][73]. It has been

shown that photosynthetic organelles such as thylakoidal membranes (TMs) from green plants [10][67][70], have the feature of selectively recognizing herbicides and remaining active once extracted from their native organism. Nevertheless, features such as stability and analytical sensitivity toward pesticides of TMs-based biosensors, very similar to those of whole algal cells biodevices, together with time-wasting extractions of organelles, have not encouraged their diffusion as potential commercial instruments [10] [78].

1.4 Aim and develop of PhD project

An innovative amperometric biosensor equipped with flow injection system was designed and realised for the detection of pesticides in water samples. It relies on the well-known ability, exhibited by the photosynthetic PSII protein complexes of selectively binding some classes of pesticide compounds such as triazine and ureic herbicides, within the so-called quinone Qb site of PSII. Therefore there is a competition between the native PSII cofactor of the Qb site, a quinone, and the added herbicide molecules (see above)

The aim of this PhD project, within the European Project "Bio-sensor for Effective Environmental Protection and Commercialization - Enhanced" (BEEP-C-EN), is to enhance the sensitivity and the stability of the photosynthetic-based biosensors to identify different herbicides classes and subclasses in the environment and agrofood. In this project two different photosynthetic microorganisms will be used: a green algae (*Chlamydomonas reinhardtii*) and a purple bacterium (*Rhodobacter sphaeroides*). These microorganisms were chosen for the sensitivity towards herbicies (*C. reinhardtii*) [10] [72] [79] and stability (*R. sphaeroides*) [73] [80] of their reaction centres.

Two parallel approaches were undertaken: 1)developing a new amperometric biosensor using whole cell algae as biosensing element, and 2) a genetic engineering to realize a Reaction Center chimera protein as a new biomediator potentially joining the sensitivity feature of the green alga plus the stability feature of the purple bacterium.

1.4.1 Development of biosensor whole cell based C. reinhardtii

Although thylakoid membranes extracted from spinach leaves and suitably immobilized over electrodes have been revealed to be quite stable (half-life of ~9 h), reusable and very sensitive to herbicides (limit of detection of ~ $1*10^{-8}$ M with most common triazine and urea compounds) we showin this PhD thesis that similar and even better results may be reached by means of algal cells

immobilized over cheap screen-printed electrodes (SPEs). Compared to thylakoid membranes, algal cells present the strong advantage of requiring no time-consuming extraction from photosynthetic organisms except a simple cell concentration by centrifuge nor the use of electrochemical mediators such as Tetramethyl-p-benzoquinone (duroquinone) or 2,6-dichlorophenol-indophenol (dichlorindolphenol) for amperometric measurements[10].

We selected as most versatile photosynthetic biomediator for our amperometric measurements were *Chlamydomonas reinhardtii* algae cells.

On the basis of recent literature [81] [82] [83] [84] [85], giving priority to easy and biocompatible (i.e. compatible to algal biomediator) immobilization procedures, we decided to adopt and compare only two simple techniques among those above mentioned: (a) coating of algae cells with a Nafion® (Figure 1.11a) membrane and (b) physical gelation of alginate (Figure 1.11b), entrapping algae cells.

Nafion® , that is a sulfonated tetrafluoroethylene based fluoropolymer-copolymer discovered in the late 1960s by Walther Grot of DuPon [86]. In biosensor field, this polymer was often used to immobilize enzymes, nucleic-acids, and other macromolecules [87] [88], but it was never used to immobilize photosynthetic whole cell algae.

Another of the most promising encapsulation material, already used for algae immobilisation, is the alginate hydrogel [78]. Alginates, extracted from brown seaweeds, are linear polysaccharide copolymers of (1-4)-covalently linked β-D-mannuronate and α-L-guluronate

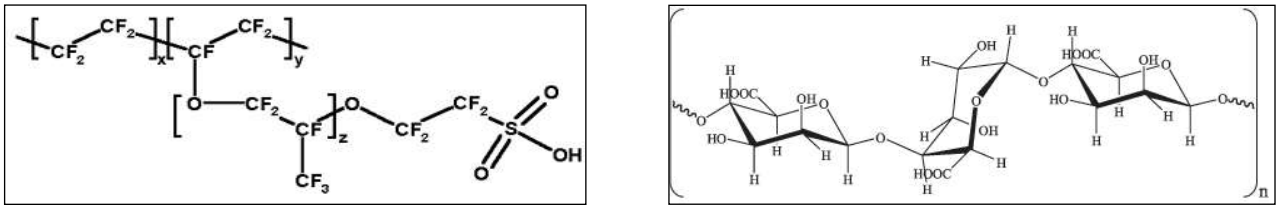

Figure 1.11 (a) Nafion polymer repeating and (b) repeating unit of a common alginate copolymer

monomer residues arranged in different sequences (Figure1.11b). Due to their abundance, lack of toxicity and compatibility with biological systems, alginates are widely used for immobilization procedures [89] [90] [91]. Gelation of alginate is achieved by an ion exchange between sodium from the guloronic acid salts and divalent cations such as Ca^{2+}. Unique properties of alginates are: (a) the possibility of exploiting a room temperature gelation/encapsulation process; (b) a relatively inert aqueous environment within gels; (c) high gel porosity, allowing high diffusion rates for macromolecules. These properties have enabled them to be used as matrices for the entrapment of several proteins.

With these two different immobilization techniques, a biomediator to detect pesticides was developed optimizing the experimental condition to enhance its stability and sensitivity.

1.4.2 Development of Chimera RC Protein

The first experimental approach to create a Chimeric RC was to check the feasibility of the *"L-D1 loop"* by bioinformatic study with the support Prof. Fabio Polticelli of the Computational Biochemistry Lab, University of Roma3. After the bionformatic study , I produced the Chimera in the laboratory of Biochemistry School, Medical Science of University of Bristol under the supervision of Mike R. Jones. The Chimera was created, and further will be tested as biomediator to develop a new biosensor for detection of low concentration of pesticides able to control the limits imposed in the European Country.

2.Experimental Section

2.1 Development of biosensor based on whole cells of Chlamydomonas reinhardtii

2.1.1 Chlamydomonas reinhardtii growth

C. reinhardtii is a soil organism, it can be grown in laboratory either in liquid culture or on agar in simple mineral salts, and many of the recipes proposed for algae are in general sufficent for its culture.

C. reinhardtii cultures, all strains, IL (intron less) [92] F274Y(Phenylalanine in position 274 was substituted with a Tyrosine), were grown in liquid Tris–Acetate-Phosphate (TAP) medium pH 7.0÷7.2 in 250 ml flasks, at 50 µmol/m^2s light intensity, 25°C temperature and 150 rpm stirring. [78]. When required, this medium was solidified with 1.5 % w/v agar to prepare Petri dishes to have "solid" culture (Figure 2.1b), able to store the algae for about a month. After this period usually the dishes need to be plated again. The plate is useful to produce the liquid culture: a small algae quantity is taken from the dish with a sterile handle and inserted in a Erlenmeyer flask containing the medium (Figure 2.1a) and grown in agitation as above described.


a


b

Figure 2.1 Example of the liquid (a) and solid algae culture (b)

TAP medium [93] is well buffered and relatively low in phosphate, making it the best medium for 32P labeling and for studies requiring optical clarity of agar, but it is the most expensive of the usual media to prepare. TAP medium contains 17.4 mM acetate as originally formulated. A

minimal medium can be made by omitting acetic acid and titrating with HCl to pH 7.0. In addiction of TAP the "trace elements" (as EDTA, citrate, iron salts etc.) are added, asthe most used trace elements developed by Hutner et al. (1950) [94]. It is possible to see the production in Protocol Section, Protocol 1.

2.1.2 Chlamydomonas reinhardtii characterization

Before immobilization, algae cells withdrawn from culture flasks within their early, mid-exponential growth phase (0.4÷0.6 absorbance at 750 nm) were always characterized in terms of chlorophyll content, cell density and fluorescence yield to ensure reproducible procedures on viable cells.

2.1.2.1 Chlorophyll content.

In according with Porra et al. (1989) [95] the total chlorophyll concentration was calculated: 1 ml of culture was centrifuged at 2000 g for 2 min (Heraeus Biofuge Pico tabletop centrifuge, Kendro, Newport Pagnell, UK). 800 µl of supernatant were discarded and substituted by 800 µl of pure acetone (Carlo Erba, HPLC grade, 99.9 % minimum purity), then the resulting mixture was vortexed for 2 min and centrifuged for 4 min at 13800 g to eliminate the cell starch present as pellet. The chlorophyll content in the supernatant, referred to 1 ml of original culture (µg/ml), was determined spectrophotometrically at 652 nm against 80 % V/V acetone/water, according to the formula $(Abs_{652nm} \times 1000)/34.5$ [96]. Usually values as 10÷15 µg/ml were obtained.

2.1.2.2 Cell density.

When cultures showed Abs750= 0.4÷0.6 [97], the cells were daily counted with a Bio-Rad TC-10 automated cell counter (Hemel Hempstead, UK) providing an average cell density of $(8\pm2)*10^5$ cells/ml.

2.1 2.3 Fluorescence yield.

The cell viability was evaluated also by measuring the chlorophyll fluorescence induction curves with a Plant Efficiency Analyzer instrument (PEA, Hansatech Instr. Ltd, Kings Lynn, Norfolk, UK) on 5 ml algal culture samples suitably diluted (OD_{750}~ 1) after 10 min of dark-adaptation. The excitation light, a 5 s saturating pulse (600 W/ m^2), was provided by an array of six red light emitting diodes (LEDs with maximum emission at 650 nm) focused on the sample surface. As

indicator of the cell photosynthetic performance the maximum quantum yield of PSII photochemical reaction, $F_v/F_m = (F_m-F_0)/F_m$, was used, where F_0 and F_m indicate the minimum (50 µs after the onset of the excitation light) and Fm fluorescence intensities, respectively. The variable fluorescence, F_v, is calculated as F_m-F_0 and represents the fraction of photosynthetically active PSII [98].

2.1.2 Algae cells Nafion® immobilization on screen-printed electrodes

C. reinhardtii cells were concentrated by 2 minutes centrifugation at 15400 x *g* and the pellet was washed for 2 times with immobilization buffers (2 or 3, respectively composed by Tricine 20mM-NaOH pH 7.2, Sucrose 70mM, NaCl 50mM, $MgCl_2$ 5mM, Ac-K 2mM, and Tricine 20mM-NaOH pH 7.2, Sucrose 70mM, NaCl 10mM, $MgCl_2$ 5mM, Ac-K 2mM) by 2 minutes centrifugation at 15400 x *g*. The suspension of cells obtained was spotted on the SPE (WE) and left at 4°C in the dry box for few minutes until it were dried. After that, 1% Nafion® solution (prepared in immobilization buffer) was spotted onto the biologic material, and dried following the same procedure mentioned before. On each SPE, 224500 cells were immobilized.

2.1.3 Algae cells Alginate immobilization on screen-printed electrodes

An aliquot of *C. reinhardtii* culture in its exponential phase growth (usually within 10÷18 ml and characterized as above reported), corresponding to ~$1.2*10^7$ cells was collected and centrifuged at 2000 x g for 5 min at 15°C with a refrigerated ALC PK121R centrifuge (UK). : the withdrawal operation has been standardized also on the basis of culture Abs_{750} values, with similar results. Withdrawals from cell cultures standardized on the basis of 750 nm absorbance provided the same results [6]

After washing the supernatant was discarded, while the pellet was resuspended with Tricine-NaOH 50 mM pH 7.2 to a final volume of 50 µl, then mixed with 100 µl of 2 % w/V sodium alginate solution in the same buffer, obtaining 150 µl of viscous algae/alginate suspension. 5 µl of the suspension (containing ~$4*10^5$ cells, see Results) were dropped over a Multi-Walled Carbon Nanotube (CNT) working electrode surface (diameter 4.0 mm) of a commercial Screen-Printed Electrode (SPE) (DRP-110CNT, DropSens, Oviedo, Spain, counter and reference electrodes were made of CNT and Ag/AgCl respectively). Then the CNT-SPE (Figure 2.3c) with spotted material (*biomediator*) was immersed for 20 minutes in Tricine-NaOH 50 mM, $CaCl_2$ 200 mM (Gelation buffer) prior to use, in order to obtain a physical gelation of the alginate polysaccharide and

consequent entrapment of the biomediator on the working electrode. A single preparation of 150 µl suspension provided over 20 SPEs bearing the immobilised biomediator (hereafter referred also as s*creen-printed biosensors*, SPE-Chlamy) took ~ 40 min including gelation time.

2.1.4 Biosensor instrument setup

The whole measuring setup was made of 3 components: (1) An electro-mechanical device equipped with suitable software (AMPBIO-SPE instrument developed by Biosensor s.r.l., Rome, Italy) coupled to a peristaltic pump [99] and a potentiostat (PG581 model, Uniscan Instruments Ltd, Buxton, UK) (Figure 2.2). (2) A disposable screen-printed cell with classical three electrodes design: screen-printed CNTs as working electrode, Ag/AgCl as reference electrode and an auxiliary CNTs electrode. (3) (Figure 1.2 and 2.3) An immobilized photosynthetic material (unicellular algae) responsible of the target analyte recognition. The AMPBIO-SPE is a portable instrument specifically designed for electrochemical measurements on biological samples immobilized on disposable SPEs suitably connected to the potentiostat.

Voltammetric and amperometric measurements on SPE whit the immobilized algae (SPEs-Chlamy) were carried out using the above mentioned apparatus. For this purpose SPEs-Chlamy were easily inserted upside down through a slit into a leakproof flow chamber made of Delrin® (polyoxyethylene), 30 mm wide in diameter and 25mm high (Figure 2.2 bc). Two red LEDs (λ= 650nm, 325 µmol/m^2s^1 total light intensity) positioned below the transparent bottom surface of the cell stimulate the photosynthetic activity of the biomediator during electrochemical measurements. Amperometric tests were carried out in dynamic mode with a suitable buffer solution flowing at rate of 0.1 ml/min through the measurement chamber by means of a peristaltic pump equipped with silicone (Masterflex®) tubes, (lying downstream from the chamber and working in aspiration mode). The output tube from the measurement buffer solution container and upstream from the chamber instead was made of chemically inert polytetrafluoroethylene (Teflon). The whole apparatus was equipped also with electronic control board for data read-out, processing and storage. Programmable parameters were LED intensity and time of illumination (light/dark sequence), flow rate, and other than specific electrochemical parameters. Keyboard and display can be used to set the parameters, while a USB connection allows data transfer to PC.

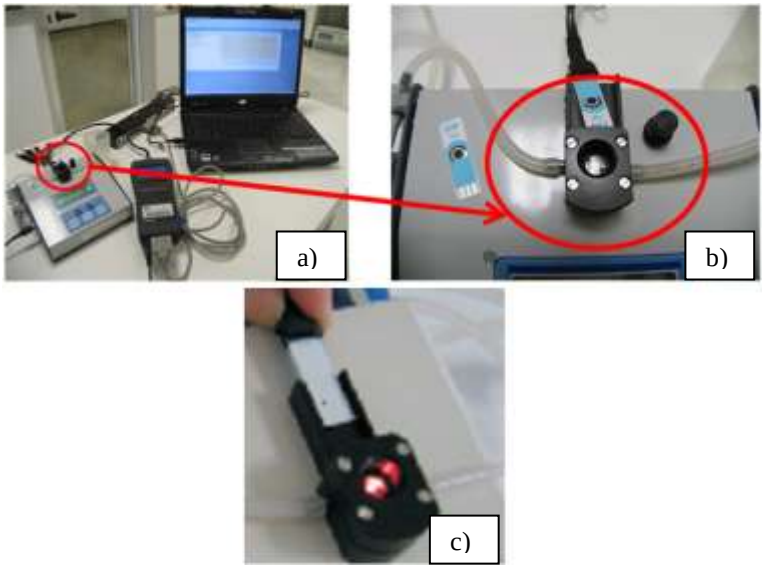

Figure 2.2 a) Biosensor Instrument is shown with all its key stakeholders: of a potentiostat PG581 (Uniscan Instrument Ltd) (a) the a peristaltic pump into a 70µl chamber containing on the button two red leds (650nm, 1500mcd) (b)(c). In c, a particular of the cell and the right positioning of the SPE-Chlamy.

2.1.5 Amperometric Measure

2.1.5.1 Electrode Choosing

Different screen printed electrodes (SPEs) with different working electrode (WE; graphite, graphite nanotube, gold Figure 2.4) were used and tested.

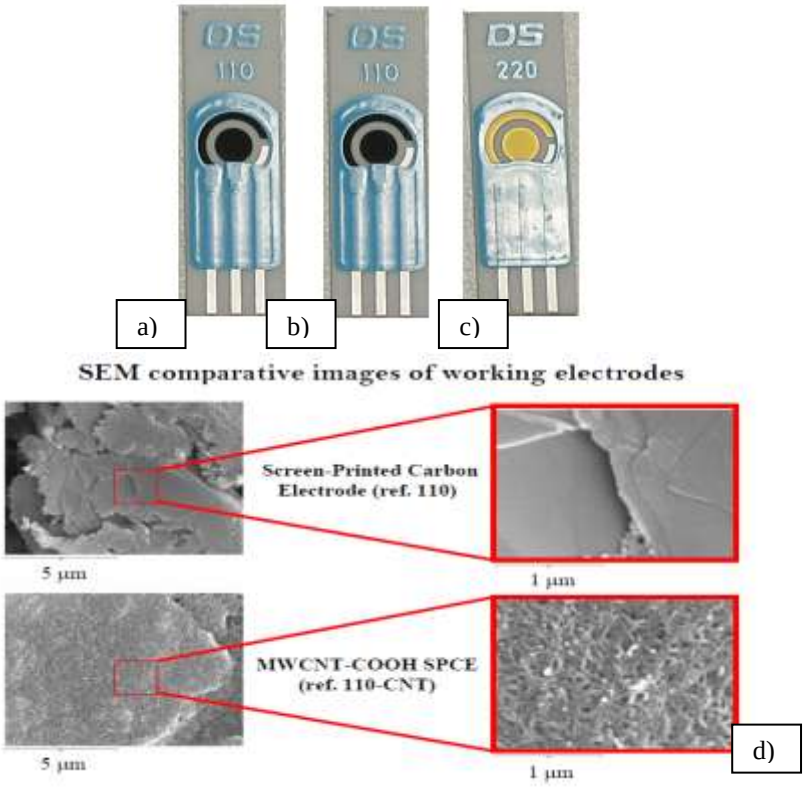

Figure 2.3 - Example of Screen Printed Electrode: (a)carbon SPE, (b) carbon nano-tube one (CNT, the difference between a and b working surface composition is illustrated in Figure d by SEM analysis, http://www.dropsens.com/) and (c) gold one

These WE were purchased from by our partner of the European project Dropsens (http://www.dropsens.com, Oviedo Asturias, Spain) .With the cyclic voltammetry (CV) the best electrode usable at our work potential (-0.7V) [81][82] (Figure 2.4) was chosen.

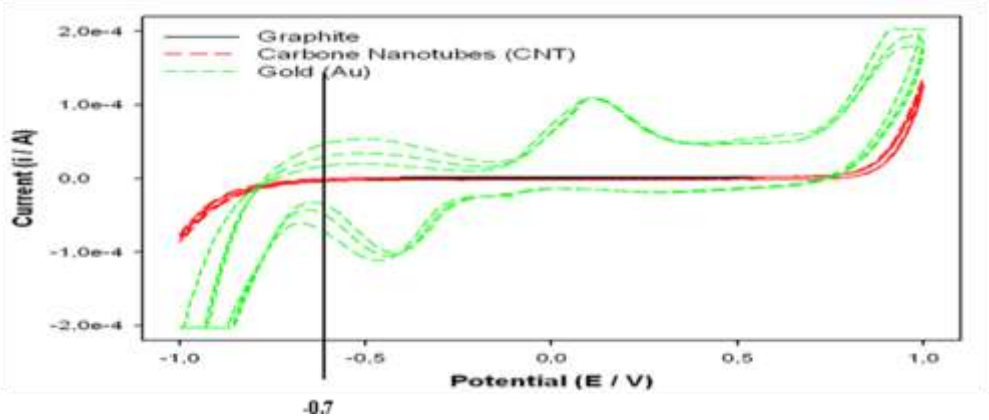

Figure 2.4- Cyclic Voltammetry comparison of three different SPEs, shows the carbon-nanotubes is the most suitable on the biomediator work potential (-0.7V)

2.1.5.2 Setting of Electrochemical Measures (Nafion® immobilization)

A set of buffers was tested as electrochemical buffer to find out which gave the best and stable signal over time. The buffers used were: buffer 1 composed of Tricine-NaOH pH 7.2 20mM, Sucrose 70mM, NaCl 50 mM, $MgCl_2$ 5mM ; buffer 2 composed of Tricine 20mM, Sucrose 70mM, NaCl 50 mM, $MgCl_2$ 5mM, potassium acetate (Ac-K) 2mM; buffer 3 composed of Tricine 20mM, Sucrose 70mM, NaCl 10 mM, $MgCl_2$ 5mM, Ac-K 2mM; buffer 4 composed of Tricine 20mM, Sucrose 70mM, NaCl 10 mM, $MgCl_2$ 5mM; and buffer 5 composed of Tricine 20mM, Sucrose 70mM, $MgCl_2$ 22mM. Some of these buffers were used as immobilization buffers, or measure buffer or for both purposes. In this initial experiment only the IL strain was tested in different conditions (using different buffers) Herbicides inhibition of electrons transport was verified.

For Chronoamperometry analysis (CA) the potential was set at -0.7 V vs. Ag/AgCl according to Shitanda [82], at this potential the oxygen is reduced.

From two references 1 min light followed by 4 min dark and 15 s light/45 s dark sequences are drawn as staring conditions. Subsequently, in order to allow a longer dark relaxation time, a sequence of 1 min light/5 min dark has been adopted. After that a careful observation of time evolution for amperometric signals under illumination clearly showed that a light interval of only 30 s was enough to reach the maximum height of the peak, the following 30 s being unnecessary.

Consequently for all experiments a sequence of 30 s light/ 5 min dark has been always maintained. It has been verified then that a halved illumination interval did not lead to any decrease in the S/N ratio, sometimes recording instead an increase in S/N.

It is well known that due to components of mass transfer occurring specifically and distinct in static and dynamic measurements, signals and, consequently S/N ratios, registered in static chronoamperometric (CA) measurements conditions usually are lower when compared to that registered in dynamic conditions in the same experimental conditions. Slow flow rates have been chosen for the measurements buffer solution: initially 0.2 ml/min, then 0.1 ml/min revealed to be more satisfactory.

2.1.5.2 Setting of Electrochemical Measures (Alginate immobilization)

2.1.5.2.1 Cyclic voltammetry tests on screen-printed biosensors.

CV tests in both dark and light conditions (2 LEDs, λ= 650nm, 325μmol*$m^{-2}s^{-1}$ total light intensity) were carried out at (25±1)°C in steady-state mode on SPEs-Chlamy inserted in the measurement chamber and hydrated with 70 μl of measurement buffer solution (Tricine 50mM pH=7.2, $CaCl_2$ 20 mM, $MgCl_2$ 5mM, NaCl 50mM, sucrose 70mM, MBS). The applied potential ranged from -1.0 to + 0.5 V, at 0.02 V/s scan rate, with three consecutive scans (not show) on each SPEs-Chlamy. Further CV experiments were performed at different scan rates (0.01÷0.15 V/s) in order to shed light on the electrochemical reaction dynamics occurring at the working electrode surface (Figure 3.5)

2.1.5.2.2 Chronoamperometry tests on screen-printed biosensors.

CA tests at constant potential, SPEs-Chlamy were kept in the flow cell at -0.7 V vs Ag/AgCl while the MB solution flows through the chamber at 0.1 ml/min rate, (25±1)°C temperature. Also for Alginate immobilization dark/light sequence for CA tests revealed to be 5 min dark/30 s light was optimized. The current peak generated by algae cells upon illumination was in the order of few microampere (μA). The dynamic flow was guaranteed by a peristaltic pump in aspiration mode, while Teflon tubes upstream from the SPEs-Chlamy cell prevented any possible adsorption of buffer components or herbicides on tube walls [100]. However, daily a 25 % V/V ethanol/water solution is used to wash the flow cell and the tubes, then rinsing with abundant distilled water.

2.1.5.2.3 Chronoamperometry tests: storage stability and stability during measurements.

Storage stability tests were performed leaving a wide set of freshly prepared SPEs-Chamy immersed in Tricine 50mM pH=7.2, $CaCl_2$ 20 mM, $MgCl_2$ 5mM, sucrose 70 mM buffer (Storage

Buffer, SB) at (25±2) °C and under environmental room illumination. The current signal of every used SPE-Chlamy was checked at the starting day, obtaining a 5 % maximum variation around the average value. At least two independently prepared SPEs-Chlamy were drawn from storage buffer for CA tests of the residual current peak at precise time intervals, till a maximum of 40 days.
The biosensor stability during measurements was instead evaluated by means of standard CA tests running for many hours (till 24 hrs.) at (25±2)°C under 30 s red light/5 min dark sequences.

2.1.5.2.4 Chronoamperometry tests: evaluation of herbicide inhibition
The detection of pesticides by SPEs-Chlamy is based on the principle that an herbicide solution flowing through the SPEs-Chlamy chamber induces a decrease of the current signal due to inhibition of the photosynthetic electron transfer activity, in a concentration-dependent manner.
Firstly, the time evolution of the current signal in the absence of herbicide (i_0) is recorded, keeping into account a necessary stabilization of the current signal (usually within 5 peaks). i_0 was generally averaged on three stable peaks. Subsequently, a herbicide solution suitably diluted in the measurement buffer was pumped through the flow cell and the residual photosynthetic activity was measured as residual current peak (i_H), after signal stabilization. Each of the two steps of measurements are always concluded within 30 min, giving a maximum total time of one hour. Every experimental test (i.e. every single herbicide concentration test) was always repeated at least three times until signal variations fall below 10 %, however.
Additional inhibition reversibility (known also as *recovery*) tests were instead carried out by removing the herbicide solution once i_0 and i_H were acquired, and by flowing again buffer solution through the SPE-Chlamy sample. By this way, after stabilization a recovered current peak (i_R) was obtained. Also in this case, complete measurements of i_0, i_H and i_R values were repeated at least three times.

2.1.6 Alternative measurements for the evaluation of herbicide inhibition
2.1.6.1 Oxygen Evolution Rate tests
Inhibition of the oxygen evolution rate (OER) by algal culture samples in the presence of herbicides was measured on algal cultures in their early exponential growth phase by a Clark-type oxygen electrode (Chlorolab 2, Hansatech Instr. Ltd, Kings Lynn, Norfolk, UK). The measurements were performed at 24 °C and under continuous stirring on 1 ml cell aliquots containing 15 µg chlorophyll per ml, in the presence of 10 mM $NaHCO_3$ as additional carbon source [101]. The registration of OER was initiated right after the introduction of the herbicide solution in the electrode chamber,

followed for a period of 5 min under saturating radiation (350 µmol/m^2s, provided by an array of red LEDs). The maximum final concentration of methanol in algal samples was always lower than 0.02 % V/V, value not altering the algal performance

2.1.6.2 Fluorescence tests.

The chlorophyll fluorescence induction (already used for the evaluation of the algal viability) was exploited also to study the specific response of the biosensor to herbicides. For this purpose, algal cultures in early exponential growth phase were concentrated up to 15 µg chlorophyll per ml and incubated for 10 min under 50 µmol/m^2s irradiation, at 24 °C temperature and 150 rpm agitation in the presence of the desired herbicide concentration. The maximum final concentration of methanol in algal samples was always lower than 0.02 % V/V, value by itself not altering the algal performance. The herbicide toxicity was evaluated by the inhibition of the electron transport efficiency between PSII primary (Qa) and secondary (Qb) quinone acceptors, represented by the decrease of parameter $1\text{-}V_J$, where $1\text{-}V_J = 1\text{-}((F_{2ms}\text{-}F_0)/(F_m\text{-}F_0))$ [98]. F_{2ms} is the fluorescence level 2 ms after the onset of excitation, the so-called *J* step in the fluorescence induction transient, while F_0 and F_m have been defined above. In the presence of herbicides, the relative variable fluorescence at *J* step (V_J) increase proportionally to the herbicide concentration, revealing the progressive inhibition of the Qa-Qb electron transfer and the accumulation of quinone Qa in the reduced form.

2.2 Chimera Creation

2.2.1 Bioinformatics analysis and future RC genetic manipulation

The possible genetic engineering of biological material could be carry out after bioinformatics feasibility's study in collaboration with Prof. Fabio Polticelli of the Computational Biochemistry Lab, University of Roma3 and Mike R. Jones of School of Biochemistry, Medical Science, University of Bristol.

The primary sequence of the D1 and L proteins was analyzed by BLAST (http://blast.ncbi.nlm.nih.gov/Blast.cgi) (Figure 3.12 Discussion) and the tridimensional modeling was carried out to have the information about the feasibility of the complete substitution of D1 protein (*C.reinhardtii*) with L protein (*R.sphaeroides*) (Figures 3.13 3.14 Discussion) following of procedures described in Rea *et al.* 2009 [102].

The design of the *Chlamydomonas* sequence encoding the aminoacidic Qb binding niche was carried out also by exploiting bioinformatic tools using the *R. sphaeroides* codon usage.

The sequence has been achieved by a PCR procedure and cloned in the pCR2.1® TOP vector between the restriction sites EcoRV and SalI, giving rise to the pCR2.1®Chlamy (Figure 3.16).

2.2.2 Genetic engineering on R. sphaeroides and C. reinhardtii organisms

R. sphaeroides strains were grown on $M22^+$ minimal medium under dark/semiaerobic conditions at 34°C (Protocols section, Protocol 2 [103]).

The pCR2.1®Chlamy vector was amplified in *E. coli* DH5α over night at 37°C and Bacterial DNA was extracted by Wizard® Plus Minipreps DNA Purification System -Promega (Protocols Section, Protocol 4).

After an EcoRV and SalI double digestion, the deriving fragment of 452 bp was cloned into plasmid pUCXB, which is a derivative of the pUC19, containing a 1841bp *Xba*I–*Bam*HI fragment encompassing pufLM [104] (Figure 3.18).

The sample digestion scheme follows:

S 2.1)

"Reagents"	µl
DNA	5
10x buffer	5
Sterile distilled H_2O	36
EcoRV	2
SalI	2
TOT	50

After 1 hour of incubation 1.5% Agarose electrophoretic gel is run, in tris-acetate-EDTA (TAE) [105] (Protocols Section, Protocol 5) (Figure 3.17-3.18)

Usually Tris-Borate-EDTA (TBE) (Protocols Section, Protocol 6) is better for smaller DNA (<300-bp on 2% agarose gel) migrated faster and thus yield better results TBE. Beneficial usage of tris-borate for obtaining a higher resolution of small DNA fragments by agarose gel electrophoresis. For the difference in the buffers for agarose gels [106]. The borate seems to make the gels more rigid which helps when you are handling them. For the same reason, it was better no to use TBE gel to ligation gel where the TBE inhibit the ligase enzyme.

The EcoRV-SalI digested bands was cut off from the gel and purify with Wizard® SV Gel and PCR Clean-Up System (Protocols Section Protocol 7).

The interesting fragment was introduced in pUCXB plasmid by ligation (the scheme following) and cloned again in E. coli DH5α.

S 2.2)

	Volume(µl)
Vector	5
Insert	6
10xBuffer	2
PEG	2
H_2Odd	-
Ligase T4	5
Total	20

Polyethylene glycol (PEG) greatly increases the rate of ligation of blunt-ended DNA. EcoRV cut the fragment produced a sticky end and a blunt end, for this reasons the PEG use is advised. [107]
The reaction was performed at 16°C for 1 hour and then 10 µl for each samples were put in frozen competent cells (Protocols Section, Protocol 8) containing in 1.5ml eppendorf tube, leaving them in ice for 1 hour following an heat shock of 1 min at 42°C to permit the transformation, and after in ice for 5 minutes again. 800µl of Luria Bertani (LB) liquid medium (Protocols Section, Protocol 9) was add for each tube, and then left at 37°C for 1 hour and 30 minutes. Each sample was centrifuged full speed for 5 minutes, and all supernatant was discarded and the pellet dissolved in the rest. When the suspension was plate in the Petri dishes with solid LB placed over night at 37°C. The colonies produced were the transformed ones, some of them were taken with a sterile toothpick. Each one was left in liquid LB again over night, to have DNA enough for the following steps.
The modified pUCXB plasmid obtained was subsequently digested with the XbaI–BamHI endonucleases (the scheme S 2.3) and the excised fragments (GR02 and GR03) purified analysed by the dideoxy sequencing in order to confirm the identity of the inserted sequence

S 2.3)

"Reagents"	µl
DNA	1
10x buffer	2
Sterile distilled H_2O	15
XbaI	1
BamHI	1
TOT	20

The enzymatic digestion was verify by TBE 1% Agarose gel (Figure 3.17 Discussion)

The GR02 band was cut, purified and cloned following the procedure above described.

The XbaI-BamHI fragments containing the mutations were then shuttled into plasmid by ligation (S 2.4) pRKEH10 (Figure 2.5a), which is a derivative of broad-host-range vector pRK415 containing a 6.55 kb EcoRI–HindIII fragment encoding pufQBALMX.

The derivatives of plasmid pRKEH10 were introduced into *R. sphaeroides* strain DD13 by conjugative transfer [108]. Transconjugant strains contained RCs and the LH1 antenna complex, but lacked the LH2 antenna. Strains with an antenna deficient (i.e. RC-only) phenotype were also constructed by shuttling the mutated GR02 fragments into plasmid pRKEH10D (S 2.4) (Figure 2.5b) [109], a derivative of pRKEH10 with a 300 bp deletion in the structural genes for the LH1 antenna complex (pufBA), so it is a RC only strain.

S 2.4)

	Volume(µl)
Vector10/10D	10
Insert(GR02)	4
10xBuffer	2
PEG	-
H_2Odd	3
Ligase T4	1
Total	20

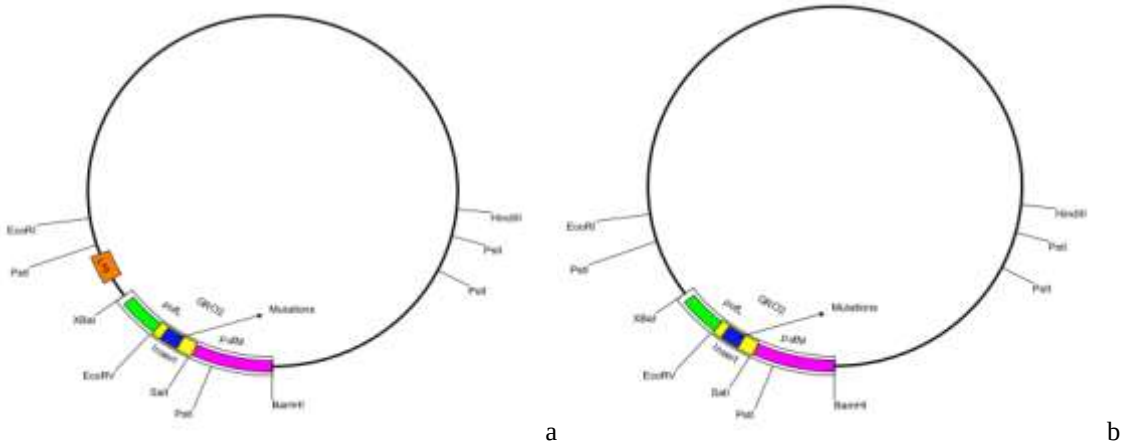

a b

Figures 2.5 Rhodobacter transformation vectors: XbaI-BamHI restriction fragment get out of plasmid pUCXB and shuttled into two expression plasmids called pRKEH10 (a) (containing also pufBA which codify LH1) and pRKEH10D (b) (RC only plasmid, without LH1 genes)

Before the Rhodobacter transformation, the GR02 ligation in pRKEH10 and pRKEH10D was verified with a PstI digestion (S2.5) (Figure 3.19).

S 2.5)

"Reagents"	µl
DNA	10
10x buffer	2
Sterile distilled H_2O	7
PstI	1
TOT	20

S17-1 *Escherichia coli* was transformed with pRKEH10 and pRKEH10D and by diparental filter mating transformation of *R.*sphaeroides DD13 [110] [111] (Protocols Section, Protocol 9) obtaining 2 chimeras, one containing only the RC and second one containing the RC plus the LH1 antenna (Figure 2.6)

Figure 2.6 *R.sphaeroides* mutant expressing just Reaction Center and mutant expressing the RC and LHI

R.sphaeroides chimeras were grown onto $M22^{+}$ plates supplemented with Vitamins, Neomycine and Tetracycline, the transformed bacteria colonies can be seen in Figure 2.7.

Figure 2.7 Chimera was created and grown in proper medium ($M22^{+}$ plates supplemented with Vitamins, Neomycine and Tetracycline)

2.2.3 Photosynthetic membranes isolation

Recombinant bacterial cells were disrupted by French pressure and intracytoplasmic membranes isolated by 15-40% sucrose gradient ultracentrifugation at 38,000 rpm 4 °C for 2 h, according to Jones et al. (2004) [102] (Protocols Section, Protocol 10) In Figure 2.8 it may be see the intracytoplasmic membranes isolated band.

2.2.4 Absorbtion spectroscopy characterization

The chimeric RC-assembled was analyzed by classic spectrophotometry absorption scan measurements between 300 to 1000 nm of wavelength. The obtained spectra were compared to those obtained by the wild type strain (Figure 3.20).

Figure 2.8 Intracytoplasmic membranes isolated band obtained by sucrose gradient extraction

2.3 Protocols Section

2.3.1 Protocol 1 TAP Production

1 liter 1X TAP is composed by:

Volume (ml)	Solution
10ml	2M Tris-Acetate 100X(pH 7.0)
10ml	Phosphate Buffer 100X(pH 7.0)
10ml	Nutrient Stock 100X
1ml	trace metals by Hutner 1000X [3]

Tris Acetate stock 100X: 242g Tris base, Dissolve in 600ml distilled water while titrating to pH 7.0 with glacial acetic acid. Bring to 1litre.

Phosphate Buffer 100X: 10.8g K_2HPO_4, 5.6g KH_2PO_4, bring to 1 liter

Nutrient Stock: 40g NH_4Cl, 10g $MgSO_4$ $7H_2O$, 5g $CaCl_2$ $2H_2O$, bring to liter.

Trace elements 1000X

The Trace elements by Hutner [3]

Dissolved 50g of Acid free EDTA in 250ml of ddH_2O, heat to dissolve.

Dissolve the following, one by one, in order, heating to approximately 100°C in 550ml.

Weight (g)	Reagents
11.40	BO_3H_3
22.00	$ZnSO_4$ $7H_2O$
5.06	MnCl2 $4H_2O$
4.99	$FeSO_4$ $7H_2O$
1.61	$CoCl_2$ $6H_2O$
1.57	$CuSO_4$ $5H_2O$
1.1	$Mo_7O_{24}(NH_4)_6$ $4H_2O$

Mix the solution a) and b) together. The result solution should be blue green (temperature should be around 100°C). Cool slightly, but don't let the temperature dorp below 80°-90°C.

Adjust pH to 6.5 to 6.8 with KOH (approximately 83ml). Don't let the temperature drop below 70°C until after the pH is adjusted.

Make up to 1l and let stand in a 2l Erlenmeyer flask. The color should change form green to purple over a period of days (it should be rest at 4°C in the dark for 2 weeks before use).
Remove the rust colored precipitate by filtering, with suction, through 3 layer of Whatman® filter paper in a Buchner funnel. Repeat until more precipitate is seen on the filter paper.
Stored in dark bottle at 4°C.

2.3.2 Protocol 2 Growth Rhodobacter sphaeroides

$M22^+$ medium is made up as a 10-fold concentrate and autoclaved. The recipe is given in Appendix A. It is kept at room temperature for several weeks.
For growth in liquid culture, we make up the $M22^+$ medium from the 10-fold concentrate and also add casamino acids (see Appendix B). After re-autoclaving the medium will keep at room temperature for several weeks. 10^4 Vitamins solution (see Appendix C) and tetracycline and neomycin (see Appendix F) were added aseptically immediately before inoculation of the medium. Growth is carried out in a dark orbital incubator running at 34°C and 180 rpm. If the incubator is fitted with lights then switch them off, and if it has a glass front or top panel, then cover it with foil. Ideally the incubator platform should be fitted with flask clips that can cope with 100 ml conicals and 2 litre conicals. The 2 litre ones will have 1.5 litres of medium and will be heavy, so make sure the flask clips can cope. Don't use the "sticky pad" type of platform unless you want to spend several hours on your hands and knees cleaning broken glass and bacterial culture out of the incubator.
For growth on agar plates, we make up an $M22^+$ solid medium as described in Appendix E. Once autoclaved the medium has a shelf life of several weeks if the bottle lids are on tight. 10^4 Vitamins solution (see Appendix C) and tetracycline and neomycin (see Appendix F) are added aseptically once molten agar has cooled sufficiently, immediately before pouring the plates.
To grow a culture, make up 3 types of $M22^+$ medium. Starter medium consists of 10 ml aliquots of $M22^+$ in 30 ml screw cap glass universals ("10 ml bottles"). Intermediate medium consists of 70 ml aliquots of $M22^+$ in 100 ml glass conical flasks with a cotton wool bung ("70 ml flasks"). Final medium consists of 1.5 litre aliquots in 2 litre glass conical flasks with a cotton wool bung ("2 litre flasks"). On day 1, inoculate a 10 ml bottle with a lump of cells from a glycerol stock, or a lump of cells scraped from an agar plate. A lump the size of a match-head is ideal. Incubate upright in the orbital incubator. On day 2, aseptically transfer the entire contents of the 10 ml bottle into a 70 ml flask and return to the incubator. On day 3, aseptically transfer the entire contents of the 70 ml

flask into a 2 litre flask and return to the incubator. Grow for 36-48 hours and harvest by centrifugation on day 5. The large-scale culture should have a deep colour (orangey-red for RC-only strains), and a nice frothy "head". You can monitor the culture using a spec – cultures ready for harvesting usually have an OD at 650 of about 1.5 and you can see discrete bumps at 760 and 800 nm due to the RC. If you want to grow more than one two litre flask of a particular mutant, grow the first 2 litre flask for 24 hours and then use this to inoculate further flasks.

Tips – if everything goes well your 10 ml culture should be a distinctly orangey-red colour 24 hours after inoculation. If instead it looks very pale then you can either (1) add a second aliquot of vitamins and incubate for a further 24 hours – this often causes the starter culture to colour-up, (2) cross your fingers and go ahead and inoculate the 70 ml flask anyway – the 70 ml flasks often grow fine even though the starter culture looked dodgy, (3) chuck the starter culture away and set up another one. I often set up at least two 10 ml starter cultures for each strain I am growing, then use the best looking one on day 2. Once you have a decent 70 ml culture growing then the rest of the growth is usually straightforward.

Tips – for 10 ml bottles you will need 2 μl each of vitamins, tetracycline and neomycin. For 70 ml flasks you need 14 μl of each, for 2 litre flasks you need 300 μl of each, and for 200 ml volumes of $M22^+$ agar you need 40 μl of each.

Glycerol stocks - Cells from a 70 ml culture grown under dark/semiaerobic conditions are harvested by centrifugation using a sterile centrifuge tube and are resuspended in approximately 1 ml of a filter sterilised mixture of 30% glycerol/70% LB medium. Store at –80°C (will remain viable for many years) Appendix G

2.3.2.1 Appendix A : M22+ medium 10x concentrate

Amounts per 4 litres:

Reagents	Amounts
KH_2PO_4	122.4 g
K_2HPO_4	92.0 g
Na lactate Solution (60% w/w syrup)	100.0 ml
$(NH_4)_2SO_4$	20.0 g
NaCl	20.0 g
Solution C (see Appendix B below)	800.0 ml

Na succinate	173.7 g
Na glutamate	10.8 g
Aspartic acid	1.6 g

Make up to approximately 3.8 l with deionised water then adjust to pH 6.8 with solid NaOH (takes quite a lot – but try not to overshoot). Top up to 4 l with deionised water, autoclave at 15 p.s.i. for 20 min. Store at room temperature. We usually split the 4 litres into 10 x 400 ml lots and dispense into 500 ml glass bottles prior to autoclaving. Don't panic if the 10x M22+ develops a precipitate either before or after autoclaving – this is normal and does not prevent the medium being used. You don't have to redissolve the precipitate before making the 1x M22+ medium.

2.3.2.2 Appendix B: Solution C

Amounts per 4 litres:

Reagents	Amounts
Nitrilotriacetic acid	40.0 g
$MgCl_2$	96.0 g
$CaCl_2$	13.36 g
EDTA	500.0 mg
$ZnCl_2$	1044.0 mg
$FeCl_2$	1000.0 mg
$MnCl_2$	360.0 mg
$(NH_4)_6Mo_7O_{24}.4H_2O$	37.0 mg
$CuCl_2$	31.0 mg
$Co(NO_3)_2$	49.6 mg
Boric acid	22.8 mg

Dissolve in deionised water, make up to 4 l. Store at -20°C.

We usually split the 4 litres into 5 x 800 ml aliquots and freeze in plastic bottles. You then thaw out one 800 ml aliquot for every 4 litres of 10x $M22^+$ you make.

2.3.2.3 Appendix C: $M22^+$ liquid medium

Amounts per litre:

10x M22+ concentrate (see Appendix A)	100 ml
5% (w/v) tryptone	20 ml
Deionised water	880 ml

Autoclave at 15 p.s.i. for 20 min. Store at room temperature.

We usually make this up as 10 ml aliquots in 30 ml glass universals, or 70 ml aliquots in 100 ml conical flasks, or 1.5 litre aliquots in 2 litre conical flasks. For the conical flasks, stopper them with a bung made from non-absorbent cotton wool and cover in the top in foil. For the 2 litre flasks a piece of autoclave tape around the foil at the neck of the flask will stop bungs from popping out (sometimes happens to 2 litre flasks in a large autoclave).

For the casamino acids, you can either make up a 50 g $litre^{-1}$ stock solution, autoclave it, and then aseptically add 20 ml to every litre of $M22^+$ liquid medium you make (before autoclaving the $M22^+$), or you can add 1 g of solid casamino acids to each litre of $M22^+$ medium you make up (again just before you autoclave the $M22^+$).

2.3.2.4 Appendix D: 10^4 Vitamins

Amounts per 100 ml:

Nicotinic acid	100.0 mg
Thiamine	50.0 mg
pABA (paramino benzoic acid)	10.0 mg

Biotin	1.0 mg

Dissolve in 100 ml of deionised water, then filter sterilise through a 0.2 μm syringe filter into sterile universals or Falcon tubes. Long term storage at -20°C, short term storage at 4°C.
Although it is a 10^4 concentrate we routinely add twice the amount needed to $M22^+$ medium (i.e. 200 μl per litre of medium). This makes the volume of Vitamins to be added the same as that for tetracycline and neomycin (see below), and so minimise the chances of making mistakes.

2.3.2.5 Appendix E: M22+ agar
Amounts per litre:

10x $M22^+$ concentrate (see Appendix A)	100 ml
Deionised water	900 ml
Agar	15 g

Autoclave at 15 p.s.i. for 20 min. Store at room temperature.
For $M22^+$ agar, we usually make up a litre of $M22^+$ (note that you don't need casamino acids for plates), then split this into 5 x 200 ml aliquots in 500 ml glass medium bottles. We then add 3 g agar to each bottle and autoclave. If you don't pour it straight away you can either melt the agar in an autoclave or in a microwave.

2.3.2.6 Appendix F: Antibiotics
Amounts per litre:

Antibiotic	Stock	used for growth	Dilution of stock
Tetracycline	5 mg/ml	1 μg/ml	200 μl per litre of medium
Neomycin	100 mg/ml	20 μg/ml	200 μl per litre of medium

For tetracycline, weigh out 250 mg and dissolve in a mixture of 25 ml water and 25 ml 100% ethanol. Filter sterilize as ~ 25 ml aliquots into sterile plastic universals or Falcon tubes wrapped in foil. Store at -20°C (will remain liquid).
For neomycin, weigh out 3 g and dissolve in 30 ml water. Filter sterilise and dispense into sterile 1.5 ml eppendorf tubes – store at -20°C. Individual aliquots can be freeze/thawed many times.

2.3.2.7 Appendix G: Glycerol Stocks

Grow up the desired *Rb. sphaeroides* strain until you have a strong 70 ml culture.

Transfer the culture into sterile 30 ml universals.

Centrifuge at 3000 rpm for 10-15 min.

Discard the supernatant and leave to drain thoroughly.

Resuspend the pellet(s) in ~1 ml of 30 % glycerol/ 70% LB medium which has been filter sterilised or autoclaved.

Transfer to clean, sterile Eppendorf(s).

Store at –80 ºC.

2.3.3 Protocol 3: Wizard® Plus Minipreps DNA Purification System -Promega

	Culture Volume		
Prepare Cleared Lysate	1-3ml	3-5ml	5-10ml
1 Pellet cells	1-2 min 10000 x g	10min 10000 x g	10min 1400xg
2. Suspend pellet in Cell Resuspension Solution	200µl	300 µl	400 µl
3. Add Cell Lysis Solution. Invert 4 times to mix	200µl	300 µl	400 µl
4. Add Neutralization Solution. Invert 4 times to mix	200µl	300 µl	400 µl
5.Centrifuge lysate for 5 min at 10000 x g			

6. Remove plunger from 3ml Luer-Lok® syringe (Becton-Dickinson Cat.# 9585)

Attach syringe barrel to Luer-Lok® extension of Minicolumn

7. Resuspend resin. Add 1ml resin to each Minicolumn/syringe assembly

Carefully transfer cleared lysate (from Step 5) to resin in each assembly

8. Insert plunger and push resin and lysate into Minicolumn*

Washing

9. Detach syringe from Minicolumn; remove plunger from syringe barrel

Reattach barrel to Minicolumn

10. Add 2ml Column Wash Solution containing ethanol. Insert the plunger and

push the Column Wash Solution through the Minicolumn

11. Remove syringe and transfer the Minicolumn to a 1.5ml microcentrifuge tube

Centrifuge at 10,000 × g for 2 minutes

Elution

12. Transfer Minicolumn to a new microcentrifuge tube

13. Add 50µl of Nuclease-Free Water to the Minicolumn and wait 1 minute

For plasmids ≥10kb, use water preheated to 70°C; for plasmids ≥20kb, use water preheated to 80°C

14. Centrifuge at 10,000 x g for 20 seconds at room temperature

15. Remove and discard Minicolumn. Store DNA at –20°C or below

2.3.4 Protocol 4: Wizard® SV Gel and PCR Clean-Up System

Gel Slice and PCR Product Preparation

A. Dissolving the Gel Slice

1. Following electrophoresis, excise DNA band from gel and place gel slice in a

1.5ml microcentrifuge tube

2. Add 10µl Membrane Binding Solution per 10mg of gel slice. Vortex and

incubate at 50–65°C until gel slice is completely dissolved

B. Processing PCR Amplifications

1. Add an equal volume of Membrane Binding Solution to the PCR amplification

Binding of DNA

1. Insert SV Minicolumn into Collection Tube

2. Transfer dissolved gel mixture or prepared PCR product to the Minicolumn assembly. Incubate at room temperature for 1 minute

3. Centrifuge at 16,000 × g for 1 minute. Discard flowthrough and reinsert Minicolumn into Collection Tube

Washing

4. Add 700µl Membrane Wash Solution (ethanol added). Centrifuge at 16,000 × g

5. Repeat Step 4 with 500µl Membrane Wash Solution. Centrifuge at 16,000 × g for 5 minutes

6. Empty the Collection Tube and recentrifuge the column assembly for 1 minute with the microcentrifuge lid open (or off) to allow evaporation of any residual ethanol

Elution

7. Carefully transfer Minicolumn to a clean 1.5ml microcentrifuge tube

temperature for 1 minute. Centrifuge at 16,000 × g for 1 minute

9. Discard Minicolumn and store DNA at 4°C or –20°C

2.3.5 Protocol 5 TAE

50× TAE Stock *1 l*

Reagents	Amount
Tris	242 g
Glacial acetic acid (100 %)	57.1 ml
EDTA	18.6 g

pH to 8 with HCl

TAE Buffer

Reagents	Amount
50× TAE stock	50 ml
Ethidium bromide*	125 µl of 10 mg/ml stock
Water	up to 2.5 l

* HIGHLY TOXIC AND CARCINOGENIC!

2.3.6 Protocol 6 TBE

Reagents	*Amount*
10× TBE Stock	*1 l*
Tris	108 g
(Ortho)boric acid	55 g
EDTA	7.45 g

pH to 8 with HCl.

TBE Buffer

Reagents	Amount
10× TBE stock	250 ml
Ethidium bromide*	125 µl of 10 mg/ml stock
Water	up to 2.5 l

* HIGHLY TOXIC AND CARCINOGENIC!

2.3.7 Protocol 7 Competent Cells

Plate out *E. coli* cells (DH5α or S17-1) onto SOB agar and incubate overnight at 37 °C.

Take a 'large amount' of *E. coli* from this plate and disperse in 1 ml of SOB. Use to inoculate 200 ml of SOB*.

Incubate at 37 °C, 250 rpm until the OD at 550 nm is 0.35-0.5 (start checking after 2 h).

Collect the culture in a sterile centrifuge pot and chill on ice for 15 min.

Pellet the cells at 4 °C, 5750 rpm for 20 min.

Drain thoroughly.

Resuspend the cell pellet in 1/3 volume (132 ml) of RFI media and chill on ice for 15-20 min.

Pellet the cells at 4 °C, 5750 rpm for 20 min.

Drain thoroughly.

Resuspend the cell pellet in 2/25 volume (32 ml) of RFII media and chill on ice for 15-20 min.

Aliquot as 200 µl samples in dry ice-chilled sterile Eppendorf tubes and flash freeze on dry ice.

Carry out a competency test.

* Before inoculating the SOB remember to take 1 ml as a spectrophotometer blank.

2.3.8 Protocol 8 Luria Bertani (LB) Medium

Liquid media 1 l

Reagents	Amount
Tryptone	10 g
NaCl	10g
Yeast extract	5 g

pH to 7.5 with NaOH

For solid media add 3 g agar to every 200 ml of liquid media.

Autoclave at 15 psi for 20 mins.

Antibiotics	10 ml	200 ml (agar)
Ampicillin	20 µl	400 µl
Tetracycline	20 µl	400µl

Antibiotics should be added to molten agar when it is cool enough to be held comfortably (~50 °C).

Protocol 9 Mating Protocol

Grow *Rb. sphaeroides* DD13 to 70 ml in $M22^+$ supplemented with Neomycine(Neo) and Vitamins (Vits) No tetracycline (Tet.)
Transform *E. coli* S17-1 cells with pRKEH10D, and plate onto LB-Tet agar. Incubate overnight at 37 ºC
Spin down the *Rb. sphaeroides* culture in a benchtop centrifuge (3000 rpm for 10 min). Drain well and then resuspend the pellet in 1 ml of M22 (no supplements)
Take a scrape of *E. coli* from the agar plate (size of a match head) and resuspend in 50 µl of LB (no supplements)
In a clean Eppendorf mix 100µl of the *Rb. sphaeroides* with 5 µl of the *E. coli*
Pipette* onto a dry LB agar plate[#] (no antibiotics) and allow to dry
Incubate for 6-8 h at 34 ºC
Scrape up the mating product using a sterile toothpick and resuspend in 200 µl of $M22^+$ (no supplements)
Take 10 µl of this resuspension and mix with 190 µl of $M22^+$ (no supplements) to give a ~20 fold dilution
Plate out both 190 µl samples onto $M22^+$ plates supplemented with Vits, Neo and Tet.
Incubate at 34 ºC for 3-5 days
Streak out several colonies onto a fresh plates (M22 agar with Vits, Neo and Tet) to check for contamination
Use *Rb. sphaeroides* from the restreak plates to produce glycerol stocks

* When pipetting the mating mixture out ensure that surface of the agar is flat (to prevent running) and that there are no bubbles in the pipette (to prevent spraying).[#] To dry the LB plates put them in an incubator overnight, or better still make them a week in advance.

2.3.10 Protocol 10 Membranes – sucrose cushion

Membranes for spectroscopy are best made on a sucrose gradient. The very best quality membranes seem to come from a 40/15% gradient, however you can be lazy and just spin the membranes down on to a 60 % sucrose cushion.

Harvest *Rb. sphaeroides* 1.5 l cultures at 4000 rpm for 20 min at 4 °C. be careful you don't get any cotton wool mixed in with the cells as this can block the French Press

Resuspend the cell pellet in 20 mM Tris (pH 8) (20 ml per 1.5 l culture)
Homogenise to break up any clumps of cells
Add a little DNase I
French press to lyse the cells (18,000 psi – one pass is usually enough)
Centrifuge at 20,000 rpm, 4 °C for 20 min to pellet cell debris. Keep the supernatant and discard the pellet. I sometimes do 2 spins to make sure all crap is removed
To make a 15%/40% step gradient, for each ~70 ml ultracentrifuge bottle add 30 ml 40% sucrose (see below) and overlay with 20 ml 15% sucrose. Then layer about 20 ml supernatant on top
Centrifuge at 38,000 rpm, 4 °C for 2 h
The membranes form a band on top of the 40% sucrose
You can concentrate membranes by spinning them down onto a 60 % sucrose cushion. Take your membrane suspension and dilute with about 2 volumes of 20 mM Tris (pH 8.0). Add about 50 ml to an ultracentrifuge tube, then pipette 10 ml of 60% sucrose into the bottom of the tube. Top up with more membranes or Tris and spin at 38,000 rpm, 4 °C for 2 h. The membranes will form a tight band on top of the 60% sucrose
Aliquot the gloopy membrane suspension and freeze at –20 °C

3.Results and Discussion

3.1 Development of biosensor

The photosynthetic activity was verified by amperometric detection measures, i.e. a detection method in which the current is proportional to the concentration of the species generating the current. Electrochemical biosensors are normally based on enzymatic catalysis of a reaction that produces or consumes electrons. The exploited sensor was based on Screen Printed Electrodes (SPEs) could be made in carbon, carbon nano-tubes, gold etc.). Any SPE was constituted of a working electrode where the biologic material is immobilized, the reference electrode (generally) be made of Ag/AgCl) and an auxiliary electrode (also known as a counter electrode usually graphite made) may also be present as an ion source. (Figures 1.2 and 2.3)

The target analyte is involved in the reaction that takes place on the active electrode surface, and the produced ions create a potential which is subtracted from that of the reference electrode to give a signal. We can either measure the current (rate of flow of electrons is now proportional to the analyte concentration) at a fixed potential or the potential can be measured at zero current, this giving a logarithmic response. [112].

In order to enhance the sensitivity and the stability of our biosensor, we followed two different research parallel lines:,1) development an innovative electrochemical biosensor based on whole algae *Chlamydomonas reinhardtii* immobilized Screen Printed Electrode by testing two different and classic immobilization methods (Nafion® and Algiante methods [113]); 2) production of a chimeric RC with a native *C.reinhardtii,* to improve sensitivity toward herbicides and maintaining the characteristic stability of this bacterium. [9][10][11][12].

In the first phase of this PhD activity, immobilization and amperometry measurements were set up, and of the sensor support choice was performed. SPEs with different working electrodes were tested. The best results in term of stability of biological material immobilization, signal intensity, baseline noise, are produced by SPE with carbon nanotubes working electrode.

Alternative common materials for the Working Electrodes (WEs) were chosen by Cyclic Voltammetry (CV) experiment (Figure 2.4) With this electrochemical technique the potential of reaction was identified.

We checked if graphite [10], gold, and carbon nanotubes WEs could be used for our purposes. Unfortunately, in voltammograms recorded on bare SPEs out of the range graphite (-0.5, +0.5 V) exhibited parasite currents, while gold was able to discharge of undesired species at every potential.

In the last case the biologic material did not adhered and was removed easily. Furthermore, electrodes CNT WEs show current increments, since they allow a more efficient electron transfer network. These features oriented us toward the choice of CNT SPEs (with CNT WEs inside), allowing electrochemical measurements with less interferences and improved response. CV

3.1.1 Nafion immobilization methods

Nafion® is a polymer widely used to immobilized enzymes for biosensor purposes. [114][115][116][117][118][119]

The number of algal cells to be immobilized were calculated from the Optical Density at 750nm [120], various SPEs containing cultures at different cell concentration were analyzed, the best sample and the cells number being counted by cells counter (see Experimental Section).

Us mentioned above, different immobilization and measure buffers were tested, comparing various amperograms, we deduced that the use of a buffer with low NaCl concentration is preferable probably because high salt concentration inhibits the algal vitality and stability. The presence of potassium acetate (Ac-K), in the same buffer used to immobilize the algae seems to have an importance in the amplitude signal and in the ratio between the signal and noise (the reasons can be explained by the fact that *C. reinhardtii* can grow heterotrophically utilizing acetate and acetate may have an effect on photosynthesis and related processes [121]). Different buffers were tested as measure buffers. Electrolytic concentration is important to have a good signal performance, but also the type of electrolytic salts used has a relevance. For instance, the photosynthetic structure has a good response in the presence of magnesium salt, thus a buffer with high concentration of $MgCl_2$, was used to provide a good signal.

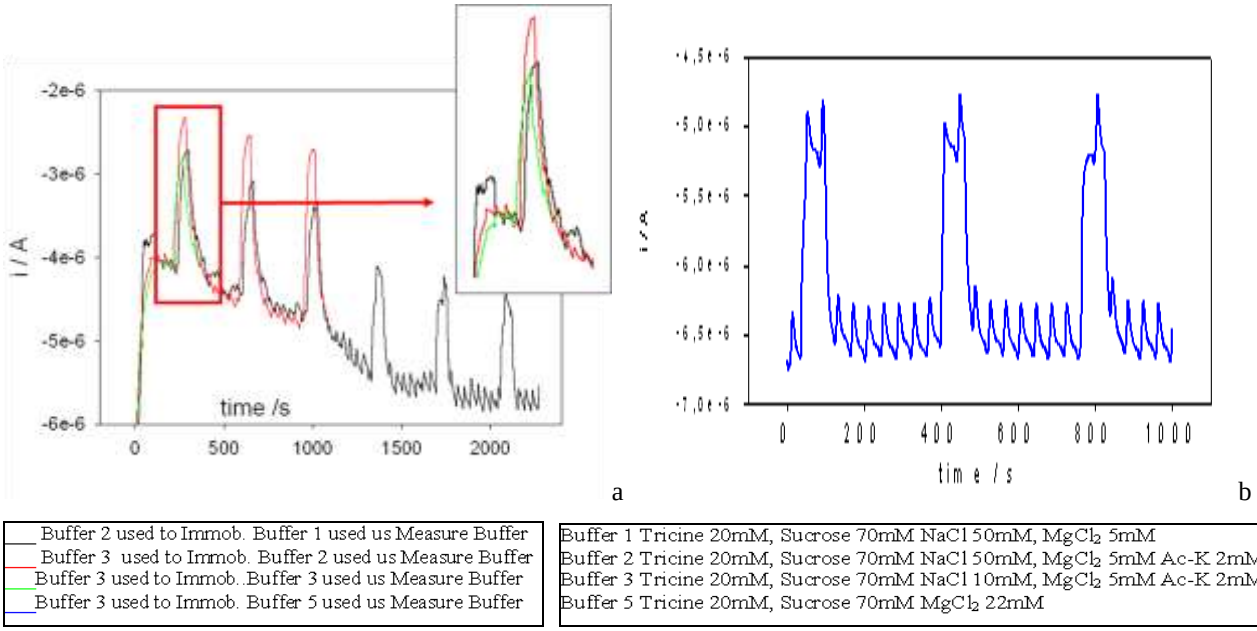

Figure 3.1- Comparison of the signal among different buffers used for immobilization and measure shows that the buffer 3 is the best immobilization buffer and buffer 1 and 5 are the best for measurements

3.1.1.2 Viability of immobilized algae in chronoamperometry: "half-life" measurements.

In the optimized experimental conditions the viability of immobilized algae was tested by means of "long-term" chronoamperometric (CA). The measurements were carried out with whole algae at a constant flow rate of 0.1 ml/min, in order to determine the time necessary to reach halving of the amperometric signal (hence defined as algae "half-life"). Such measurements differ from standard CA only because they are extended over several hours timescale, needing larger volume of flowing solution.

Different half life during the measure were obtained out in different conditions, varing from 19 hours on CNT- SPE and using Buffer1, to more than 40 hours using CNT-SPE and using Buffer 4 for the measurement. The best immobilization buffer Buffer 3. These results are certainly due to variation of concentration of NaCl. Up to now, the best measure buffers appeares to be the buffer 1 giving the best compromise between signal intensity and stability of measure time.

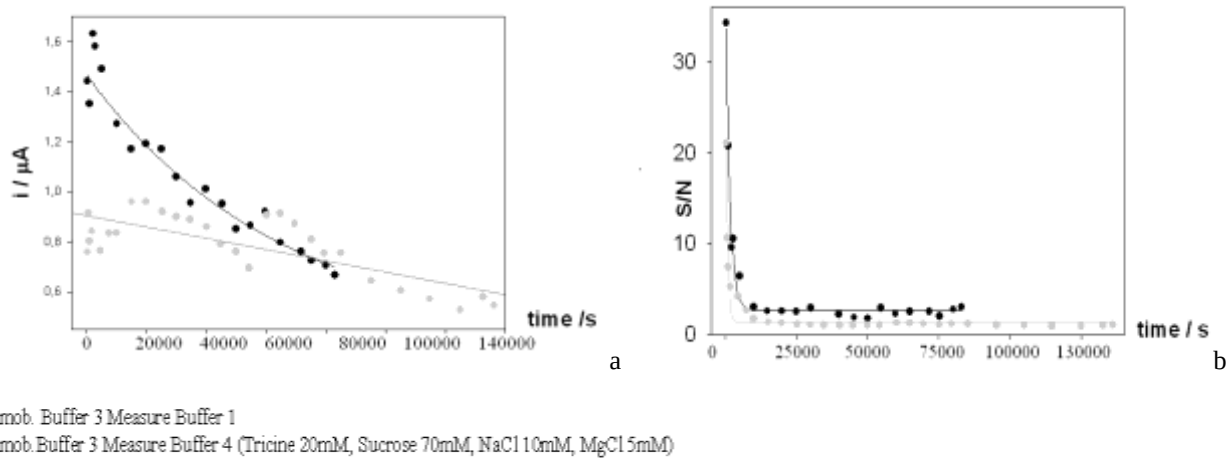

Figure 3.2 Carbone Nanotubes SPE half life during the measurements with *C.reainhardtii* cells immobilized: comparison of signal on time (a) and rate of the Signal on Noise (b) using two buffer buffers with different electrolytic concentration

The algae half-life indicates a long stability for algae cells immobilized with Nafion over CNT SPEs, especially when compared to literature data obtained with similar biomediator and procedures. Indeed spinach thylakoids immobilized over printed electrodes by BSA-GA chemical networking provide an already successful half-life of 16.7 hrs [10]. At the end of the measurements, 23 hrs long, the S/N ratio is still about 35 % of the maximum S/N, this latter is very similar to the initial value but occurring after ~ 1 hr stabilization of the biosensor; moreover, the noise increased in relatively slight percent after 23 hrs (37 %); from table 1 the S/N ratio starts with a great value (higher than 20), remaining for the largest part of the measurements higher or close to 10; it is noticeable that S/N is maximum at the beginning of the measurement and then suddenly starts decreasing while the noise intensity increases; instead the maximum intensity for the signal occurs after ~ 1 hr from the measurement start, attributable to a necessary stabilization of the biomediator/SPE interface; from a comparison with signals reported in literature for analogue biosensing systems, our highest measured amperometric peaks (1.3÷1.6 µA) have the same magnitude order as those from an alginate gel-based algal biosensor (~ 2 µA [82] while they are much higher than those reported in an "upgraded version" of the biosensor just mentioned, based on an algal film (~ 0.3 µA [81]). Both examples chosen for comparison employ the unicellular algae *Chlorella vulgaris*, since biosensors made of *Chlamaydomonas reinhardtii* immobilized algae do are not reported in the literature to our knowledge.

To measure the herbicides inhibition, an analyte sample at 10^{-6}M of Linuron was prepared in Buffer 5, the algae immobilized since to give the best electrochemical performance, and fluxed on the SPE. The percentage of herbicide inhibition was 29% (Figure 3.3).

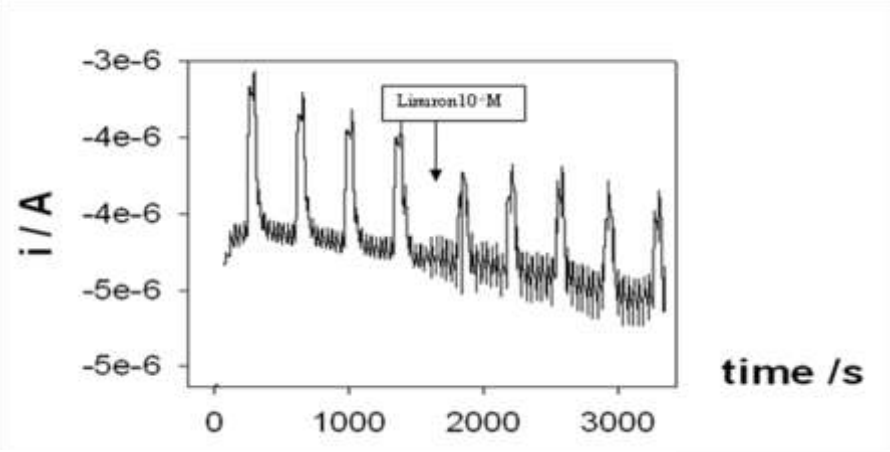

Figure 3.3 29% of inhibition herbicides(Linuron 10^{-6}M) was verified

Due to the poor sensitivity toward Linuron, we have chosen to investigate another method of immobilization, varying also the experimental setup details.

Alginate hydrogel is one of the most promising encapsulation material, already used for algae immobilization, is the [83] Alginates, extracted from brown seaweeds, are linear polysaccharide copolymers of (1-4)-covalently linked β-D-mannuronate and α-L-guluronate monomer residues. Due to their abundance, lack of toxicity and compatibility with biological systems, alginates are widely used for immobilization procedures [89][90][91]. Gelation of alginate is achieved by ion exchange between sodium and calcium divalent cations. Unique properties of alginates are: (a) the possibility of exploiting a room temperature gelation/encapsulation process; (b) a relatively inert aqueous environment within gels; (c) high gel porosity, allowing high diffusion rates for macromolecules. These properties enabled them to be used as matrices for the entrapment of several proteins. For these reasons the alginate gelation method has been selected to immobilize over SPEs whole *Chamydomonas rheinhardtii* cells.

3.1.2 Alginate immobilization method

Basic parameters in determining the amperometric biosensor performances are algae cell density and chlorophyll content on the working electrode, generally proportional within the same algal strain (IL in our case) [122] Specifically, the current signal and the signal to noise ratio (S/N) depend on many experimental factors such as cell density, chlorophyll content, the composition of the buffer solution used for the measurements and the surface characteristics of the immobilized

cells/SPE interface, etc.. Withdrawal of suitable volumes from incubated algae cultures has always been performed in the limited Abs_{750} = 0.4÷0.6 range, corresponding to the mid-exponential phase of cell growth. Several SPEs with different number of immobilized cells were tested in order to optimize the electrochemical signal in relation to cell density and chlorophyll content, in terms of peak current intensity and S/N.

Figure 3.4 shows that the highest signal is reached with ~ $4*10^5$ cells over the SPE. Data points follow an inverted U-shaped trend, typical of hormetic models describing many biological systems fitting with a quadratic function. Such models rely on U-shaped or inverted U-shaped dose vs response curves, depending on the parameter observed. If the parameter is cell growth or viability, the dose/response curve would describe an inverted U-shape, while it describes a U-shape in case of alteration of physiological functions. In particular, *hormesis* is considered an adaptive response characterized by biphasic dose/response curves due to similar quantitative features (with respect to amplitude and range of the stimulatory response), either directly induced or the result of compensatory biological processes [123]. In our case, opposite processes leading to mutual compensation and then to a signal maximum may be due to the number of PSII complexes/SPE, increasing with cell density and prevailing in the growing branch of the trend; an optimal electrical contact between cells and electrode surface, which decreases after a certain cell density is reached.

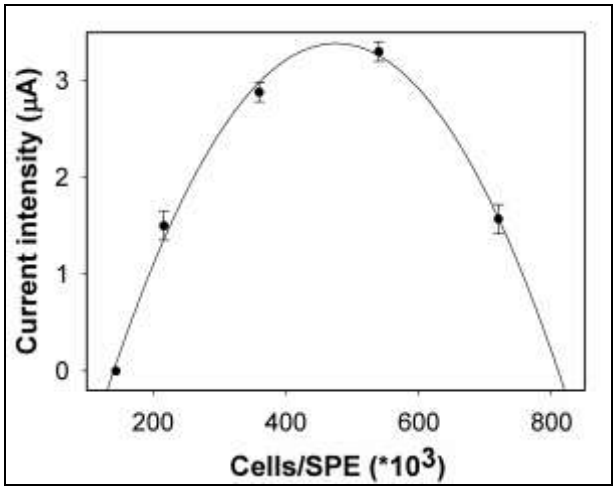

Figure 3.4 :Current intensity peak obtained upon illumination of the algal biomediator as a function of the cell

3.1.2.1 Cyclic voltammetry: investigation on the electrochemical reaction at electrode surface.

CV tests were always preliminary to CA measurements the aim of the former is finding the most suitable potential to set the measurement, where maximum current signal difference can be obtained

after stimulation by illumination. Figure 3.5 represents a typical single scan CV test carried out on a SPE-Chlamy, in dark and light conditions overlaid (dashed and continuous lines respectively). A cathodic reduction peak at - 0.7 V vs Ag/AgCl present only under at 650 nm continuous illumination, dominates the voltammogram. Multiple scan traces (e.g. triple, *not shown*) recorded in the same conditions result quite overlapped, with peak current intensities not significantly decrease, that indicates that electrodes of SPEs are electrochemically stable. Therefore, the optimal potential to set in CA tests was unambiguously identified as - 0.7 V vs Ag/AgCl.

Since in literature references illustrating algal biosensors almost no attention is dedicated to the electrochemical reaction occurring at the SPE/algae cells interface, we decided to investigate the nature of this reaction, also in order to optimize the biosensor signal (the sharp current peak at 0.7V originated by photosynthetically generated oxygen upon illumination) [**Errore. Il segnalibro non è definito.**][30] (Figure 3.5).

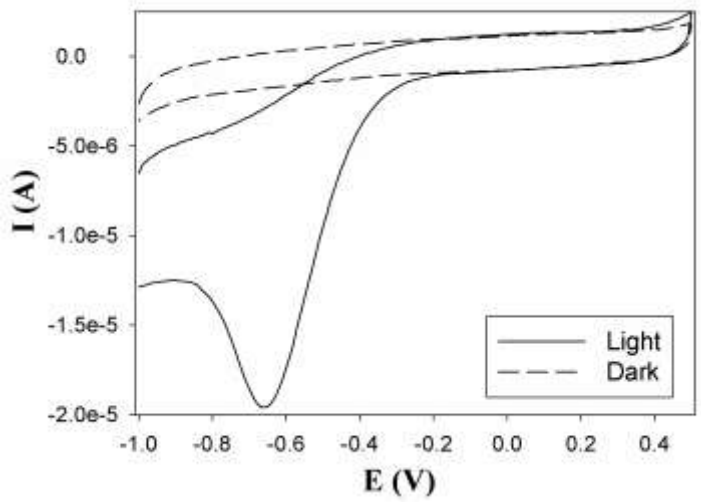

Figure 3.5 Cyclic voltammograms at 0.02 V/s scan rate of *C. reinhardtii* cells immobilized over CNT SPEs, in dark (dashed t race) and continuous light conditions (650 nm LED, solid).

In addition, CV measurements at different scan rates were performed in order to investigate the nature of the photosynthetic oxygen reduction and the electrode mechanisms. In fact, in view of the SPE-Chlamy optimization it is fundamental to evaluate the relative contributions of faradic and capacitive currents, respectively related to the discharge of chemical species the electrode surface (to maximize in CA tests) and to the formation of electrically charged layers. Beyond a very slight shift toward positive peak potential at higher rates (Figure 3.6a) (indicating a quite reversible electrode reaction) peak current intensities (I_p) plotted vs square root of scan rate ($v^{1/2}$) exhibit a

linear increment at increasing rates(Figure 3.6 b). According to analogous electrochemical studies on immobilized biomaterials [124], such linear dependence indicates that the oxygen reduction kinetics is controlled by diffusion processes toward a planar electrode surface (i.e. the rate of the electron transfer step is fast compared to the rate at which the electroactive species diffuse from the bulk solution to the electrode surface due to a concentration gradient). Since electroactive species such as oxygen, protons and electrolytes strongly adhere to the alginate matrix the mechanism may be explained by the transport of the ion of the supporting electrolyte to and from the electrode surface due to charge compensation [122]. Therefore the alginate matrix seems to offer low hindrance to migration of electroactive species, the whole electrochemical reaction resulting to be in optimal conditions.

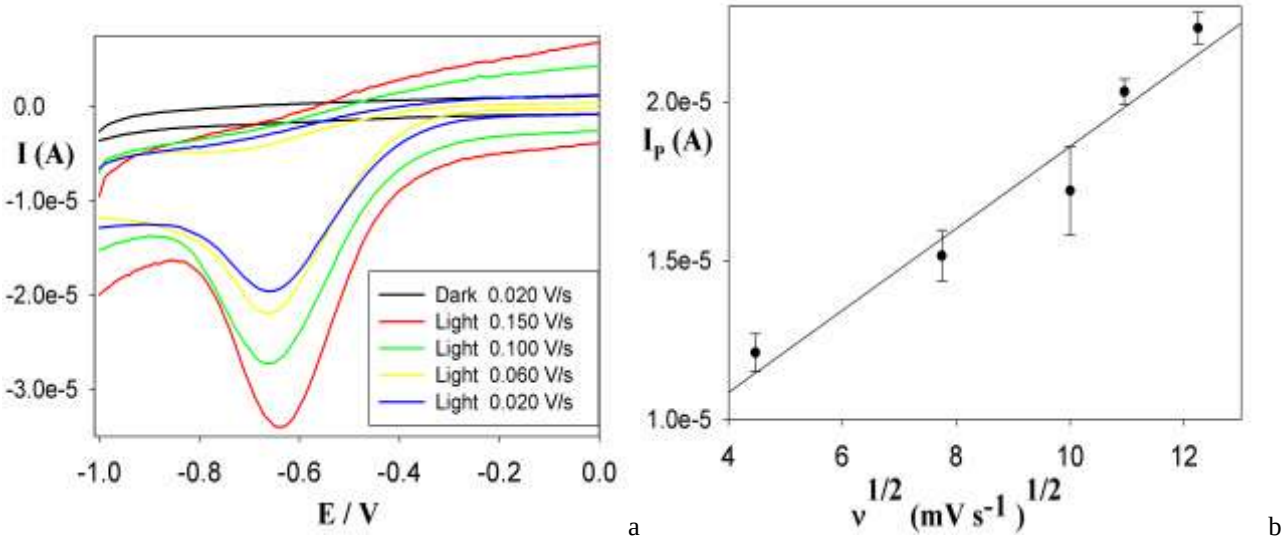

Figure 3.6 (a) Cyclic voltammograms obtained at different scan rates (v) from 0.020 to 0.150 V/s under dark/light conditions. Only the 0.020 V/s trace is reported among very similar dark adapted ones. (b) Peak current intensities (I_p, obtained by the tangent method) linearly increase with the square root of the corresponding scan rates ($v^{1/2}$).

3.1.2.2 Chronoamperometry: the principles of the herbicide detection.

CV analysis on SPE-Chlamys allowed an unambiguous attribution of the electrochemical reaction exploited as principle of the herbicide detection and its wide characterization.

Figure 3.7 shows typical time evolution of CA current responses of the alginate gel-based algal CNT-SPE biosensor (SPE-Chlamy). The first two current peaks (in the absence of herbicide) exhibit a signal higher than 7 μA high and S/N ratio of higher than 50. Of course, these parameters

may slightly vary for each test and from a SPE-Chlamy to another, but surely they are representative of high quality and reliable experimental data.

The potential was set at -0.7 V vs Ag/AgCl because of its ability to reduce oxygen. As already seen in Figures 3.7, the oxygen reduction current was significantly increased when the SPE-Chlamy was illuminated, since oxygen concentration increased at the electrode surface as a result of the algal photosynthesis. A saturation steady state was reached only within 30s upon illumination: this may be explained in terms of small alginate/algae cells layer thickness, the concentration of oxygen accumulated in a thin layer taking a shorter time to reach steady state. Subsequently, a dark time interval of 5 min was left for relaxation of the algal photosystem. When light was turned off the reduction current suddenly decreased, due to dissipation of oxygen previously generated by photosynthesis and its consumption by the dark respiration of the algae. Such results demonstrate that the immobilized algae retained sufficient photosynthetic activity.

The light/dark sequence was set at 30 s/5 min in order to reach steady illumination state and allow full relaxation of the biomediator, thus maximizing the S/N ratio. Moreover, the oxygen reduction current was found to slightly vary upon repeated dark/light cycles, however well under 5 % after a stabilization time of 5÷10 min. This may be due to the biomediator adaptation to the applied potential and dynamic flow measurement conditions. Optimal signal and S/N were found with 0.1 ml/min flow rate.

A careful optimization work was carried out also for the choice of the working electrode (WE) material and the composition of the buffer solution used for the measurements, in addition to the examination of other experimental factors already mentioned such as immobilization procedures, illumination sequence, cell density and chlorophyll content.

On the other side, for the composition of the measurement buffer many possibilities were open: beyond the selected composition (Tricine 50mM pH=7.2, $CaCl_2$ 20 mM, $MgCl_2$ 5mM, NaCl 50mM, sucrose 70mM). $CaCl_2$ 20 mM was found to be the lowest concentration sufficient to maintain calcium–alginate gel physical integrity over hours of flow measurements; $MgCl_2$ and sucrose are essential nutrients in photosynthesis, while NaCl 50 mM is important for the electrical conductivity. Figure 3.7 shows also that the oxygen reduction current decreased upon addition of linuron herbicide. The inhibition ratio percentage (*Inh%*) of the signal was given by E 3.1

3.1) $$Inh\% = \left(1 - \frac{i_H}{i_0}\right) * 100$$

where i_0 and i_H were photosynthetic oxygen reduction currents (i.e. peak amplitudes from the baseline level) before and after the injection of herbicide, respectively. The inhibition percentage is

normalized since it refers to each single SPE-Chlamy: by this way, inhibition data obtained in the same conditions but in different days may be compared. Inh % values were drawn from an average of at least three stable and comparable peaks (within 3 %). For this purpose, often a limited equilibrium stabilization time (≤ 15 min) was left, both in the absence and in the presence of the herbicide. Each SPE-Chlamy was always used once when in the presence of herbicide.

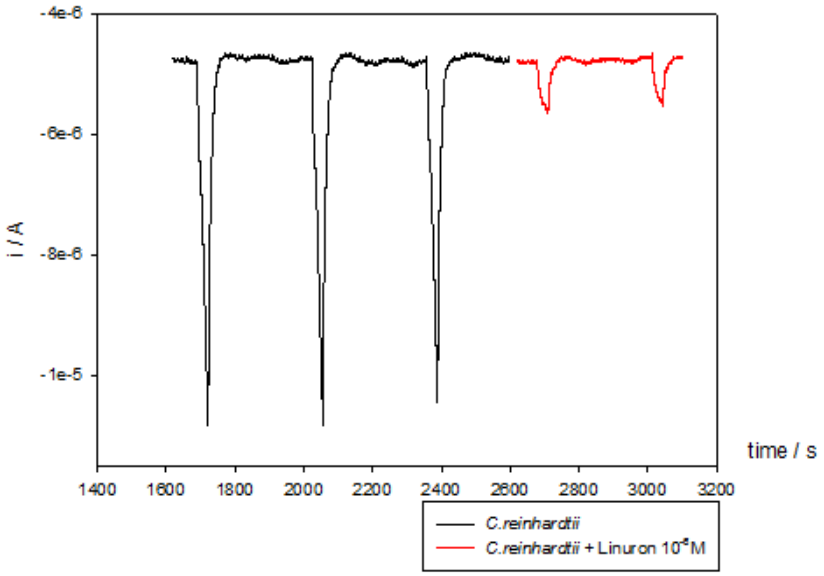

Figure 3.7 Current changes of the algal biosensor in response to switching of light (solid trace, 325 µmol*m^{-2} s^{-1} light intensity, 30s of 650 nm red LEDs/ 5 min dark) and addition of linuron 10^{-6} M at – 0.7 V vs Ag/AgCl in a Tricine 50mM pH=7.2, $CaCl_2$ 20 mM, $MgCl_2$ 5mM, NaCl 50mM, sucrose 70mM solution (pH 7.2) at 25 °C.

3.1.2.3 Biosensor performances in the absence of herbicides.

For the first 3 days after preparation SPE-Chlamys (stored at (25±2) °C under environmental illumination in Tricine 50mM pH=7.2, $CaCl_2$ 20 mM, $MgCl_2$ 5mM, sucrose 70mM optimized buffer) exhibit no detectable loss of photosynthetic activity. After 10 days in the same conditions they retained ~90 % of their original photosynthetic activity, 75 % within 20 days (Figure 3.9). In the following period a more pronounced drop of the current signal and of S/N ratio occurs, with 20% of the original current still detectable after 40 days. In the storage stability tests at least two independently prepared SPE-Chlamys were evaluated at every selected time interval, obtaining a reproducibility within 7 % error. While running CA measurements the prolonged use of each SPE-Chlamy did not affect their reliability and reproducibility for the first 3 hours. After a progressive drop of the signal and S/N ratio took place due to a decrease of algal photosynthetic activity. The slope of biomediator decomposition was biphasic with half-life ~9 hours.

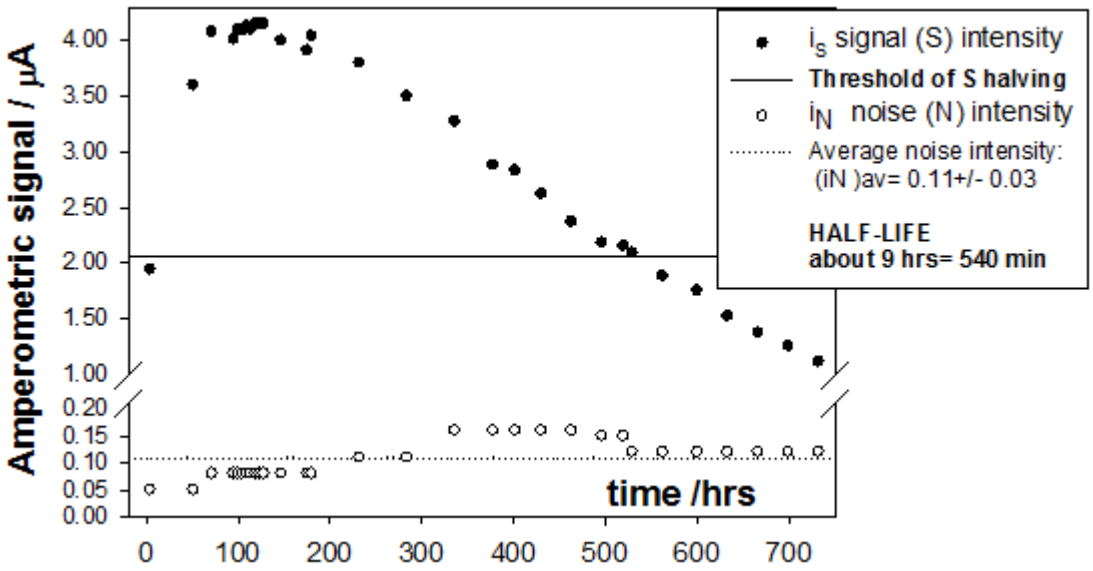

Figure 3.8 Half-life during a continuing measure reached in ~9 hours (half of the initial current signal)

Such results allow a reliable use of SPE-Chlamys even after 10÷20 days after preparation when necessary. Nevertheless, for a better reproducibility all tests reported in this work were carried out on freshly prepared SPE-Chlamys and were finished within 3 hours, although clues of their possible re-use after washing of herbicide were given (see below).

Moreover, our algal amperometric biosensor revealed to be suitable for field operations of herbicide determination: SPE-Chlamys may be prepared before hand and stored until measurements.

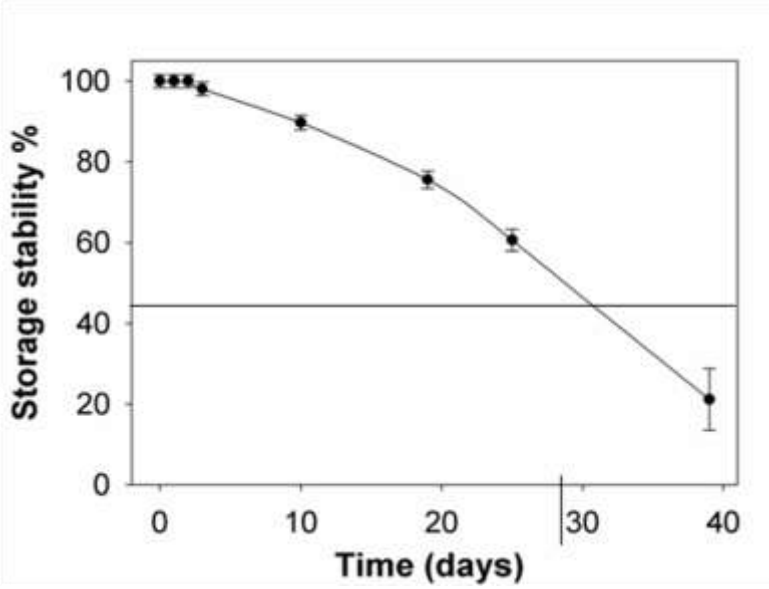

Figure 3.9 Storage stability (expressed as percentage of the initial current signal) of the SPBs in Tricine 50mM pH=7.2, $CaCl_2$ 20 mM, $MgCl_2$ 5mM, sucrose 70mM buffer at (25±2) °C and under environmental room illumination.

3.1.2.4 Biosensor performances in the presence of herbicides. Suggestions about QC site.

The sensitivity of our SPE-Chlamys was evaluated for two toxic pesticides, linuron and simazine, an urea derivative and a triazine only respectively. Such herbicides bind the D1 protein of algal PSII complex blocking the photosynthetic electron flow from plastoquinone A (Qa) to plastoquinone B (Qb) [125]The dose-response curves reporting the inhibition ratio percentage of the oxygen reduction current (*Inh%*) vs molar herbicide concentration for linuron and simazine are depicted in Figures 3.10a-b At least three independently prepared SPE-Chlamys were used for each concentration and the reproducibility on *Inh%* values was usually obtained within 8 %. They both indicate a very good agreement with amperometric SPE-Chlamys data, sharing all the three a common experimental trend.

Moreover, two distinct fitting curves in each one of Figures 3.10a-b a dashed and a solid one, indicate typical isothermal binding equations at one and two sites, respectively. Indeed, the theoretical response of the inhibition ratio (*Inh%*) of the oxygen reduction current for algal cells SPE-Chlamys treated with a triazine or urea herbicide of concentration [H] is given by the equation E 3.2a

E 3.2a) $$Inh\% = \frac{I_{MAX}*[H]}{I_{50}+[H]}$$

for a single binding site, e. g. the well-known Qb site within the D1 protein of algal PSII complex [81] [126]. I_{MAX} and I_{50} are the maximum inhibition induced by concentrations of herbicide leading to a 50 % signal decrease, respectively. Unfortunately, equation (E3.2a) provides an unsatisfying fit of experimental CA data (dashed line) corresponding to low concentrations ($1*10^{-9} \div 5*10^{-8}$ M for linuron, $1*10^{-8} \div 5*10^{-6}$ M for simazine). Instead of dropping this issue, [10][81][82] we examined further possible approaches and explanations.

Since 1980s literature proofs accumulated about the existence within eukaryotic PSII complexes of a second site of quinone binding and herbicide inhibition other than the well-characterized Qb site. Such evidences may be grouped into two cathegories: those collected before detailed crystallographic knowledge of PSII structure was available [125][127],[128], dealing with indirect clues of the existence of an additional site without possibility of identification; on the other side, proofs based on available PSII structures [129] leading to a precise description of the functional implications of a so-called novel Qc site [58] and of mechanisms of its interaction with the Qb pocket.[59].

On these bases the inhibition ratio of the current signal by herbicide might be related to a two sites binding equation E.3.2:

(E 3.2 b) $$Inh\% = \frac{I_{MAX,1}*[H]}{I_{50,1}+[H]} + \frac{I_{MAX,2}*[H]}{I_{50,2}+[H]}$$

where $I_{MAX,1}$ and $I_{MAX,2}$ were the maximum percentage contributions of the two binding sites separately to maximum total inhibition, while $I_{50,1}$ and $I_{50,2}$ were I_{50} values for the two sites. In this view it must be noted that sites are distinguished as 1 and 2 not in relation with their chronological identification (therefore as Qb and Qc) but rather with their binding affinity for the specific herbicide. Therefore Equation E 3.2a and E 3.2b were the first and second site interacting with herbicide molecules at increasing [H] concentrations (Qc and Qb respectively), Qc showing an higher affinity toward herbicides than Qb. The unique constraint to the fit operation was setting $I_{50,1}$ and $I_{50,2}$ different by at least one order of magnitude in order to observe Qc and Qb (nr. 2) as distinguished binding sites, exactly as literature reports [58].

Fitting data to the 3.2b equation provides the solid line curve in Figures 3.10a and 3.10b, characterized by parameters reported in Table 3.1. [130], I_{50} and K_d are both referred to the binding process of herbicides to the D1 protein of algal and cyanobacterial PSII complexes, respectively: in this purpose they may be compared and used interchangeably [80].

Herbicide	**$I_{MAX,1}$**	**$I_{50,1}$ (mol*L^{-1})**	**$I_{MAX,2}$**	**$I_{50,2}$ (mol*L^{-1})**
Linuron	6 ± 3	(1.0 ± 0.5)*10^{-9}	89 ± 4	(1.2 ± 0.2)*10^{-7}
Simazine	6 ± 2	(1.0 ± 0.5)*10^{-8}	94 ± 2	(2.3 ± 0.2)*10^{-6}

Table 3.1 Fitting parameters obtained for linuron and simazine inhibition experiments. For the fit operation literature results suggested a factor of separation of minimum 10 between $I_{50,1}$ and $I_{50,2}$ ($I_{50,2}$ >10* $I_{50,1}$).

The fit uncertainty reflects mainly on $I_{MAX,1}$ and $I_{50,1}$ values referred to Qc site, which bear errors until 50 %. This is the reason why statements leading beyond the intervention of an additional herbicide binding site should be carefully limited in this stage of study. Further investigations are necessary to clarify this hypothesis. On the other side the more accurate $I_{50,2}$ parameter, related to half of the Inh% increment due to the herbicide binding with the less sensitive Qb site, was responsible of at least 90 % total inhibition. Therefore Qb site is by far the most quantitatively determinant in the inhibition process, allowing to use $I_{50,2}$ as an I_{50} value referred to an approximate single-site binding ($I_{50,2} \approx I_{50}$). Moreover, such prevalence of Qb ver Qc in terms of "relative

proportions" of quinone and inhibitor binding would easily explain why in the past it has been so difficult to distinguish between Qb and Qc functions, as well as to investigate on Qc.

The I_{50} provides a reliable estimation of the limit of detection (LOD) of our biosensors in the determination of linuron and simazine [75] (formula F3.1 following). LOD is the lowest analyte concentration which detection is feasible, the assumption is that if analyte is present, it will produce a signal greater than the analytical noise in the absence of analyte [131]

$$\text{F 3.1) LOD} = \frac{2.6 \times \sigma \times I_{50}}{100 - 2.6 \times \sigma}$$

where $2.6 \times \sigma$ represents the mean standard error of the measurements increased by a factor of 2.6. This latter value corresponds to a 99 % confidence interval for a normal statistical distribution of values. According to definition (F 3.1), LOD result to be ~ $6*10^{-9}$ and $9*10^{-8}$ M for linuron and simazine respectively.

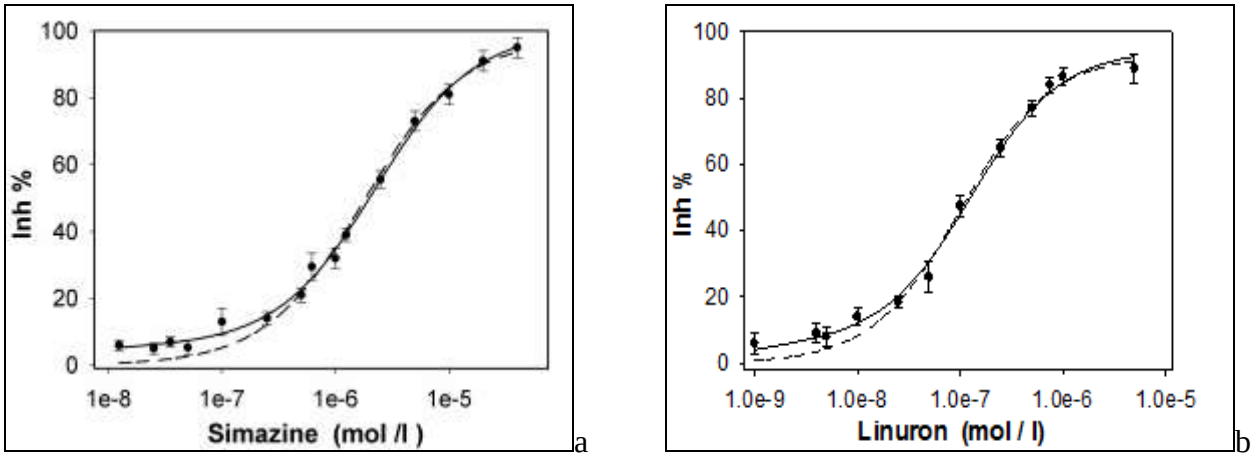

Figure 3.10 Semilogaritmic dose-response (inhibition percentage vs. concentration) curves of the SPE-Chalmy after exposure to linuron (a) and simazine (b) herbicides. Dashed and solid curves, based on typical isothermal binding equations, represent one and two binding sites respectively. The option of two sites clearly exhibits a much better agreement with experimental data, the largest difference lying in the lower concentrations range

It should be stressed that data in Figures 3.10 to our knowledge were the first successful in describing the herbicide inhibition of algal cell biosensor well in line with theoretical dose-response curves, where other pioneering efforts failed [81][82].

In our case, adaptation of experimental results to simple model equations more than a success *per se* represented a valid way to push the discussion toward cutting edge biochemical issues about Qb and Qc sites, as indicated below.

In order to strengthen our observations about a possible additional binding site Qc, revealed to be more sensitive than Qb, we have carried suitable chronoamperometric measurements intended to

evaluate the reversibility of the inhibition, known also as *recovery* tests [10]. They consist in flowing again buffer solution (without herbicide added) through the SPE-Chlamy chamber just after the measurement of the inhibition at a given herbicide concentration (equation 1) and recording the recovered current signal (i_R). In order to possibly discriminate between Qc and Qb site inhibition low and high concentrations of both linuron and simazine were selected with respect to their $I_{50,1}$ and $I_{50,2}$ values

Recovery data were analyzed in terms of: (a) Inh%; (b) Apparent Recovery percentage (AppRec %), defined as $(i_R/i_0)*100$ and including also the "never-inhibited" binding sites (indicated as NotInh% = 100- Inh%), thus explaining the meaning of "apparent recovery"; (c) Net Recovery Percentage (NetRec %), i.e. the apparently recovered sites minus the "never-inhibited" ones (AppRec % - NotInh%). Complement to 100 of AppRec % was the percentage of not recovered binding sites (NotRec %), i.e. sites still occupied by the herbicide. Finally, the reversibility of the algal biomediator inhibition at low and high herbicide concentrations was evaluated as inhibition reversibility percentage (InhRev %), defined as 100*{1- [(NotRec %)/(Inh%)]} (Table 2).

Herbicide/concn.	[Herb.] (M)	Inh%	NotInh%	AppRec %	NetRec %	NotRec %	InhRev%
Linuron/low concn.	$4.0*10^{-9}$	9 ± 3	91	91 ± 4	0	9 ± 4	0
Linuron/high concn.	$2.5*10^{-6}$	81 ± 2	19	72 ± 3	54	28 ± 3	65
Simazine/low concn.	$3.5*10^{-8}$	7 ± 3	93	91 ± 4	0	9 ± 4	0
Simazine/high concn.	$5.0*10^{-6}$	73 ± 3	27	97 ± 3	70	3 ± 3	96

Table 3.2 Summary of recovery measurement and analysis data. While only i_0, i_H, i_R current signals represent experimental results providing Inh% and AppRec % as above defined, other parameters come from these latter as above explained. Measurements were repeated and data averaged at least three times for each concentration.

AppRec % data at high concentrations are in a discrete agreement with those obtained on immobilized thylakoids from *Spinacea oleracea* (80 and 56 % recovery for diuron and simazine both $1*10^{-6}$ M, respectively). Despite evident differences in the biomediators and herbicides employed the agreement suggests that analogous biochemical mechanisms may occur.

Table 3.2 results undoubtedly confirm that two binding sites are responsible of the inhibition process: a high affinity site intervening at very low inhibitor concentrations and a lower affinity site Qb interacting with herbicides only at concentrations from ~10 nM (linuron) and from ~100 nM (simazine) on. Out of the uncertainty, AppRec % values are coincident with NotInh % ones only at low herbicide concentrations, showing that an apparent recovery higher than 90 % (i.e. reversibility)

is due only to "never-inhibited" binding sites, the net recovery and the inhibition reversibility being null. In other words, Qc site strongly binds herbicide molecules, not leaving them any possibility of release within the experimental timescale. On the contrary, high herbicide concentrations leading to significant inhibition (70÷80 %) exhibit high AppRec % values which, corrected for the "never inhibited" site fractions, indicate high net recovery and inhibition reversibility results, reaching ~ 100 % reversibility for simazine, which interacts less strongly with Qb site compared to linuron. In fact, because of its lower affinity Qb interactions with herbicides is characterized by a much higher degree of reversibility compared to Qc.

3.1.2.5Comparison with analogous biosensing devices and conventional methods.

A detailed comparison of some technical and analytical features between our SPE-Chlamys and similar recent algal biosensing devices will complete the issue. Characteristics such as measurement time, storage stability, half-life during tests and I_{50}, LOD (toward herbicides) were compared with those of *Chlorella vulgaris* algal amperometric biosensor exploiting a similar electrochemical signal [81][82] or, in a minor extent, with those obtained for immobilized spinach thylakoids [10] (Table 3.3).

Biosensor features	Present SPE-Chlamys	C. vulgaris biosensor	Immob. spinach thylak.
Electrochemical signal (μA)	5÷7	0.2÷0.3	0.020÷0.040
Measurement signal/noise	> 20	~ 5	Not av.
Measurement time (min)	≤ 30	4	10÷50
Storage stability	98 % after 3 days	Not av.	Not av.
Half-life (hrs)	~ 9	Not av.	10÷17[1]
I_{50} (mol*l-[1])	$2.3*10^{-6}$ (simazine)[2] $1.2*10^{-7}$ (linuron)[2]	$1.2*10^{-5}$ (atrazine) $1.0*10^{-6}$ (diuron)	$1.0*10^{-7}$ (simazine) $1.0*10^{-7}$ (diuron)
LOD (mol*l-[1])	$9*10^{-8}$ (simazine) $6*10^{-9}$ (linuron)	$1*10^{-6}$ (atrazine)	$4.1*10^{-8}$ (simazine) $1.5*10^{-8}$ (diuron)

1. *Spinacia oleracea*, depending on the immobilization procedure.

2. $I_{50,2} \approx I_{50}$.

Table 3.3: Comparison with analogous photosynthetic biomediator

The assay time of our SPE-Chlamys was certainly longer than *C. vulgaris* biosensors, although the sensitivity parameters (I_{50} and LOD) largely favoured our biosensors.

Our I_{50} for simazine took nearly the same value of that measured with an algae-immobilized Clark-type oxygen electrode ($1.3*10^{-6}$ M for atrazine), reporting also similar measurement times (30 min) and LOD (2*10-7 M for atrazine) [132].

3.1.2.6Preliminary results with C.reinhardtii mutant

We tried to improve the sensitivity of our biosensor to using different photosynthetic Chlamydomonas mutants.

C.reinhardtii RC subunit D1 has long been a target for genetic engineering many mutants were created for different purposes [72][133] [134] [135] following different transformation techniques [136] [122], though the most used chloroplast transformation is the biolistic one.

Amino acid residues lining this binding niche provide ligands to a diverse set of inhibitors, which can lose or gain affinity upon substitution of certain amino acids. One can exploit this and other properties of the D1 protein by changing the corresponding *psb*A gene which is located on the chloroplast genome in algae and higher plants as well.

The Chlamydomonas mutants can be obtained or by site directed mutagenesis if a single specific aminoacid changing occured or by random mutagenesis (by Error Prone-PCR) to create a pool of random mutants. The first approach to generate DNA sequences with mutated codons, insertions or deletions instead the second approach the Error-prone PCR is the method for introducing random mutations into a defined segment of DNA (being too long to be chemically synthesized as a degenerate sequence). Also the second technique is carried out by PCR introducing a specific primer designed specifically for the interested sequence.

In our specific study two PCR-based mutagenesis procedures for the introduction of random and site-directed mutations into the recipient strain were performed as follows: for random mutagenesis an error-prone PCR in the presence of $MnSO_4$ and dGTP was used. For site-directed mutagenesis a mutagenic primer M was used. PCR fragments were precipitated directly onto tungsten particles and introduced by particle gun transformation without further cloning or purification, in the cells occurred a homologues recombination between the exogenous and endogenous DNA[122] [137].

Previously a bioinformatic analysis could be carried out to design specific mutants regarding a specific aim [102].

In our case we have chosen a mutant kind gift of Prof. Johanningmeier called F274Yrm (a Phenylalanine in position 274 replaced with a Tyrosine). Considered tridimensional structure of PSII we expected this substitution should be close to Qc binding site and may interfere with the herbicides inhibition.

Using our biosensor whole algae based, F274Yrm was immobilized over the CNT-SPE and herbicide inhibition was analyzed. A semilogaritmic dose-response curve with Linuron (Figure 3.11) was observed with IL strain. Though it was possible detect with high repeatability low concentrations of herbicide, 10^{-10} M of Linuron gave about a 9% decrease of the amperometric signal (Definition (1)). More analysis need, also to calculate the I_{50} [10] [81] [82], the statistic LOD value (definition (3), [75] [131]], and check if "inhibition points" fit with equations (3.2a) or (3.2b).

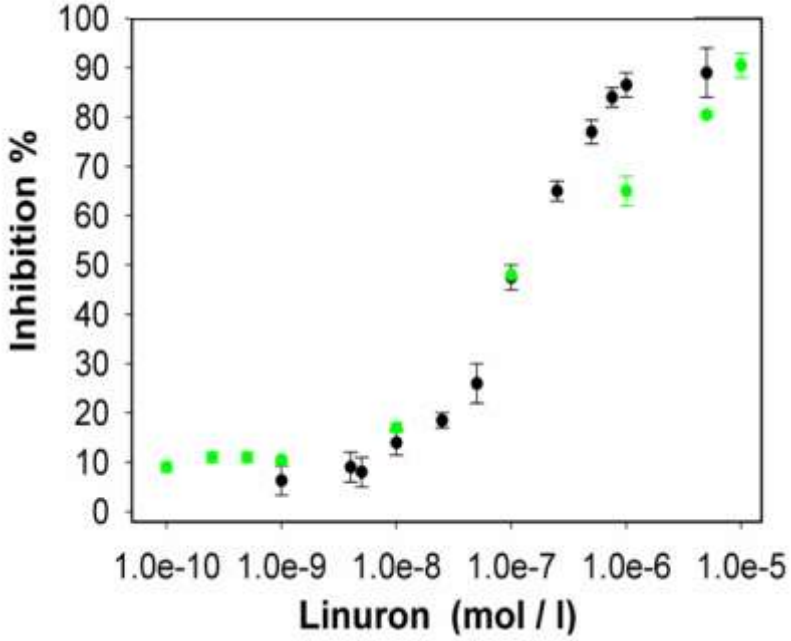

Figure 3.11 Preliminary semilogaritmic dose-response (inhibition percentage vs. concentration) curves of the SPE-ChalmyF274Yrm (green) compared with SPE-ChalmyIL after exposure to linuron.

3.2 Engineering of Rhodobacter sphaeroides Reaction Center

3.2.1 Chimera Creation to biosensoristic purpose

The *Rhodobacter sphaeroides* Reaction Center (RC) is composed of three subunits termed H (heavy), M (medium) (corresponding to D2 protein of higher plants and green algae of PSII) , and L (light) (corresponding to D1 protein of higher plants and green algae PSII) and the binding sites for each quinones were present in H and L protein respectively, as the high plant homologues protein D1, D2, such as in high plant and green algae the photosynthetic inhibitors in purple bacteria compete with Qb for the binding on the L protein interfering with photosynthesis.

Biosensor based on RC or its chromatophores were developed resulting more stable respect high plants thylokoids or chloroplasts [10][73][74][138].

For this reason a parallel experimental line, was followed for the production of a chimeric RC able to maintain high sensitivity toward herbicides typical of *C.reinhardtii* maintaining the characteristic stability of *Rhodobacter sphaeroides*

The possible genetic engineering of biological material was carry out after bioinformatics feasibility's study made in collaboration with Prof. Fabio Polticelli of the Computational Biochemistry Lab, University of Roma3.

3.2.2 Bioinformatics feasibility's study

Three work hypothesis were made: the first one is the production of *C. reinhardtii* mutant strains carrying *pufL* gene (encoding the L protein) of *R. sphaeroides* in substitution of the *psbA* gene (encoding the D1 protein). This first hypothesis was discarded because the sensitivity towards pesticides depends on Qb binding site present on D1 protein and the stability feature depends probably on bacterial background; for this reasons as second hypothesis of work it was though to produce *R. sphaeroides* mutant strains carrying *psbA* gene (D1 protein) of *C. reinhardtii* in substitution of *pufL* gene (L protein); finally as third hypothesis was considered the production of *R. sphaeroides* mutants carrying a chimeric form of L protein encompassing the *C. reinhardtii* Qb binding site.

The feasibility of the second hypothesis was verified by bioinformatics analysis The primary protein sequences of *C.reinhardtii and R.sphaeroides* were aligned and analyzed; 46 identical residues over 344 were found and few conserved residues in Qb pocket regions were identified (from 200 to 220 a.a., from 250 to 270 a.a., from 270 to 290) and interfacial regions (Figure 3.12).

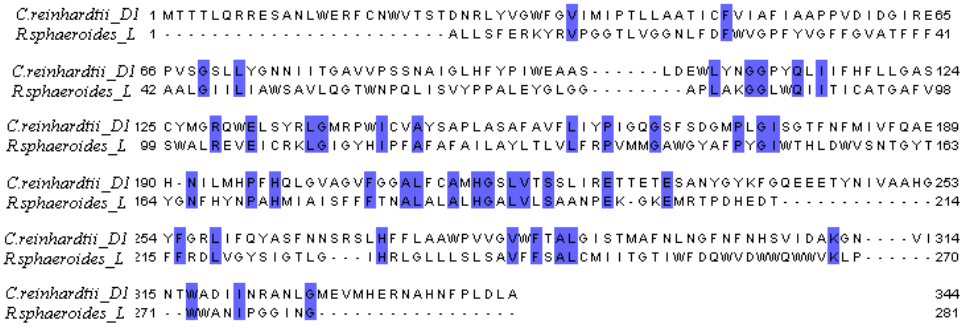

Figure 3.12 Alignment of the D1 protein of *C. reinhardtii* and L protein of *R. sphaeroides:* 46 identical residues over 344 are found and few conserved residues in Qb pocket regions are identified (from 200 to 220 a.a., from 250 to 270 a.a., form 270 to 290)

with other proteins and cofactors were carried out; it is evident a general compatibility (Figure 3.14) [72], but some violation problems were checked: the worse violation identified was the 250s helix,

part of Qb binding site and the D1-M interface nearby the Mn cluster and more several violation with lipids and cofactors. For this reason the second hypothesis of substitution of D1 protein with L protein is considered to be not a solution practicable (Figure 3.13)


a


b
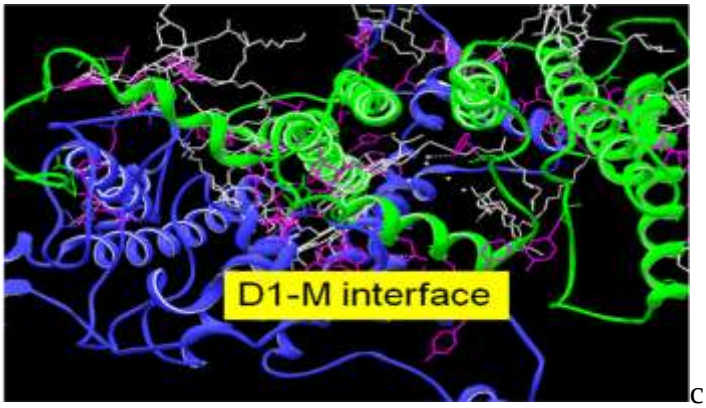

c

Figure 3.13 The modeling of the possible interaction from D1 and the others photosynthetic proteins, lipids and cofactors

However the backbone of the two protein fold high compatibility in the 190-291 region (approximate 25% of identity). There are some deviations of this compatibility just in the Qb loop (Figure 3.14).

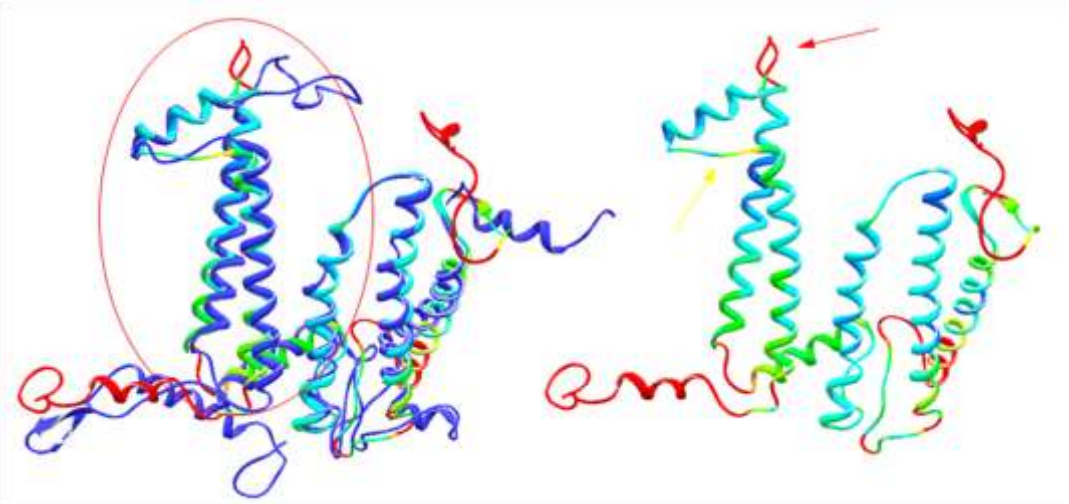

Figure 3.14 Feasibility of construction chimera: backbone fold highly compatible in the 190-291 region (approximately 25% of identity), higher deviation is in loop regions indicated of the warm colors.

It is possible to replace the specific L protein sequence with the D1 protein, from 182 to 202 residues; from 205 to 238 residues of L protein must be substitute with the specific sequence of D1 from 207 to 227 residues, from 244 to 282 residues, but the loop it is very important for the Qb binding. In conclusion the best hypothesis resulted the loop grafting from Rhodobacter 220-230 L sequence with the 259-271 Chlamydomonas D1 sequence.

A further bioinformatics analysis was led in collaboration with Mike R. Jones of School of Biochemistry, Medical Science, University of Bristol, confirming the previous analysis therefore we finally decided to replaced the Rhodobacter sequence from Glycine in 221 position to Isoleucine 229 with the D1 sequence present in Qb binding site from 260 to 271(FQYASFNNSRS) (Figure 3.15)

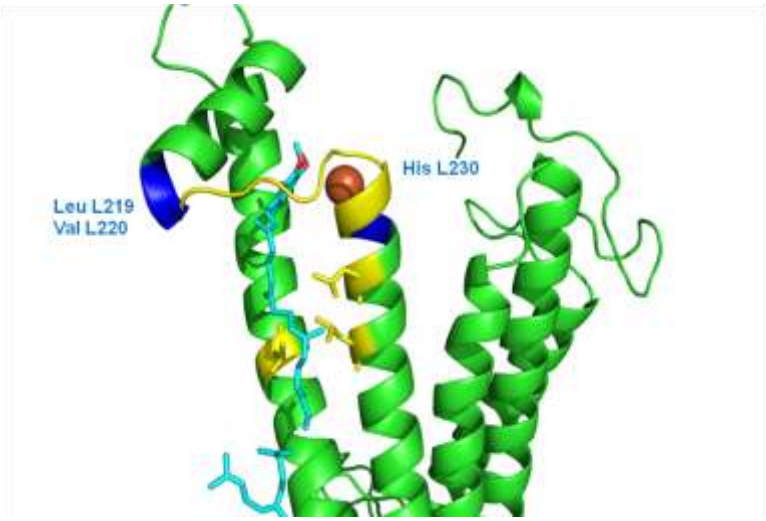

Figure 3.15 Loop grafting replecement modeling representation of Rhodobacter aminoacid G^{221}YSIGTLGI^{229} sequence with Chlamydomonas F^{260}QYASFNNSRS^{271}

Amino acids are encoded by triplets of RNA (DNA in genes). Because DNA and RNA are composed of 4 different nucleotides, there are 64 possible triplets (codons) combinations of these 4 nucleotides. With only 20 amino acids, there is approximately a 3-fold excess of triplet combinations available to encode these amino acids. In most organisms the codons for a given amino acid are not equally used; some triplets are used more frequently, other some triplets are used only rarely. The pattern of usage differs, however, between different genes and between organisms. The design of the *Chlamydomonas* sequence encoding the aminoacidic Qb binding niche was carried out by exploiting bioinformatic tools using the *R. sphaeroides* codon usage

The sequence (TTCCAGTACGCCTCGTTCAACAACTCGCGCTCGCTG (Chlamy-sequence) includes a part of L protein of the bacterium (Tranformation Chlamy construct), as reported in Figure 3.16.

The sequence has been achieved by a PCR procedure and cloned in the pCR2.1® TOP vector between the restriction sites EcoRV and SalI, important for the introduction in plasmid.

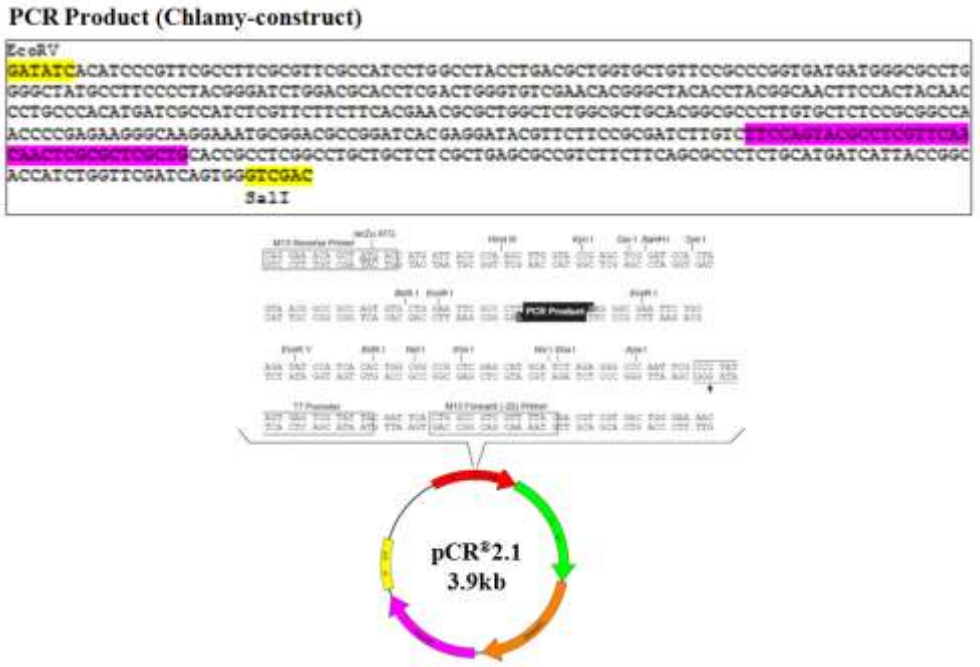

Figure 3.16 Transformation construct designed and producted with *R.sphaeroides* codon usage in pCR®2.1, TOP*E.Coli* TOP10; at the ends of transformation sequence they are present two restriction site, one for EcorV and one for SalI.

3.2.3 Chimera creation

After amplification in *E.coli* DH5α cells, the plasmid was extracted and the fragment sub-cloned into modify plasmid pUC19 (plasmid called pUCXB): In the gel shown in Figure 3.17 it is possible to see the EcoRV-Sal digests in lanes 3 and 4 of the pCR2.1® TOP and pUCXB plasmid. To check the correctly DNA transfer, the DNA sequencing was carried out.

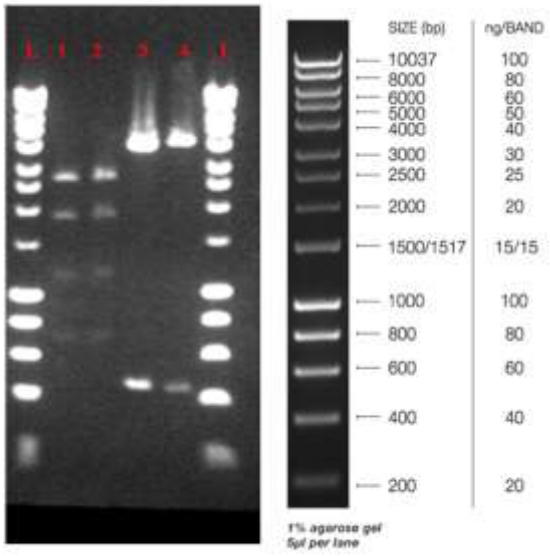

Figure 3.17 In this figure it is shown the EcoRV-SalI digests (the lower band should be 424 bp, and is running just above the 400 bp) marker in lanes 3 and 4 of the pCR2.1® TOP and pUCXB plasmid, and XbaI-BamHI restriction digestion in lanes 1 and 2 showing XbaI/BamHI digests. the top band is the pUCXB plasmid at 2700bp, the next band is the XbaI—BamHI fragment at 1850 bp It was used HyperladderI as size marker

pUCXB plasmid has three restriction sites which are not in the original puf operon, an EcoRV site at position 2011bp, a PstI site at position 2752bp and a SacI site at position 3208bp. A map of the puf operon mutated is in Figure 3.18 and it is possible to see XbaI-BamHI fragment encompassing pufLM.

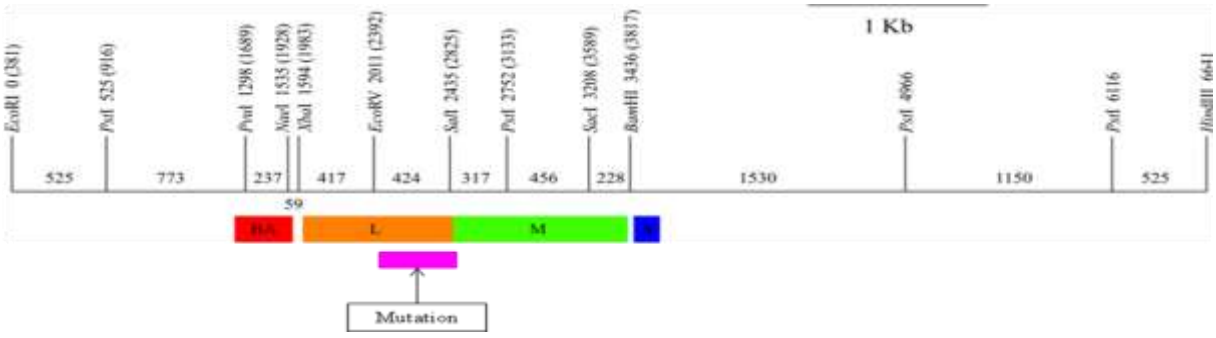

Figure 3.18 pUCXB derived from pUC19 with the gene coding reaction center and plus 3 restriction site EcoRV, PstI, SacI. Chlamy sequence was introduce by enzymatic digestion.

The new generated mutant was subjected to XbaI-BamHI restriction digestion (lanes 1 and 2in the Figure 3.17) . show XbaI/BamHI digests of the two clones we checked by sequencing, called GR02 and GR03. the top band is the pUCXB plasmid at 2700bp, the next band is the XbaI—BamHI fragment at 1850 bp), and the produced fragment was cloned into the two expression plasmids called pRKEH10 (Figure2.6a) and pRKEH10D (Figure 2.6b) containing the *puf*LMX..

These plasmids have two different versions of the full EcoRI-HindIII Rhodobacter restriction fragment cloned into a broad host range vector called pRK415. Neither of these plasmids have the PstI site at position 2752, but they acquire a PstI site when we replace the wild type XbaI-BamHI restriction fragment with the mutated one.

Plasmid pRKEH10 has the full puf operon which includes genes *pufBALM* and *X*. Plasmid pRKEH10D has the section between the PvuI site at 1298 and the NaeI site at 1535 missing, so only has *PufLMX* (pufBA are missing, it do not code the antenna LH1).

In order to check the success of these cloning, a restriction analyses with the PstI enzyme has been carried out. Neither of these plasmids have the PstI site at the cloning site position 2752, but (see above) it can be created replacing the wild type XbaI-BamHI restriction fragment with the mutated one. In pRKEH10, the digestion profile on agarose gel indicated the occurrence of 4 PstI-PstI bands up 8000bp, one at 1,150 bp and two closely-spaced bands at 2227 and 2214 (Figure 3.19, lanes 1-3). In case of no cloning, the PstI site at 2752 is missed and just 3 bands will appear.

In pRKEH10D plasmid (Figure 3.19, lanes 4-6 on the right on the gel) has Pst-Pst bands at 2214 and 1930, would be a single band instead at 4204.

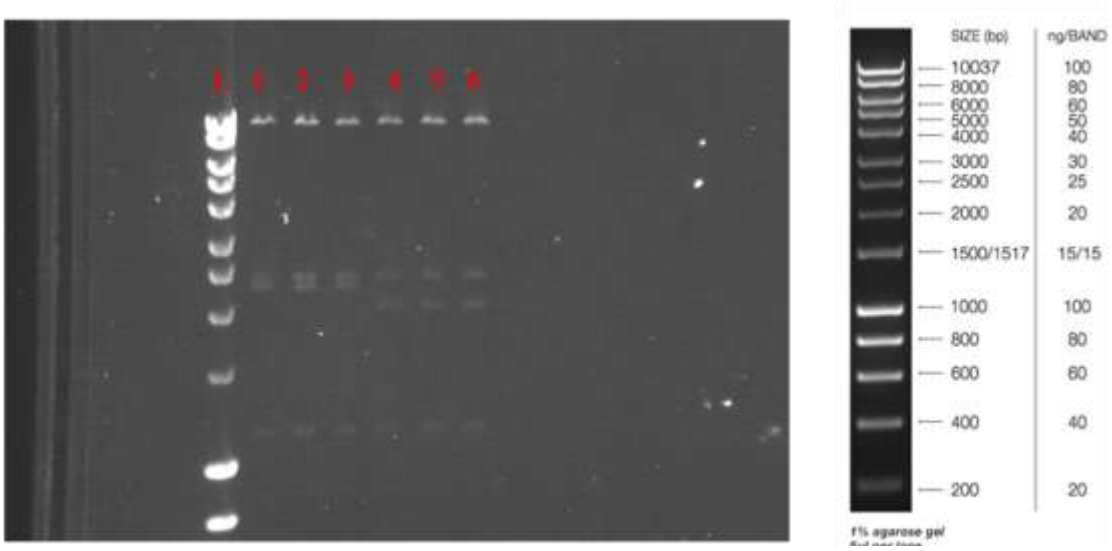

Figure 3.19 Electrophoresis PstI digestion: pRKEH10 (three on the left) it possible to see 4 Pst-Pst bands, the heavy (up 8000bp) one and one at 1150 bp, then two closely-spaced bands at 2227 and 2214 were present. If it hasn't worked the Pst site at 2752 will be missing and just 3 bands would be. In pRKEH10D plasmid (three on the right) are presented Pst-Pst bands at 2214 and 1930, if not would be a single band instead at 4204. It was used HyperladderI as size marker

S17-1 *Escherichia coli* was transformed with pRKEH10 and pRKEH10D and by diparental filter mating transformation of *R.sphaeroides* DD13 to obtain 2 chimeras, one containing only the RC and second one the RC plus the LH1 antenna.

After extraction of the photosynthetic membranes by sucrose gradient extraction, they were characterized by spectroscopy (Figure 3.20). The spectra reported in Figure 3.20a, indicates the that RCs are present, even if the expression level is very much lower compared to the wild-type. In addition, in the figure is possible to see an extra peak absorbance at ~760 nm (the green spectrum is just a blow-up of the black one) which indicated. The occurrence of free bacteriochlorophyll, maybe due to assembling problems. The lower expression level can also be seen in the LH2-deficient membranes (Figure 3.20b). The graph shows that the RC band at 800 nm is much less pronounced in the black spectrum than in the red one (wild type), this is a small effect than you might expect from the RC-only spectrum, perhaps because LH1 helps to stabilize the "sick" RC.

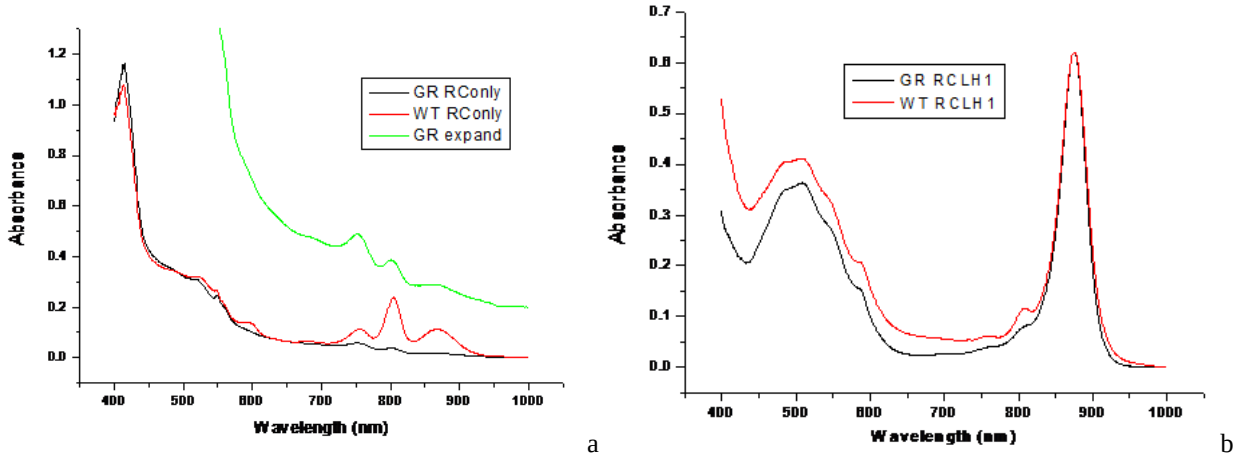

Figures 3.20 Memebrane Spectra: in RC only strain (a) the expression level of the mutant is very much lower than normal and there is extra absorbance at ~760 nm. In strain with LH1 (LH2-deficient membranes)(b) RC band at 800 nm is much less pronounced in the black spectrum than in the red.

4.Conclusion

The possibility of producing this new generation of technological devices that integrate the knowledge coming from various fields (chemistry, biology, computer science, electronics, engineering) is attracting increasing attention. Thanks also a new technological science called "molecular electronics" or "nanotechnology". It is a technology based on the use of molecular scale components such as a single or a few molecules, carbon nanotubes, nanoscale metallic and/or semiconductor wires, etc. that function as electronic components [3]. Biosensors were developed to meet the demand for analytical instrumentation at low cost, robust, sensitive, compact, easy to use, as a fast *in situ* measurement.

In our case for the pesticide detection, the photosynthetic organisms help us thanks the interaction between these molecules and the photosystem II apparatus, in fact some pesticides are able to inhibit PSII, are especially suitable because of their physiological activities can be easily monitored by amperometric, potentiometric and optical systems.

Although conventional techniques such as HPLC and GC still represent the best solution for more accurate analyses, most of them are time consuming, especially in the case of routine analyses, and require very expensive equipments. For this reason our biosensor is specifically intended for an easy, low-cost, and fast pre-screening of photosynthetic herbicides in water samples.

The construction of photosynthetic-based devices requires a multidisciplinary approach where the device is obtained in various stages: first of all the physiology of the photosynthetic organism should be considered since it is essential before designing the biodevice, for instance the biomediator should be guarantees the stability of biosensors for monitoring herbicides.

The second stage is the isolation of the biomediator, its stabilization and immobilization by biochemical and chemical techniques. Using molecular biology, mutations on PSII that produce specific properties can be carried out: e.g., a modification of a single amino acid on D1 protein generates a resistance towards herbicide subclasses. Then bioinformatics is then applied to optimize the molecular modifications on the biomediator. The next stage is the study of suitable transduction systems for the detection of the chosen PSII activity and the analyses of the data. Finally, biosensor prototypes for specific applications are designed (e.g., field portable, device for laboratory, miniature size prototype etc.) [3].

Photosynthetic based biosensors are not immune to problems and difficult in realization: 1)problems related to the variability of biological element especially if it is a life organism (growth condition, strain, manipulation, etc.); 2) problems related to possible photosynthetic apparatus

extraction steps (time consuming, and in is necessary expensive machines); 3) improvement the sensitivity and stability of biologic elements, usually it is a big challenge, and requires working on the setup of biosensor (immobilization, buffer, flux, and so on) and on biomediator genetic engineering; 4) immobilization methods, it is necessary to develop a technique compatible with biologic material that does not compromise the photosynthetic signal and the biosensor performance.

In my PhD project all these issues have been addressed to have a stable and sensitive biosensor able to detect pesticides for possible future commercial uses too. We have chosen two well-known photosynthetic microorganisms *(Chlamydomonas reinhardtii and Rhodobacter sphaerodies*) used in different fields of application, also in biosensoristic one.

To avoid the photosynthetic apparatus extraction and permit a rapid procedure to produce SPE immediately usable and disposable, we focused our efforts to develop a *C.reinhardtii* whole cells immobilization protocols, using two polymers Nafion® and Algiante, the last one showed the best results. Thus the effect of two pesticides on algal photosynthetic performance was analyzed and, linuron and simazine LOD of ~ $6*10^{-9}$ and $9*10^{-8}$ M respectively was determinated. Concerning the stability of the biomediator, a reduction of 25% of initial signal was verified after 20 days of storage at RT. The analysis of inhibition and recovery data lead to the conclusion of a possible Qc binding site in according with recent literature. Using *C.reinhardtii* mutants close Qc binding site it is expected to enhance the sensitivity of the biosensor.

A parallel experimental line, were the production of a chimeric RC with a native *Chlamydomonas reinhardtii* sequence able to improve sensitivity toward the herbicides, maintaining the characteristic stability of this *Rhodobacter spahaeroides*, was followed. After a bionformatic feasibility study, we decided to replace a *R.sphaerodes* native sequence (in the Qb binding loop) with a part of *C.reinhardtii* Qb binding site sequence. Chimeric reaction centres were succesfully created. Some assembly or stability problems seems perhaps to exist in the chimeric formand further analyses will be carried out in order to verify the photosynthetic functionality of these new strains.

The next step will be RC extraction and purification to check its real stability in term of protein folding, after the herbicide binding test will be necessary to verify if the herbicides affinity is really improved as expected by the bioinformatic model. That will develop of a new aperometric biosensor system to detect low concentration of pollutants in the environment.

Finally we can conclude that from two parallel research lines followed we satisfied our purpose of obtaining a stable biosensor based on *Chlamydomonas reinhardtii* whole cells capable of detecting

low concentrations of herbicides and a potential biomediator based on *Rhodobacter sphaeroides* chimer.

5. References

[1] Thevenot D. R., Tòth K., Durst R. A.,. Wilson G. S, 1999 Electrochemical Biosensors: Recommended Definitions and Classification Pure Appl. Chem. 71 2333

[2] Duglas V, Elaissari A., Chevalier Y., 2010 Surface Sensitization Tecniques and Recognition Receptors Immobilization on Biosensor and Microarrays In Recognition Receptors in Biosensors- Eds Zourob M. Springer

[3] Giardi M.T., 2005 Introduction: The Emergence of a new Technology In Technological applications of Photosynthetic proteins, Eds M.T. Giardi and E. Piletska. Landes Bioscience/ eurekah.com, Georgetown, Texas, U.S.A

[4] Cavalcanti A, Shirinzadeh B, Zhang M, Kretly LC, 2008. Nanorobot Hardware Architecture for Medical Defense. Sensors 8 (5): 2932–2958

[5] Mascini M., 2005 A Brief Story of Biosensor technology In Technological applications of Photosynthetic proteins, Eds M.T. Giardi and E. Piletska. Landes Bioscience/ eurekah.com, Georgetown, Texas, U.S.A.

[6] Rouillon R., Piletsky S.A., Piletska E.V., Euzet P., Carpentier R., 2005, Comparison of the Immobilization Techniques for Photsystem II, In Technological applications of Photosynthetic proteins, Eds M.T. Giardi and E. Piletska. Landes Bioscience/ eurekah.com, Georgetown, Texas, U.S.A.

[7]Spichiger-Keller U. E., 1998 Chemical Sensors and Biosensors for Medical and Biological Applications, Willey-VCH

[8] Newman J.D., Turner A.P.F., 2005 Home Blood Glucose Biosensors: A Commercial Perspective Biosensors and Bioelectronics. 20, 2435-2453

[9] Vo-Dinh T. and Cullum B. Biosensors and biochips: advances in biological and medical diagnostics, 2000 Fresenius Journal of Analytical Chemistry 366, 6-7

[10] Touloupakis E, Giannoudi L., Piletsky S.A.,. Guzzella L,. Pozzoni F,. Giardi M.T, 2005 A multi-biosensor based on immobilized Photosystem II on screen-printed electrodes for the detection of herbicides in river water Biosensors and Bioelectronics 20, 1984–1992

[11] Hofstadler S.A., Sampath R., Blyn L.B., Eshoo M.W., Hall T.A., Jiang Y., Drader J.J., Hannis J.C., Sannes-Lowery K.A., Cummins L L., Libby B., Walcott D.J., Schink A., Massire C., Ranken R., Gutierrez J., Manalili S., Ivy

C., Melton R., Levene H., Barrett-Wilt G., Li F., Zapp V., White N., Samant V., McNeil J.A., Knize D., Robbins D., Rudnick K., Desai A., Moradi E. and Ecker D.J., 2005 TIGER: the universal biosensor. International Journal of Mass Spectrometry 242 (1): 23-41

[12] Pohanka M, Skladal P, Kroca M., 2007 Biosensors for biological warfare agent detection. Def. Sci. J. 57(3):185-93.

[13] Ravindra N. M., Prodan C., Fnu S., Padronl I. and Sikha S.K. (2007) Advances in the manufacturing, types, and applications of biosensors JOM Journal of the Minerals, Metals and Materials Society 59, 37-43

[14] Johanneke L. H. C. Busch, Karel Hrncirik, Emily Bulukin, Claire Boucon, and Marco Mascini 2006 Biosensor Measurements of Polar Phenolics for the Assessment of the Bitterness and Pungency of Virgin Olive Oil J. Agric. Food Chem., 54 (12), pp 4371–4377

[15] Turner, A.P.F ., Karube, I. & Wilson, G .S .(ed.) (1987) . In : Biosensors: Fundamentals & Applications, Oxford University Press, Oxford, UK

[16] Watson, L.D ., Maynard, P ., Cullen, D.C ., Sethi, R.S ., Brettle, J. & Lowe, C.R . (1987/88). A microelectronic conductimetric biosensor, Biosensors, 3, 101-115 .

[17] Blum L.J., Coulet P. R. 1991. Eds Biosensor Principles and Applications (Biotechnology and Bioprocessing) Marcel Dekker Inc

[18] Newman JD, Setford SJ: 2006 Enzymatic biosensors.Mol. Biotechnol. 32:249–268.

[19] Buerk DG: Biosensors. 1993 Theory and Applications. Technomic Publ. Co., Lancaster, Pennsylvania. p. 54

[20] Bergveld, P . 1970 . Development of an ionsensitive solid state device for neurophysiological measurements, IEEE Trans. Biomed. Eng., BME- 17, 70-71

[21] Bergveld, P. 2003. Thirty Years of isfetology What Happened in the Past 30 Years and What May Happen in the Next 30 Years. Sens. Actuators B, 88, 1-20.

[22] Eggins B.R. 2002. Chemical Sensors and Biosensors (Analytical Techniques in the Sciences (AnTs)) Willey-VCH

[23] Belluzo M.S., Ribone M.É. and Lagier C.M. 2008 Assembling Amperometric Biosensors for Clinical Diagnostics Sensors, 8, 1366-1399

[24] Pinalysa C. Longobardi F., Agostiniano A. 2005 Signal Transduction Techniques for Photosynthetic Proteins, Eds M.T. Giardi and E. Piletska. Landes Bioscience/ eurekah.com, Georgetown, Texas, U.S.A

[25] Pohanka M, Skládal P. 2008 Electrochemical biosensors – principles and applications. Review. J Appl Biomed. 6:57-64

[26]Belluzo M.S., Ribone M. É. and Lagier C. M. 2009 Assembling Amperometric Biosensors for Clinical Diagnostics-Review Sensors 8, 1366-1399

[27] Prodromidis M.I. and Karayannis M.I. 2002 Enzyme Based Amperometric Biosensors for Food Analysis-Review, Electroanalysis 14 (4) 241-261

[28] Mozas S.R, Marco M-P, Lopez de Alda M.J., Barcelo D. Biosensor for environmental application: future development trends-Review 2004 Pure Appl. Chem. 76(4)723-752

[29] Buonasera K., Pezzotti G., Scognamiglio V., Tibuzzi A. and Giardi M.T: 2010 New platform for prescreening of pesticides residues to support laboratory analyses J. Agric. Food Chem 58, 5982–5990

[30] Kissinger, P.T.; Heineman, W.R. 1983 Cyclic voltammetry J. Chem. Educ. 60, 702

[31] Van Benschoten, J.J.; Lewis, J.Y.; Heineman, W.R.; Rosten, D.A.; Kissinger, P.T. J.. **1983**, Cyclic voltammetry experiment Chem. Educ., 60, 772

[32] Mabbott, G.M., An introduction to cyclic voltammetry 1983 J. Chem. Educ. 60, 697.

[33] Baldwin, R.P.; Ravidhandran, K.; Johnson R.K. 1984 A cyclic voltammetry experiment for the instrumental analysis laboratory J. Chem. Educ. 61, 820

[34] Rajinder S.S 1994 Transducer Aspect of Biosensors Biosensor and Bioelectronics 243-264

[35] Ngeh-Ngwainbi J, Suleiman AA, Guilbault GG. 1990. Piezoelectric crystal biosensors. Biosensor and Bioelectronics 5(1):13-26.

[36] Patel P. N., Mishra V., Mandloi A. S., 2010 Optical biosensors fundamentals and trends JERS Vol. I Issue I July-Sept. 2010/15-34

[37] Singh, M.; Verma, N.; Garg, A. K. & Redhu, N. 2008. Urea biosensors. Sensors and Actuators B-Chemical, 134, 345-351

[38] Eggins, B. R. 1996. Biosensors: an introduction, Wiley

[39] Nunes, G. S. & Marty, J. L. 2006. Immobilization of Enzymes on Electrodes Immobilization of Enzymes and Cells (Methods in Biotechnology). J. M. Guisan. Totowa, NJ, Humana Press Inc. :239.

[40] Castillo M., Alonso M. C., Riu J., Reinke M., Kloter G., Dizer H., Fischer B.,. Hansen P. D, Barcelo D.. 2001 Identification of cytotoxic compounds in European wastewaters during a field experiment Anal. Chim. Acta 426, 265–277.

[41] Choi J.-W.,. Kim Y.-K, Lee I.-H., Min J., Lee, W. H. 2001Optical organophosphorus biosensor consisting of acetylcholinesterase/viologen hetero Langmuir–Blodgett filmBiosens. Bioelectron. 16, 937–943

[42] Andreou V. G. and. Clonis Y. D. 2002. A portable fiber-optic pesticide biosensor based on immobilized cholinesterase and sol–gel entrapped bromcresol purple for in-field use Biosens. Bioelectron. 17, 61–69.

[43] Andres R. T. and Narayanaswamy R. 1997. Fibre-optic pesticide biosensor based on covalently immobilized acetylcholinesterase and thymol blue Talanta 44, 1335–1352

[44] Mulchandani A, Chen W., Mulchandani P., Wang J., Rogers K. R.. Biosensors for direct determination of organophosphate pesticides Biosens. Bioelectron. 16,225–230 (2001).

[45] Cosnier S. , Innocent C. 1993 A new strategy for the construction of a tyrosinase-based amperometric phenol and o-diphenol sensor. Bioelectrochemistry and Bioenergetics 31 (2), 147-160

[46] Mozaz S.R., Lopez de Alda M.J. and Barceló D. 2006 Biosensors as useful tools for environmental analysis and monitoring Anal.Bioan Chem Anal. and Bioan. Chem. 386 (4) 1025-1041

[47] Thomas S.W.III, and Swager T. M. 2006 Trace Hydrazine Detection with Fluorescent Conjugated Polymers: A Turn-On Sensory Mechanism Adv. Mater., 18, 1047–1050

[48] Noguer T., Marty J.L. 1997 High sensitive bienzymic sensor for the detection of dithiocarbamate fungicides Anal. Chim. Acta 347, (1-2), 63-70

[49] Giardi M.T. , Koblízek M., Masojídek J. 2001 Photosystem II-based biosensors for the detection of pollutants Biosens. Bioelectronics 16(9-12) 1027-1033

[50] Buonasera K., Lambreva M., Rea G., Touloupakis E. and . Giardi M. T 2011 Technological applications of chlorophyll a fluorescence for the assessment of environmental pollutants Anal. and Bioanal. Chem. 401(4)1139-1151

[51] Koblízek M, Malý J, Masojídek J, Komenda J, Kucera T, Giardi MT, Mattoo AK, Pilloton R. 2002A biosensor for the detection of triazine and phenylurea herbicides designed using Photosystem II coupled to a screen-printed electrode. Biotechnol Bioeng. Apr 5;78(1):110-6.

[52] Stryer L, 1995 "The photosynthesis" in *Biochemistry*, chapt. 26, 4th ed., W . H. Freeman and Company, New York and Basingstoke.

[53] Nagyvary J., Bechert J., 1999 Biochem. Edu. 27, 193

[54] Rawn J. D., 1988 "The photosynthesis" in Biochemistry, vol. I, chapt. 18, p. 489, McGraw-Hill.

[55] The photobiology" (G. Forti Ed.), (1989) Le Scienze (italian edition of Scientific American), vol. 46.

[56] Hu X., Damjanovic A., Ritz T. and Schulten K., 1998 Proc. Natl. Acad. Sci. USA 95, 5935.

[57] Cogdell R., Fyfe P., Barrett S., Prince S., Freer A., Isaacs N., McGlynn P. and Hunter C., 1996 Photosynth. Res. 48, 55.

[58] Guskov A., Kern J., Gabdulkhakov A., Broser M., Zouni A., Saenger W., 2009Cyanobacterial photosystem II at 2.9-A resolution and the role of quinones, lipids, channels and chloride. Nat. Struct. Mol. Biol. 16(3), 334-342

[59] Kaminsakaya O., Shuvalov V. A., Renger G., 2007 Evidence for a novel quinone-binding site in the photosystem II (PS II) complex that regulates the redox potential of cytochrome b559 Biochemistry 46, 1091-1105.

[60] Fyfe P. K.,. Isaacs N. W, Codgell R. J., Jones M. R., 2004, Biochim. Biophys. Acta 1608 11.

[61] Feher, G., J. P. Allen, M. Y. Okamura, and D. C. Rees. 1989. Structure and function of bacterial photosynthetic reaction centers. Nature (London) 339:111-116.

[62] Govindjee, 1982 "Purple bacteria" in Photosynthesis energy conversion by plants and bacteria (Govindjee Ed.), chapt. 4 p.81, Academic Press, New York.

[63] Ackerman F. 2007The Economics of Atrazine. Intl. J. Occup. Environ. Health 13, 441-449.

[64] European Commission. Opinion of the Scientific Committee on Plants on specific questions from the Commission concerning the evaluation of atrazine in the context of council directive 91/414/EEC. Brussels, Belgium: Health and Consumer Protection Directorate-General.

[65] Wackett L. PSadowsky., M. J., Martinez B., Shapir N., 2002, Biodegradation of atrazine and related s-triazine compounds: from enzymes to field studies Appl. Microbiol. Biotechnol. 58 39–45.

[66] Rodriguez-Mozaz S., Lopez de Alda M. J., Barceló D., 2006 Biosensors as useful tools for environmental analysis and monitoring.Anal Bioanal Chem 386 1025–1041.

[67] Moreland D. E., 1993 Research on biochemistry of herbicides:, Z. Naturforsch 48c 121

[68] Giardi M. T., Koblizek M., Masojidek J. 2001 Photosystem II-based biosensors for the detection of pollutants Biosensors and Bioelectronics 16, 1027..

[69] Giardi M. T., Pace E., 2005 A review: Photosynthetic proteins for technological applications Trends in Biotechnology 23(5), 257-263

[70] Scognamiglio V., Pezzotti G., Pezzotti I., Cano J., Buonasera K., Giannini D. and. Giardi M. T, 2010 Biosensors for effective environmental and agrifood protection and commercialization: from research to market Microchim. Acta 170, 215

[71] Varsamis D. G., Touloupakis E., Morlacchi P., Ghanotakis D. F. , Giardi M. T. and Cullen D. C., 2008 Development of a photosystem II-based optical microfluidic sensor for herbicide detection Talanta 77(1), 42-47.

[72]. Giardi M.T,.Scognamiglio V, Rea G., Rodio G.,.Antonacci A, Lambreva M., G.Pezzotti, Johanningmeier U. 2009 Optical biosensors for environmental monitoring based on computational and biotechnological tools for engineering the photosynthetic D1 protein of Chlamydomonas reinhardtii Biosensors and Bioelectronics 25 294–300

[73] Mallardi A., Giustini M., Lopez F., Dezi M., Venturoli G., Palazzo G., 2007 Functionality of photosynthetic reaction centers in polyelectrolyte multilayers: toward an herbicide biosensor.J. Phys. Chem. B 111, 3304-3314.

[74] Bettazzi F., Laschi S., Mascini M., 2007One-shot screen-printed thylakoid membrane-based biosensor for the detection of photosynthetic inhibitors in discrete samples. Analytica Chimica Acta 58914–21

[75] Maly J., Masojidek J., Masci A., Ilie M., Cianci E., Foglietti V., Vastarella W., Pilloton R., 2005 Direct mediator less electron transport between the monolayer of photosystem II and poly(mercapto-p-benzoquinone) modified gold electrode--new design of biosensor for herbicide detection. Biosensors and Bioelectronics 21, 923–932.

[76] Masojìdek J., Soucek P., Màchovà J., Frolìk J., Klem K., Maly J., 2011 Detection of photosynthetic herbicides: algal growth inhibition test vs. electrochemical photosystem II biosensor. Ecotoxic. Environ. Safety 74, 117–122.

[77] Koblitzek M., Maly J., Masojidek J., Komenda J., Kucera T., Giardi M. T., Mattoo A. K. and Pilloton R., 2002 A biosensor for the detection of triazine and phenylurea herbicides designed using Photosystem II coupled to a screen-printed electrode Biotechnol. Bioeng. 78, 110.

[78] Harris E. H, The Chlamydomonas sourcebook, 2nd edn. 2009 vol. 1, chapt. 1, "The Genus Chlamydomonas", p. 1 24, Elsevier, Oxford, U.K..

[79] Tibuzzi A, Rea G, Pezzotti G, Esposito D, Johanningmeier U and Giardi MT 2007 A new miniaturized multiarray biosensor system for fluorescence detection. J. Phys.: Condens. Matter 19-395006

[80] Zhao J., Liu B., Zou Y., Xu C., Kong J., (2002) Photoelectric conversion of photosynthetic reaction center in multilayered films fabricated by layer-by-layer assembly-Electrochimica Acta 47- 2013-2017

[81] Shitanda I., Takada K., Sakai Y., Tatsuma T., 2005Compact amperometric algal biosensors for the evaluation of water toxicity, Analytica Chimica Acta 530, 191–197

[82] Shitanda I., Takamatsu S., Watanabe K., Itagaki M., 2009 Amperometric screen-printed algal biosensor with flow injectionanalysis system for detection of environmental toxic compounds. Electrochimica Acta 54, 4933–4936.

[83] Lu J., Drzal L.T., Worden R.M. and Lee I., 2007 Simple Fabrication of a Highly Sensitive Glucose Biosensor Using Enzymes Immobilized in Exfoliated Graphite Nanoplatelets Nafion Membrane, Chem. Mater. 19, 6240–6246

[84] Gogol E.V.,. Evtugyn G.A,. Marty J.-L,. Budnikov H.C,. Winter V.G, 2000 Amperometric biosensors based on nafion coated screen-printed electrodes for the determination of cholinesterase inhibitors,
Talanta 53, 379–389.

[85] Moreno-Garrido I., 2008 Microalgae immobilization: Current techniques and uses**,** Bioresource Technology 99, 3949–3964

[86] Church, Steven 2006 Del. firm installs fuel cell. The News Journal. p.B7.

[87] Moore C. M., Nick A. L. ; Hill A. D.; Johnson Z. C.; Minteer S. D. 2004 Improving the environment for immobilized dehydrogenase enzymes by modifying Nafion with tetraalkylammonium bromides Biomacromolecules 5, (4) 1241-1247

[88] Rishpon J., Gottesfeld S., Campbell C., Davey J., Zawodzinski Jr. T. A. 2005 Amperometric glucose sensors based on glucose oxidase immobilized in nafion Electroanalysis 6(1)17-21

[89] Coppi, G., Iannuccelli, V., Leo, E., Bernabei, M.T. and Cameroni, R. 2002. Protein immobilization in crosslinked alginate microparticles. J. Microenc. 19, 37-44.

[90] Tumturk, H., Demirel, G., Altinok, H., Aksoy, S. and Hasirci, N. 2008. Immobilization of glucose isomerase in surface-modified alginate gel beads. J. Food Biochem. 32, 234-246.

[91] Sriamornsak, P. 1998. Preliminary investigation of some polysaccharides as a carrier for cell entrapment. Eur. J. Pharm. Biopharm. 46, 233-236.

[92] Johanningmeier U. and Heiss S., Construction of a Chlamydomonas reinhardtii mutant with an intronless psbA gene Plant Mol. Biol. 22 (1993), 91-99.

[93] Gorman , D.S. and Levine , R.P. 1965. Cytochrome f and plastocyanin: their sequence in the photosynthetic electron transport chain of Chlamydomonas reinhardi . Proc. Natl. Acad. Sci. U. S. A. 54 , 1665 – 1669 .

[94] Hutner , S.H. , Provasoli , L. , Schatz , A., and Haskins , C.P. 1950. Some approaches to the study of the role of metals in the metabolism of microorganisms . Proc. Am. Philos. Soc. 94 , 152 – 170 .

[95] Porra, R.J., Thompson, W.A., Kriedemann, P.E., 1989. Determination of accurate extinction coefficients and simultaneous equations for assaying chlorophyll a and b extracted with four different solvents: verification of the concentration of chlorophyll standards by atomic absorption spectroscopy. Biochim. Biophys. Acta, 975, 384-394.

[96] Walker D.A., Preparation of higher plant chloroplasts. In: Methods in Enzymology (1980), , A. San Pietro ed., Academic Press, New York, 69, 94-104.

[97] Veer, B. V.D. and Bolier G. 1991. Improvement in accuracy of the interpretation of algal growth. Verh. Int. Ver. Limnol. 24, 1272-1276.

[98] Strasser R. J., Srivastava A., Tsimilli-Michael M., 2000 The fluorescence transient as a tool to characterize and screen photosynthetic samples. In: Probing Photosynthesis: Mechanism, regulation and adaptation 443–480. M. Yunus, U. Pathre, P. Mohanty eds, London: Taylor and Francis, UK.

[99] Tibuzzi A.,. Pezzotti G, Lavecchia T., Rea G., and Giardi M. T., A portable Light –Excitation Equipped Bio Amperometer for Electrogenic Biomaterials to Support the Technical Development of Most Biosensors, Sensors & Transducers Journal, 88(2) (2008), 9-20.

[100] Topp E., Smith W., 1992 Sorption of the herbicides atrazine and metolachlor to selected plastics and silicone rubbeJ. Environ. Qual. 21 316-317.

[101] Melis, A., Neidhardt, J., Benemann, J.R.,1999"Dunaliella salina (Chlorophyta) with small chlorophyll antenna sizes exhibit higher photosynthetic productivities and photon use efficiencies than normally pigmented cells"J. Appl. Phycol. 10, 515-525.

[102] Rea G, Polticelli F., Antonacci A., Scognamiglio V. ,Katiyar P., Kulkarni S.A., Johanningmeier U., Giardi M.T. 2009 Structure-based design of novel *Chlamydomonas reinhardtii* D1-D2 photosynthetic proteins for herbicide monitoring 18(10)2139-2151

[103] Jones MR, Heer Dawson M, Mattioli TA, Hunter CN, Robert B 1994 Site-specific mutagenesis of the reaction centre from Rhodobacter sphaeroides studied by Fourier transform Raman spectroscopy: Mutations at tyrosine M210 do not affect the electronic structure of the primary donor. FEBS Lett 339 18–24

[104] McAuley-Hecht KE, Fyfe PK, Ridge JP, Prince SM, Hunter CN, Isaacs NW, Cogdell RJ and Jones MR Structural studies of wild-type and mutant reaction centers from an antennadeficient strain of Rhodobacter sphaeroides: Monitoring the optical properties of the complex from cell to crystal. Biochemistry 37 (1998) 4740–4750

[105] Ogden, R.C., and Adams, D.A., 1987 Electrophoresis in agarose and acrylamide gels. Methods Enzymol., 152, 61-87

[106] Biggin M D, Gibson T J, Hong G F 1983 Buffer gradient gels and 35S label as an aid to rapid DNA sequence determination Biochemistry 80, 3963-3965

[107] Tessier D.C., Brousseau R., Vernet T.1986 Ligation of single-stranded oligodeoxyribonucleotides by T4 RNA ligase Analytical Biochemistry 158 (1) 171–178

[110] Jones MR, Fowler GJS, Gibson LCD, Grief GG, Olsen JD, Crielaard W and Hunter CN 1992a Construction of mutants of Rhodobacter sphaeroides lacking one or more pigment–protein complexes and complementation with reaction-centre, LH1, and LH2 genes. Mol Microbiol 6: 1173–1184

[111] Jones MR, Visschers RW, van Grondelle R and Hunter CN 1992b Construction and characterisation of a mutant of Rhodobacter sphaeroides with the reaction centre as the sole pigment–protein complex. Biochemistry 31: 4458–4465

[112] Lud S.Q., Nikolaides M.G., Haase I., Fischer M. and Bausch A.R. 2006. Field Effect of Screened Charges: Electrical Detection of Peptides and Proteins by a Thin Film Resistor. ChemPhysChem 7(2), 379-384

[113] Kong J, Lu Z., Vov Y.M.L, Desamero R Z.B., Frank H.A., and Rusling J.F. 1998 Direct Electrochemistry of Cofactor Redox Sites in a Bacterial Photosynthetic Reaction Center Protein J.Am.Chem.Soc. 120, 7371-7372

[114] Seago JL - 1985 Biological detection process using polymer-coated electrodes US Patent 4,517,291

[115] Seago JL – 1986 Perfluorosulfonic acid polymer-coated indicator electrodes US Patent 4,604,182

[116]. Clarke D.J, R. C. Michael, Carr R.J.G., Blake-Coleman B.C.,S. Moody.C, A. C. Timothy 1985 The development and application of biosensing devices for bioreactor monitoring and control 1(3)213-320

[117] Arnold M.A.., Meyerhoff M.E. 1984 Ion-selective electrodes Anal. Chem., 56(5) 20-48

[118] Litescu S.C., Eremia S.A.V.,Bertoli A., Pistelli L. Radu G.L. 2010 Laccase-Nafion Based Biosensor for the Determination of Polyphenolic Secondary Metabolites 43(7-8) 1089-1099

[119] T. Feng, Y. Yang, M. Chuang, S. Luo, M. Galik, G. Flechsig, and J. Wang, 2009 Thermally Stable Improved First-Generation Glucose Biosensors based on Nafion/Glucose-Oxidase Modified Heated Electrodes", Electrochem. Commun., 11-1812.

[120] Veer, B. v.d. and Bolier G. 1991. Improvement in accuracy of the interpretation of algal growth.
Verh. Int. Ver. Limnol. 24, 1272-1276.

[121] Heifetz P.B., Forster B., Barry Osmond C., Giles J.L., Boynton J.E.2000Effects of Acetate on Facultative Autotrophy in Chlamydomonas reinhardtii Assessed by Photosynthetic Measurements and Stable Isotope AnalysesPlant Physiology, 122,1439–1445

[122] Johanningmeier, U., Heiss, S., 1993 Construction of a Chlamydomonas reinhardtii mutant with an intronless psbA gene. Plant Mol. Biol. 22, 91–99. 481

[123]. Calabrese E. J,. Baldwin L. A 2002 Defining hormesis Human & Experimental Toxicology 21, 91- 97.

[124] Lima I. S., ALazarin. M., Airoldi C, 2006 Cyclic voltammetric investigations on copper α-N,O-succinated chitosan interactions Carbohydrate Polymers 64, 385–390.

[125] Carpentier R.,. Fuerst E. P, Nakatani H. Y., Arntzen C. J., Photoacoustic detection of photosynthetic energy storage in Photosystem II submembrane fractions Biochim. Biphys. Acta 808 (1985), 293-299.

[126]. Findlay J. W. A, Dillard R. F. (2007) Appropriate Calibration Curve Fitting in Ligand Binding AssayAAPS Journal 9(2) 260-267.

[127] Oettmeier W., Masson K. 1980 Synthesis and thylakoid membrane binding of the radioactively labeled herbicide dinoseb Pesticide Biochem. and Physiology 14 86-97.

[128] Thiel A, Böger P., 1984 Comparative herbicide binding by photosynthetic membranes from resistant mutants Pesticide Biochem. and Physiology 22, 232-242.

[129] Kruk J., Strzalka K, Redox Changes of Cytochrome b559 in the Presence of Plastoquinones J. Biol. Chem. 276(1) (2001), 86-91.

[130] M. Broser PhD Thesis, 2011.

[131] Armbruster D. A. and Pry T.. 2008 Limit of Blank, Limit of Detection and Limit of Quantitation Clin Biochem Rev. August; 29: 49–52.

[132] Pandard P., Rawson D.M., 1993An amperometric algal biosensor for herbicide detection employing a carbon cathode oxygen electrode Environ. Toxicol.Water Qual. 8 323.

[133]Lamb M.R., Dutcher S.K. , Worley C.K , Dieckmann Eyespot-Assembly Mutants in Chlamydomonas reinhardtii C.L.1999 Genetics 153, 721-729

[134] Inwooda W.,Yoshiharaa C., Zalpuri R., Kima K.S., Kustua S. 2008 The Ultrastructure of a Chlamydomonas reinhardtii Mutant Strain Lacking Phytoene Synthase Resembles that of a Colorless Alga. Molecular Plant 1 (6)925-937

[135] Erickson J.M., Rahire M., Bennount P., Delepelairet P., Dinert B., Rochaix J-D 1984Herbicide resistance in Chlamydomonas reinhardtii results from a mutation in the chloroplast gene for the 32-kilodalton protein of photosystem II Biochemistry 81, 3617-3621

[136] Shimogawara K., Fujiwara S., Grossman A., Usuda H. 1998 High-Efficiency Transformation of*Chlamydomonas reinhardtii* by Electroporation Genetics, 148, 1821-1828

[137] Johanningmeier U., Bertalan I., Hilbig I., Schulze J., Wilski S., Zeidler E. Oettmeier W., 2005 Engineering the D1 Subunit of Photosystem II: Application to Biosensor Technology, Eds M.T. Giardi and E. Piletska. Landes Bioscience/ eurekah.com, Georgetown, Texas, U.S.A

[138] M. Kasuno, M.Torimura , Y. Tsukatani, D.Murakami,S.Hanada, T.Matsushita, H. Tao 2009 Characterization of the photoinduced electron transfer reaction from the photosynthetic system in Rhodobacter sphaeroides to an exogenous electron acceptor Journal of Electroanalytical Chemistry 636 101–106